Master's Theses   Master's Theses and Graduate Research

2008

Flexural comparison of the ACI 318-08 and AASHTO LRFD structural concrete codes

Nathan Jeffrey Dorsey
San Jose State University

Follow this and additional works at: https://scholarworks.sjsu.edu/etd_theses

Part of the Structural Engineering Commons

FLEXURAL COMPARISON OF THE ACI 318-08 AND AASHTO LRFD
STRUCTURAL CONCRETE CODES

A Thesis

Presented to

The Faculty of the Department of Civil Engineering

San Jose State University

In Partial Fulfillment

of the Requirements for the Degree

Master of Science
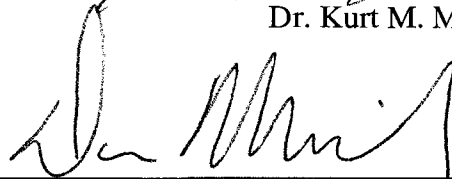
by

Nathan Jeffrey Dorsey

May 2008

APPROVED FOR THE DEPARTMENT OF CIVIL ENGINEERING

_____
Dr. Akthem Al-Manaseer
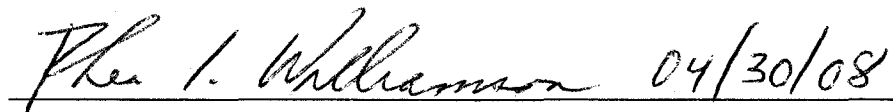
_____
Dr. Kurt M. McMullin

_____
Mr. Daniel Merrick

APPROVED FOR THE UNIVERSITY

_____
04/30/08

ABSTRACT

FLEXURAL COMPARISON OF THE ACI 318-08 AND AASHTO LRFD
STRUCTURAL CONCRETE CODES

by Nathan Jeffrey Dorsey

There are two prevailing codes utilized during the design of structural concrete

members in North America, ACI 318-08 and AASHTO LRFD. Each takes a unique

approach to achieve the same result, a safe working design of a structural concrete

section; however there are fundamental differences between the codes regarding the

calculation of member properties.

The purpose of this paper was to investigate these differences between codes

encountered during the calculation of flexural strength or moment capacity of a section.

This study focused on the code's influence during the classical approach to analysis of a

shallow reinforced T-beam and the strut and tie model method as applied to a series of

deep beams with openings. Parametric studies were conducted using software developed

by the author specifically for this purpose.

It was concluded that both codes provided similar and safe results regardless of

the very different approaches to solution taken by each.

ACKNOWLEDGEMENTS

Table of Contents

List of Tables

List of Variables

a	effective depth of the compressive block
a'	distance from center of concentrated load to edge of support
A_c'	area of concrete on flexural compression side of member
A_{ps}	area of prestressed longitudinal reinforcement placed on the flexural tension side of the section
A_s	area of flexural reinforcement
A_s	area of non-prestressed longitudinal reinforcement placed on the flexural tension side of the section
A_s	area of conventional non-prestressed tensile reinforcing steel
A_s'	area of conventional non-prestressed compressive reinforcing steel
A_v	cross sectional area of provided stirrup reinforcement within distance s
b	section width
b_v	effective web width
b_w	web width
c	distance from extreme compressive fiber to neutral axis
d	distance from the extreme compressive fiber to the centroid of the flexural reinforcement
D	overall member depth
d_c	strut width
d_e	depth from the extreme compressive fiber to the centroid of the tensile force in the non-prestressed reinforcement, i.e. reinforcing bars also called the effective depth of main flexural reinforcement
d_n	effective shear depth, can be taken as 0.9d
d_p	depth from the extreme compressive fiber to the centroid of the tensile force in the prestressed reinforcement
d_s	depth from the extreme compressive fiber to the centroid of the tensile force in the non-prestressed reinforcement, i.e. reinforcing bars
d_v	effective shear depth, taken as 0.9d
E	modulus of elasticity of the material, commonly referred to as Young's Modulus
E_c	elastic modulus of concrete
E_p	modulus of elasticity of prestressed reinforcement
E_s	modulus of elasticity of non-prestressed reinforcement
f^*_c	effective concrete strength
f'_c	compressive concrete strength
f_{ps}	stress in the prestressing steel at nominal bending resistance
f_{pu}	tensile strength of prestressing steel
f_{sy}	yield strength of main longitudinal reinforcing steel
f_y	yield strength of conventional non-prestressed reinforcing steel
k_3	ratio of the in situ strength to the cylinder strength
M_u	factored moment; taken as a positive quantity not less than $V_u d_n$
n	efficiency factor
N_u	factored axial force; positive if tensile, negative if compressive

s	stirrup spacing
t_f	flange thickness
T_u	factored torsion
V	shear force
V_c	shear strength contribution from concrete
V_s	shear strength contribution from reinforcing steel
V_u	factored shear
w	node width over which shear force is applied
z	distance between node centers
ε	strain
ε_1	major principal strain, normal to strut
ε_2	minor principal strain, parallel to strut
ε_x	strain in the horizontal direction
Ω	equivalent strut width over which ties contribute
θ	angle of strut to horizontal
θ	angle of strut to longitudinal axis
θ	σ stress

1.0 <u>INTRODUCTION</u>

1.1   General

The purpose of this thesis is to compare and contrast the ACI 318-08 and the AASHTO LRFD 3rd Ed. code provisions and design philosophies.

1.2   Scope

The crux of this thesis is the comparison of the two prevailing concrete design codes regarding the design and detailing of concrete beams in pure flexure with no other loading present. The discussion on shallow beams used a series of twelve flanged beams as its focus while the deep beam discussion focused on a series of five deep beams and the Strut-and-Tie Model (STM) method. To accomplish this a series of Excel spreadsheets were created to ensure the accuracy and consistency of all calculations performed; however as programming is not the point of this research several simplifying assumptions were made to reduce the time required to create, vet and utilize these tools.

Both sections focus solely on analytical results; no laboratory experiments were carried out. Comparisons were based on but not limited to maximum predicted allowable load.

1.3   Objective

The objective of this thesis is to clarify the differences between the two prevailing concrete design codes, ACI 318-02 and AASHTO LRFD 3rd Ed. and categorize them as

major, minor, or insignificant. For simplicity when the AASHTO LRFD 3rd Ed. is referenced, the 3rd Ed. shall be omitted. In cases where other editions are referenced, the edition under discussion shall be noted. An additional comparison will be made between the results produced by the two codes when using the method of STM and the actual experimental test loads used during experimental work carried out by Ha in 2002. A comprehensive literature review providing coverage of examples illustrating additional differences found between the ACI 318 and AASHTO LRFD codes beyond pure flexure and deep beams is included.

1.4 Outline

Chapter 2 contains a literature review of relevant academic and industry articles regarding a specific structural member type, a specific concrete design code or a comparative study of both codes. Chapter 3 provides a brief introduction and review of the design philosophy of both flexural analysis for shallow reinforced concrete beams and the STM method of design for reinforced concrete deep beams. Chapter 4 details the analytical procedure as described by each code and what methods were implemented by the software tools developed. Chapter 5 contains the results obtained from this study. Chapter 6 provides the concluding remarks on the findings of this study.

2.0 <u>LITERATURE REVIEW</u>

2.1   Introduction

The flexural resistance or moment capacity of a structural member is a

fundamental part of the overall analysis required when designing or evaluating an

assembly of structural concrete sections. This flexural resistance is only one of a myriad

of forces that needs to be considered when designing or evaluating a structural member.

Other forces due to direct loading or reactions such as axial, torsional and shear forces

must not be overlooked.

Of the many comparisons between the American Concrete Institute (ACI) 318

Building Code Requirements for Structural Concrete and the American Association of

State Highway Transport Officials Load and Resistance Factor Design (AASHTO LRFD)

Bridge Design Specifications for non-prestressed concrete members reviewed only one

article directly addressed differences when analyzing or designing a structure with

respect to the flexural resistance. However many of the conclusions presented by the

reviewed articles followed the same general trend.

Articles detailing differences in method and results when using the strut-and-tie

model (STM) method were rather numerous and articles reviewed or discussed in this

paper date back as far as 1996, older articles on these subjects were available but were

not considered for review due to the significant revisions made to the codes since the

time of publication.

2.2 Shallow Beams

Gupta and Collins (537-47) performed a study that primarily focused on the question of the safety of using traditional shear design procedures based on the failure of the Sleipner offshore platform on 23 August, 1991. To aid in their determination of the safety of these traditional methods of analysis and design 24 reinforced concrete elements having concrete compressive strengths ranging from 4280 to 12,600 psi were loaded under a variety of shear and compressive axial load combinations. The results from these tests were used to evaluate the design provisions of the ACI 318-99 and AASHTO LRFD *"Bridge Design Specifications and Commentary"* 2nd Ed.

The ACI 318-99 code provisions made a general assumption that the shear stress of a member V_n, could be defined as the sum of the shear load at which diagonal cracks form V_c, and the provided shear capacity of any stirrups present using the traditional 45 degree truss equation, V_s.

$$V_n = V_c + V_s \tag{2-1}$$

The traditional 45 degree truss equation is defined as

$$V_s = \frac{A_s f_y d}{s} \tag{2-2}$$

The code also allowed for a simplified conservative calculation to be used for V_c although the detailed approach provided for more accurate and less conservative results. Both equations are shown below. The simplified and conservative approach is detailed in

Equation 2.3 while the detailed approach is shown in Equation 2.4. Both equations

require the use of English units.

$$V_c = 2\left(1 + \frac{N_u}{2000A_g}\right)\sqrt{f'_c}\,b_w d \tag{2-3}$$

$$V_c = \left(1.9\sqrt{f'_c} + 2500\rho_w \frac{V_u d}{M_m}\right)b_w d \tag{2-4}$$

N_u in Equation 2-3 represents the load due to axial compression and M_m in Equation 2-4

represents the modified moment as defined by the relationship shown in Equation 2-5.

$$M_m = M_u - N_u\left(\frac{4h - d}{8}\right) \tag{2-5}$$

Regardless of the method utilized for calculation of the shear load at which

diagonal cracks form the ACI 318-99 code placed a restriction on the maximum value for

V_c as defined by

$$V_c \le 3.5\sqrt{f'_c}\,b_w d\sqrt{1 + \frac{N_u}{500A_g}} \tag{2-6}$$

These detailed equations for V_c were derived by ACI-ASCE Committee 326 in

1962 and were based on the principal stress as found at the location of the diagonal

tension cracking.

The AASHTO LRFD shear design procedure did not use the general assumptions

utilized by the ACI 318-99 provisions, rather it relied on the more involved modified

compression field theory (MCFT) which in turn uses relationships between equilibrium,

compatibility and stress and strain to predict the shear capacity of cracked concrete

section/elements. In addition to the obvious difference between the backgrounds of the

two code provisions note that the AASHTO LRFD used SI units of MPa whereas the ACI

318-99 provided solutions in English units of psi.

Hence the AASHTO LRFD expression for shear resistance of a section, V_n, was

more involved and incorporated several different sub-equations. AASHTO LRFD

defined shear resistance as

$$V_n = 0.083\beta\sqrt{f'_c}\,b_v d_v + \frac{A_v f_y}{s} d_v \cot\theta \quad (MPa) \tag{2-7}$$

The variables were defined as:

A_v = cross sectional area of provided stirrup reinforcement within

distance s

b_v = effective web width

d_v = effective shear depth, taken as $0.9d$

f'_c = compressive strength of concrete

f_y = yield stress of steel reinforcement

s = stirrup spacing

Values for β and θ were derived from calculating the stresses transmitted across

diagonal cracked concrete sections which contained no less than the minimum required

transverse reinforcement for crack control. This minimum amount of transverse

reinforcement $A_{v,min}$, was defined and calculated by AASHTO LRFD as

$$A_{v,min} = 0.083\sqrt{f'_c}\,\frac{b_v s}{f_y}\ (MPa)$$

(2-8)

The values for β and θ were dependant on the shear stress, v, and the longitudinal

mid-depth strain of the section, ε_x. Figure 2-1 details the idealized section used by

AASHTO LRFD in the calculation of ε_x for this procedure.
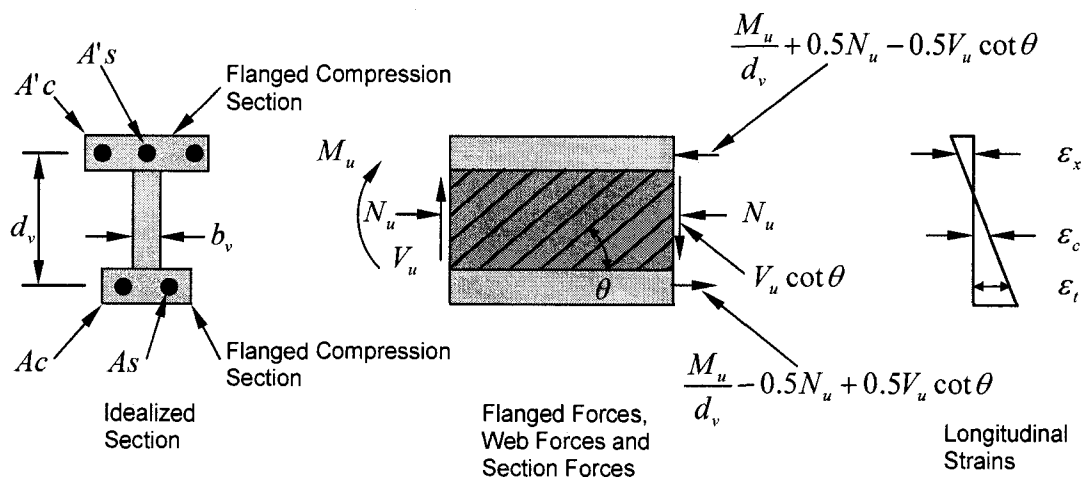
Figure 2-1 AASHTO LRFD Procedure for calculation of ε_x

Mathematically the longitudinal mid-depth strain of this section is defined by the

relationship shown in Equation 2-9.

$$\varepsilon_x = \frac{\varepsilon_t - \varepsilon_c}{2}$$

(2-9)

Where the terms ε_t represented the longitudinal tensile strain in the flexural tension flange

and ε_c represented the longitudinal compressive strain in the flexural compressive flange.

Mathematically ε_t and ε_c were calculated as shown in Equations 2-10 and 2-11.

$$\varepsilon_t = \frac{\dfrac{M_u}{d_v} - 0.5N_u + 0.5V_u \cot\theta}{E_s A_s} \tag{2-10}$$

$$\varepsilon_c = \frac{\dfrac{M_u}{d_v} + 0.5N_u - 0.5V_u \cot\theta}{E_s A_s + E_c A_c{}'} \tag{2-11}$$

The newly introduced variables were defined as:

A_c' = area of concrete on flexural compression side of member

E_c = elastic modulus of concrete

E_s = elastic modulus of steel

And v was defined by the relationship shown in Equation 2-12.

$$v = \frac{V_n}{b_v d_v} \tag{2-12}$$

The result of the relationships defined above was that for an increase in axial compression the variables N_u, ε_x and θ decreased while β would increase. This contributed to an increased shear capacity for any given section.

In order to obtain empirical data to corroborate the analytical predictions from each code's procedure a series of 24 specimens were built and tested in the University of Toronto's shell element testing apparatus. Specimens were designed to represent the

sections of a structural wall that was simultaneously subjected to high axial compression and high out of plane shear loads.

Specimen length L, overall section depth h, total percentage of longitudinal reinforcement ρ_x, and total percentage of transverse reinforcement across the specimen width ρ_y were not varied during the course of investigation. The parameters that were variable were the compression to shear ratio N/V, the concrete compressive strength f'_c, specimen width b and the shear reinforcement provided r_z.

Loads were induced by five series of six jacks that applied pressure onto steel transfer beams located on the top and bottom faces of the specimens. A compressive stress of up to 9400 psi was applied along with equal but opposite moments applied to each end of the specimen bending it in double curvature. In each test case the loads from axial, shear and moments were increased proportionally until the specimens reached failure. Tangential deformation was used as the means of quantifying the total deformation of each specimen.

Strains from the flexural tension side of the member ε_{xt} and the flexural compression side of the member ε_{xc}, were measured from locations directly adjacent to the steel end plates. Strain for the shear reinforcement was measured directly from the T-headed bars used to provide shear reinforcement and reinforcement across the member width.

Failures were classified as shear S, or flexural F, based on the observed strains in the ε_{xt} and ε_{xc} directions at the ends of the specimen when compared to the magnitude of the applied moment at the specimen ends M_E and the shear strains γ_{xz}. Of the 24 specimens tested 18 were classified as failing in shear while the remaining 6 were classified as flexural failures. In the six flexural failures it was determined that the longitudinal reinforcement yielded and the applied moment M_E, approximately equaled or exceeded the predicted moment at failure M_o.

This experiment demonstrated that when the ACI 318-99 conservative method for calculating V_c was utilized the shear strength and mode of failure for a reinforced specimen loaded under high axial compression can be consistently predicted; whereas when using the more detailed method of calculating V_c was used, the mode of failure can be brittle shear and occur at loads significantly less than those predicted, on average 68% less. It was demonstrated that it was possible to properly design a section using the detailed method described by this procedure and yet only provide a factor of safety as low as 1.10.

The AASHTO LRFD procedure for calculating V_c provided far more accurate and consistent results for shear failure and the upper limit of shear capacity as induced by an increase in axial compression was correctly predicted.

Two major recommendations arose from these results:

- The detailed expression for V_c be removed from the ACI 318 code

- The term for axial compression N_u/A_g in Equations 2-3 and 2-6 not be taken greater than 3000 psi

Rahal and Collins (277-82) undertook research to provide an evaluation of the design provisions for combined shear and torsion load cases as described by both the ACI 318-02 and the AASHTO LRFD Bridge Design Specifications, 2nd Edition.

When Rahal and Collins' report was published the current version of each code contained torsional design provisions that were similar other than the method used to determine the angle θ. Rahal and Collins noted that the AASHTO LRFD provisions had been extensively checked for shear cases whereas the ACI 318-02 provisions had been extensively checked for pure torsion as well as combined torsion and bending. It was concluded that there was a lack of data available that directly correlated the torsional provisions of each code. Hence Rahal and Collins ran four large scale experiments to compare the results of the calculated torsion-shear interaction diagrams obtained from both the AASHTO LRFD and ACI 318-02 provisions. The beams tested were solid, rectangular sections 340mm wide and 640mm deep reinforced with non-prestressed longitudinal bars.

The ACI 318-02 code described the basic truss equation relating the provided hoop reinforcement to torsional strength as follows:

$$T_n = 2A_o \frac{A_t f_{yv}}{s} \cot \vartheta \ \textit{(SI Units)} \qquad\qquad (2\text{-}13)$$

Where A_o represented the area enclosed by the shear flow path and was permitted to be taken as $0.85*A_{oh}$, and where A_{oh} represented the area enclosed by the outermost transverse torsional reinforcement. f_{yv} was the yield strength of the hoop reinforcement and A_t represented the cross sectional area of one leg of the transverse reinforcement. θ represented the angle of inclination of the compressive diagonals and was noted to have rather ambivalent instructions to its suggested versus its analyzed values. As described in ACI 318-02 §11.6.3.6 the angle θ shall not be less than 30 degrees but it is suggested that $\theta = 45$ degrees for non-prestressed members and $\theta = 37.5$ degrees for members that are prestressed.

A similar truss equation, see Equation 2-14, related the torsional strength to the quantity of longitudinal reinforcement provided.

$$T_n = 2A_o \frac{A_t f_{yl}}{p_h} \tan \vartheta \ \textit{(SI Units)} \qquad\qquad (2\text{-}14)$$

Rahal and Collins observed that when comparing equations 2-13 and 2-14 the equivalent torsional strengths could be obtained by using less hoop reinforcement but increasing the longitudinal reinforcement.

When these two equations were set equal to each other the required area of

transverse reinforcement could be solved for as shown by Equation 2-15.

$$A_l = \frac{A_t}{s} p_h \frac{f_{yv}}{f_{yl}} \cot^2 \theta \ (SI \ Units)$$ (2-15)

The ACI 318-02 equation for a non-prestressed section that described the

relationship between transverse reinforcement and shear strength is shown in Equation 2-

16.

$$V_n = V_c + V_s = 0.166\sqrt{f'_c}b_w d + \frac{A_s f_y}{s} d \ (MPa)$$ (2-16)

The variables were defined as:

A_s = area of flexural reinforcement

b_w = web width

d = distance from the extreme compressive fiber to the centroid of the flexural

reinforcement

f'_c = compressive concrete strength

f_y = yield strength of reinforcing steel

V_c = shear strength contribution from concrete

V_s = shear strength contribution from reinforcing steel

Additionally the ACI 318-02 code required that the nominal shear stress for solid

sections be limited to avoid concrete crush prior to reinforcement yield. Equation 2-17

describes this limitation.

$$\sqrt{\left(\frac{V_n}{b_w d}\right)^2 + \left(\frac{T_n p_h}{1.7 A_{oh}^2}\right)^2} \leq 0.83\sqrt{f'_c} \text{ (SI Units)} \qquad (2\text{-}17)$$

The AASHTO LRFD code used the same basic truss equation as the ACI 318-02,

Equation 2-13, to relate the area of one leg of the transverse reinforcement A_t, to the

required torsional strength T_n. However the AASHTO LRFD relationship between the

minimum required shear strength V_n and the required area of transverse reinforcement A_v

was noticeably different from that shown for ACI 318-02 in Equation 2-18.

$$V_n = V_c + V_s = 0.083\beta\sqrt{f'_c} b_v d_v + \frac{A_v f_y}{s} d_v \cot\theta \text{ (SI Units)} \qquad (2\text{-}18)$$

The variable b_v represented the web width, however d_v was defined as the

effective shear depth which can be taken as $0.9*d$. For sections containing stirrups the

values for β and θ depended on the nominal shear stress v, and the mid-depth

longitudinal strain ε_x.

Rahal and Collins noted that when β was set equal to 2.22 the AASHTO LRFD

value matched the ACI 318-02 value for V_c exactly. Also when examining non-

prestressed sections ε_x could be taken as 1.00×10^{-3} which provided a value of 36 degrees

for θ, and when the AASHTO LRFD value for θ equaled 36 degrees the results for V_s

were 24% higher than those obtained from the ACI 318-02 procedure.

Equation 2-19 details the nominal shear stress v, for a solid section as calculated under the AASHTO LRFD provisions for a solid section under combined shear and torsion which was required to be no greater than $0.25f'_c$ to avoid failures due to concrete crushing.

$$v = \sqrt{\left(\frac{V_n}{b_v d_v}\right)^2 + \left(\frac{T_n p_h}{A_{oh}^2}\right)^2} \leq 0.25 f'_c \quad (MPa)$$

(2-19)

The longitudinal stress ε_x, at the mid-plane could be taken as 1.00×10^{-3} or it could be calculated using the relationship shown in Equation 2-20.

$$\varepsilon_x = \frac{\frac{M_u}{d_v} + 0.5 N_u + 0.5 \cot\theta \sqrt{V_u^2 + \left(\frac{0.9 p_h T_u}{2 A_o}\right)^2} - 0.7 f_{pu} A_{ps}}{2\left(E_s A_s + E_p A_{ps}\right)}$$

(2-20)

Variables in Equation 2-20 were defined as:

A_s = area of non-prestressed longitudinal reinforcement placed on the flexural tension side of the section

A_{ps} = area of prestressed longitudinal reinforcement placed on the flexural tension side of the section

d_v = effective shear depth, can be taken as $0.9d$

E_s = modulus of elasticity of non-prestressed reinforcement

E_p = modulus of elasticity of prestressed reinforcement

f_{pu} = tensile strength of prestressing steel

M_u = factored moment; taken as a positive quantity not less than $V_u d_v$

N_u = factored axial force; positive if tensile, negative if compressive

T_u = factored torsion

V_u = factored shear

Rahal and Collins noted that for prestressed sections ε_x would often approach zero. In these cases the value of θ would vary from 22 to 30 degrees depending on the level of shear stress present.

The AASHTO LRFD provisions required that the tensile capacity of the longitudinal reinforcement on the flexural tension side of the section be no less than the force T_E, to prevent premature failure of the longitudinal reinforcement. T_E was calculated as shown in Equation 2-21.

$$T_E = \frac{M_u}{\phi d_v} + \frac{0.5N_u}{\phi} + \cot\theta \sqrt{\left(\frac{V_u}{\phi} - 0.5V_s\right)^2 + \left(\frac{0.45p_h T_u}{\phi 2A_o}\right)^2} \qquad (2\text{-}21)$$

The test variable in the series was the torsion to shear ratio which varied from zero to 1.216m. Specimen failures were attributed to excessive yielding of the closed stirrups as well as spalling and crushing of the concrete in the test region.

Rahal and Collins determined that use of the ACI 318-02 provisions produced very conservative results when the maximum value of 45 degrees for the angle of the compression diagonals θ, was used. Conversely when the minimum value for θ of 30

degrees was used the ACI 318-02 provisions demonstrated less consistent results and provided failure loads for high torsion-to-shear ratios much higher than those observed.

Results obtained from use of the AASHTO LRFD provisions provided a consistent value of approximately 36 degrees for θ. Use of this value provided results of a consistent and reasonable nature that closely replicated the observed crack patterns.

Naaman (209-18) investigated the differences between the ACI 318-02 and AASHTO LRFD codes regarding sections that were classified as being between tension controlled and compression controlled, i.e. in the transition zone. Naaman found and described several examples where the ACI 318-02 provisions regarding the limits of reinforcement for flexural members lead to unintended erroneous results that brought the validity of the provision into question. These flaws were not directly correlated to the corresponding AASHTO LRFD provisions but they did reflect similar results for other ACI provisions as described by several other publications where solutions appeared conservative but in reality did not provide adequate factors of safety.

Naaman noted that the changes made from the ACI 318-99 to the ACI 318-02 codes relocated the limits for tension and compression controlled sections and added the transition region between the two; the flaw lie in this definition for these regional boundaries. The various regions for reinforcement limits and the definitions and from different codes are shown in Figure 2-2.
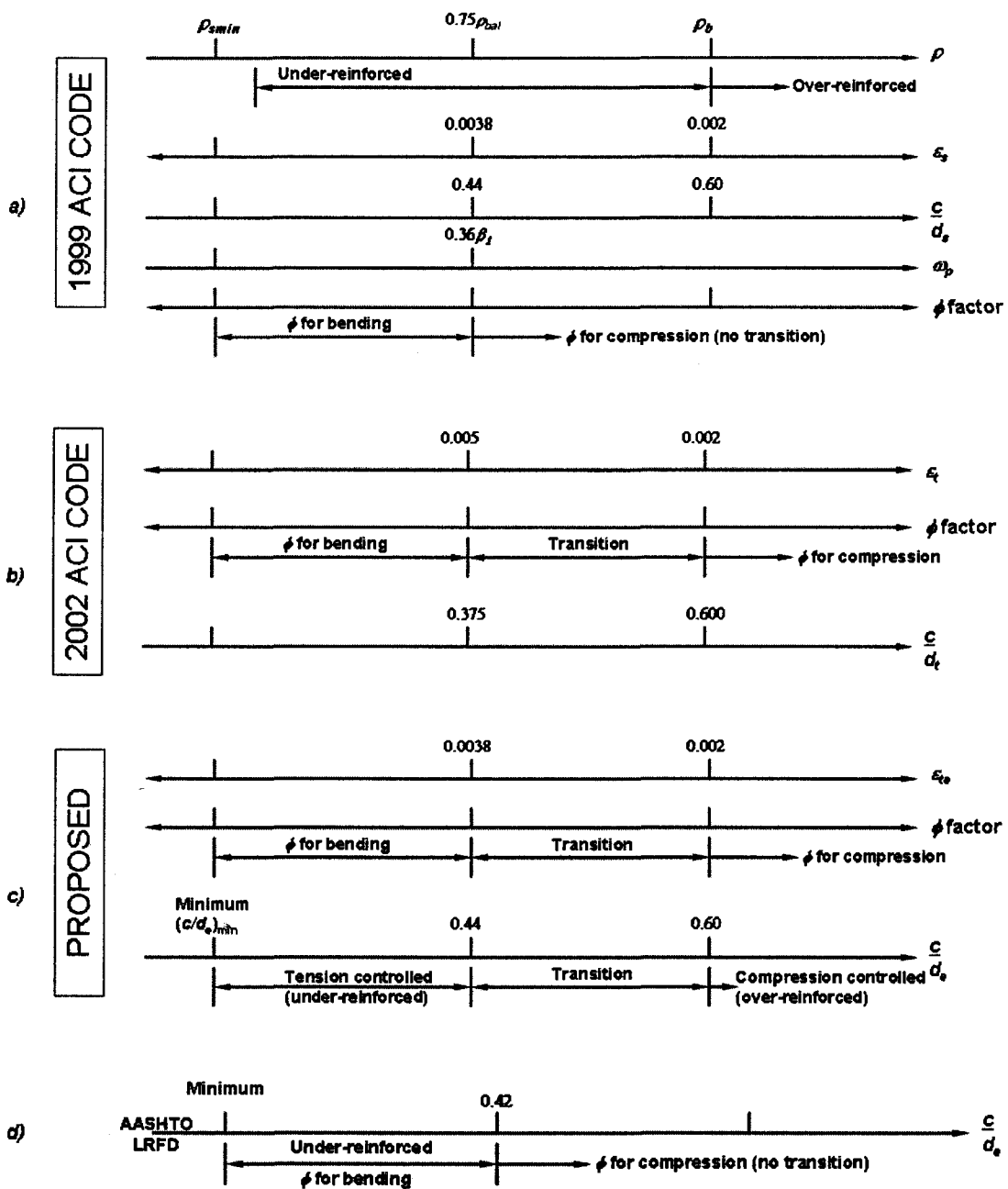
Figure 2-2 Summary of reinforcement limits by 1999, 2002 ACI codes and AASHTO LRFD and Naaman recommendation

The ACI 318-99 code used the ratio of c/d_s where c represented the depth of the compression block and d_s represented the depth from the extreme compressive fiber to the centroid of the tensile force in the non-prestressed reinforcing bars.

In the 2002 edition of the ACI 318 code the ratio was changed to c/d_t where d_t was defined as the depth from the extreme compressive fiber to the centroid of the extreme layer of the non-prestressed reinforcement. This allowed for values of ϕ found using the ACI 318-02 to be different from those obtained using the AASHTO LRFD for identical sections because the definition of d_t and its corresponding ε_t was defined as the distance to the centroid of the extreme tensile reinforcement only. This did not take into account tensile resistance provided by a multi-layered arrangement and implied that a section which contained more than one layer of reinforcement or a section having any combination of plain reinforced, partially prestressed or fully prestressed steel would be controlled by the extreme layer of reinforcement exclusively.

While the ACI 318-02 code offered this somewhat conflicting definition for the limits of reinforcement between editions the corresponding AASHTO LRFD provision detailed that for all cases the maximum reinforcement was bound by the relationship detailed in Equation 2-22.

$$\frac{c}{d_e} \leq 0.42 \qquad\qquad (2\text{-}22)$$

Where c again represented the depth of the compression block and d_e was calculated as the weighted sum assuming yield of the steel reinforcement provided. Reference Equation 2-23

$$d_e = \frac{A_s f_{ps} d_p + A_s f_y d_s}{A_{ps} f_{ps} + A_s f_y}$$

(2-23)

The variables used were defined as:

A_s = area of non-prestressed reinforcement

A_{ps} = area of prestressed reinforcement

f_{ps} = stress in the prestressing steel at nominal bending resistance

f_y = yield strength of conventional reinforcing steel

d_p = depth from the extreme compressive fiber to the centroid of the tensile force in the prestressed reinforcement

d_s = depth from the extreme compressive fiber to the centroid of the tensile force in the non-prestressed reinforcement, i.e. reinforcing bars

Naaman noted that when the quantity d_e was used to calculate the limits of reinforcement for a section the results were guaranteed to be the same, independent of whether the section was plain reinforced, partially prestressed or fully prestressed. This consistency was attributed to the fact that the equation guaranteed simultaneous equilibrium of forces as well as strain compatibility in any case. It also made the type of reinforcement present irrelevant since the tensile force T must equal the compression force C for all cases.

More specifically Naaman described that because the assumed failure strain in the concrete ε_{cu}, was taken as a constant in equations 2-24 and 2-27 there was a direct relationship between c/d_e and the tensile strain in the concrete at the centroid of the tensile force ε_{te} that was unique.

$$\frac{\varepsilon_{cu}}{\varepsilon_{cu}+\varepsilon_{te}} = \frac{c}{d_e} \tag{2-24}$$

$$d_e = d_s \text{ for } A_{ps} = 0 \tag{2-25}$$

$$d_e = d_p \text{ for } A_s = 0 \tag{2-26}$$

$$\varepsilon_{te} = \varepsilon_{cu}\frac{d_e - c}{c} = \varepsilon_{cu}\left(\frac{1}{c/d_e} - 1\right) \tag{2-27}$$

The use of d_e was proposed by Naaman to replace d_t when determining the ratio c/d_t to avoid erroneous reinforcement level classification of a section. It should be noted that the ACI 318-05 provisions did include some but not all of the recommendations proposed by Naaman. The relationship used to define the regions was changed to use the quantity d_e rather than the less accurate d_t, and the upper limit of the transition region remained 0.60 consistent with Naaman's recommendation; however the lower limit of the transition region remained set at 0.375 rather than the 0.44 that Naaman had proposed. Reference Figure 2-3 to compare the new limits of the ACI 318-05 to those of the AASHTO LRFD.
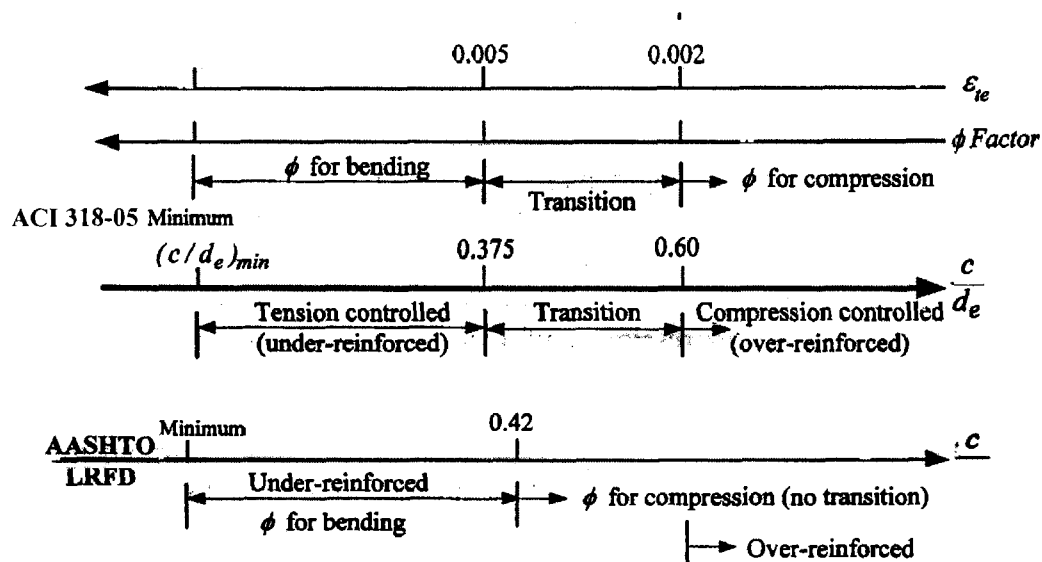
Figure 2-3 ACI 318-05 and AASHTO LRFD limits of reinforcement

Rahal and Al-Shaleh (872-78) conducted a study to examine the differing requirements for minimum transverse reinforcement as specified by the ACI 318-02 Code, Canadian Standards Association (CSA) A23.3 and AASHTO LRFD Specifications 2nd Ed. The observed cracking patterns, crack widths at the estimated service load and at the post-cracking reserve strength were used to evaluate the performance of each specimen. Their study focused on high-strength concrete (HSC) based on its increased use in construction. HSC sections require larger amounts of transverse reinforcement due to their behavior of cracking at much higher shear stresses than conventionally reinforced concrete sections.

The ACI 318-02 used detailed equations that accounted for the contribution from the concrete V_c, on the effect of the longitudinal steel as well as the stress resultants for bending moment and axial load. The AASHTO LRFD Specifications accounted for the influence of longitudinal reinforcement, flexural, torsional and axial loading in the calculation of the strain indicator ε_x, which has effects on both concrete and steel reinforcement contributions V_c and V_s respectively.

The CSA A23.3, the ACI 318-02, and the AASHTO LRFD were not united in their approached to longitudinal reinforcement provisions and were noted to have differed significantly. Regardless of the difference in the approach to provided longitudinal reinforcement none of the aforementioned codes accounted for the *influence* of the longitudinal reinforcement; addressing this influence from longitudinal reinforcement was the objective of Rahal and Al-Shaleh's test program.

Eleven four point load shear tests were performed on 65 MPa (9500 psi) beams that had minimal transverse reinforcement and two levels of longitudinal reinforcement. Beam dimensions for all specimens were 200 mm (7.87 in.) wide, 370 mm (14.57 in.) deep and 2750 mm (108 in.) long with a shear span of 900 mm. The average concrete cylinder strength f_{cy} was 75% of the concrete cube strength f_{cu} and split tensile strength f_{sp} was approximately $0.74\sqrt{f_{cy}}$.

Their study produced the following conclusions:

- Behavior of members containing large amounts of longitudinal steel was far superior when compared to members that contained very little or no longitudinal steel

- The ACI 318-02 and CSA A23.3 provided adequate performance for members containing large amounts of longitudinal reinforcement

- No evidence was found in performance between beams designed with the maximum stirrup spacing as defined by each code

- Shear capacity equations in the ACI 318-02 and AASHTO LRFD 2nd Ed were conservative

2.3   Deep Beams

Brown, Sankovich, Bayrak and Jirsa (348-55) completed a study of the behavior and efficiency factors assigned to bottle shaped struts when used in calculations as described by the method of STM. Historically these efficiency factors were assigned based on good practice rather than actual results from experimentation. A fundamental difference found between the two provisions was in the calculation of the strength of a strut based on specified concrete strength as determined by a cylinder test f'_c, and the strut efficiency factor β_s.

ACI 318-05 defined f_{cu} as shown in Equation 2-28.

$$f_{cu} = 0.85\beta_s f'_c \qquad\qquad (2\text{-}28)$$

The strut efficiency factor β_s, is based on the type of strut under consideration and the amount of transverse reinforcement present. When ACI 318-05 is used in cases of a bottle shaped strut that was crossed by adequate transverse reinforcement as defined by ACI 318-05 Equation A-4 (Equation 2-29) the strut will control the strut-node interface in all cases other than CTT, i.e. an interface node having one strut and two ties.

$$\sum \frac{A_{si}}{bs_i}\sin\gamma_i \leq 0.003 \qquad (2\text{-}29)$$

The AASHTO LRFD utilized the MCFT to define f_{cu} and therefore the definition is much more involved than that described by the ACI 318-05 method. Equation 2-30 repeats the AASHTO LRFD Equation 5.6.3.3.3-1

$$f_{cu} = \frac{f'_c}{0.8 + 170\varepsilon_1} \leq 0.85 f'_c \qquad (2\text{-}30)$$

where

$$\varepsilon_1 = \varepsilon_s + (\varepsilon_s + 0.002)\cot^2\alpha_s \qquad (2\text{-}31)$$

α_s was defined as the smallest angle between the compressive struts and the adjoining tie. It was noted that many engineers have difficulty choosing an appropriate tensile concrete strain to be used during design and have therefore expressed reservations about using the MCFT based ASSHTO LRFD provisions.

To more directly measure the effect these two approaches had on modeling struts 26 concrete panels measuring 36 x 36 x 6 in. (914 x 914 x 152 mm) were loaded using a 12 x 6 x 2 in. (305 x 152 x 51 mm) steel bearing plate. One test used a different panel thickness and bearing plate to observe and examine the effect of specimen geometry on the efficiency factor.

Each specimen had a unique amount and placement of reinforcing steel and in each isolated strut test the same mode of failure was observed. Failure was first indicated by a vertical crack which would form in the center of each panel. That crack then propagated from panel midheight to the loading points but would not intersect them, rather it would change direction. Failure was described as crushing and spalling of the concrete near but not adjacent to the loading plate.

The same failure mode was observed in every test regardless of the boundary conditions present. Of the 26 specimens tested the efficiency factors presented in ACI 318-05 provided a safe estimate of the isolated strut capacity. Of these 25 specimens it was noted that the results were conservative but erratic when compared to the test data. When the average value for the experimental efficiency factor was divided by the predicted ACI 318-05 efficiency the result was 1.68.

Of the 26 test specimens 20 of the AASHTO LRFD determined efficiency factors yielded results for the isolated struts that were less conservative but more consistent with

the test data. All of the AASHTO LRFD data was governed by the limitation placed on the maximum strut strength of $0.85f'_c$ as described by AASHTO LRFD Equation 5.6.3.3.3-1 (Equation 2-30).

Foster and Malik (569-77) reviewed a comprehensive set of test data on deep beams and corbels and compared them to the proposed efficiency factors. The STM model that was most extensively investigated was the plastic truss model where all truss members enter the nodal zones at 90°. The plastic truss model has two possible failure modes; concrete crush in the struts and yielding of the ties. A third failure mode was proposed by in 1998 by Foster where splitting or bursting of the strut should be considered. Due to the well known behavioral and material properties of reinforcing steel tension failures can be predicted with a high degree of confidence and therefore this mode is not discussed.

To simplify their discussion regarding deep beams and corbels Foster and Malik standardized the nomenclature used in their study. They defined the clear span a, as the distance from the centers of the strut nodes and they also split up the in situ strength factor k_3 and the strut efficiency factor v; historically these two strength factors were combined into a single parameter. All relevant equations were then recalculated to incorporate this split between variables.

The fundamental plastic truss model equations that relate material properties,

geometry and strength of a member in equilibrium are shown below.

Material:

$$T = A_s f_{sy} \tag{2-32}$$

$$C = f^*_c b d_c \tag{2-33}$$

$$f^*_c = k_3 \nu f'_c \tag{2-34}$$

Geometry:

$$a = a' + \frac{w}{2} \tag{2-35}$$

$$z = d + \frac{\Omega}{2} \tag{2-36}$$

$$\tan\theta = \frac{z}{a} = \frac{w}{\Omega} \tag{2-37}$$

$$\Omega = d - \sqrt{d^2 - 2aw} \leq 2(D - d) \quad (SI) \tag{2-38}$$

$$d_c = \frac{w}{\sin\theta} \tag{2-39}$$

Strength:

$$V = \min\left(\frac{A_s f_{sy} z}{a}, f^*_c b w\right) \tag{2-40}$$

The variables were defined as:

a = shear span

a' = distance from center of concentrated load to edge of support

A_s = area of tensile reinforcement

b = section width

d = effective depth of main flexural reinforcement

d_c = strut width

D = overall member depth

f'_c = compressive concrete strength

f^*_c = effective concrete strength

f_{sy} = yield strength of main longitudinal reinforcing steel

k_3 = ratio of the in situ strength to the cylinder strength

V = shear force

w = node width over which shear force is applied

z = distance between node centers

v = efficiency factor

θ = angle of strut to longitudinal axis

Ω = equivalent strut width over which ties contribute

Using these relationships Foster and Malik calculated the efficiency factor as shown in Equation 2-41.

$$v = \frac{V}{k_3 f'_c bw}$$ (2-41)

This efficiency factor was used to reduce predicted member capacity to compensate for the fact that concrete is not a perfectly plastic but rather a brittle material. In 1986 the MCFT was proposed to describe and define that concrete is not perfectly plastic and the corresponding loss of strut capacity due to transverse tension fields.

Foster and Malik also investigated the controversy and debate surrounding the assignment and values used for efficiency factors in this same report. A 1986 study suggested $v = 0.6$, whereas another undertaken in 1997 suggested $v = 0.85$ and placed greater emphasis on the selection of an appropriate truss model. Models created in 1987, 1990 and 1997 also used efficiency factors that were functions of strut or node location and the degree of disturbance these struts or nodes experienced. The greater this disturbance the lower the efficiency factor assigned. ASCE-ACI Committee 445 offered a comprehensive review of this work.

In 1978 Nielsen introduced an efficiency factor to calibrate the concrete plasticity models they had developed for members in shear. In 1998 Chen revised these factors for deep beams and proposed the following relationship v.

$$v = \frac{0.6(1 - 0.25D)(100\rho + 2)(2 - 0.4\frac{a}{d})}{\sqrt{f'_c}} \text{ for } \begin{bmatrix} a/D \leq 0.25 \\ \rho \leq 0.02 \\ D \leq 1.0 \end{bmatrix} \text{ (SI)} \quad (2\text{-}42)$$

Where ρ was defined as the reinforcement ratio for main longitudinal steel

In 1986 Batchelor and Campbell proposed a reduction of the effective compressive strength based on their theory that the diagonal struts are in a state of biaxial tension which in turn reduced the strength of the web concrete. Based on their parametric study Bachelor and Campbell proposed the following equation be used to define the efficiency factor.

$$\ln\left(v\frac{d}{b}\right) = 3.342 - 0.1991\left(\frac{a}{d}\right) - 7.471\left(\frac{b}{d}\right) \ (SI) \tag{2-44}$$

Warwick and Foster investigated the effects of concrete strength on the efficiency factor using a range of 20 to 100MPa and proposed

$$v = 1.25 - \frac{f'_c}{500} - 0.72\left(\frac{a}{d}\right) + 0.18\left(\frac{a}{d}\right)^2 \leq 1 \ for \ a/d \leq 2 \ (SI) \tag{2-45}$$

and

$$v = 0.53 - \frac{f'_c}{500} \ for \ a/d \geq 2 \ (SI) \tag{2-46}$$

Equations 2-44 and 2-45 were developed in parametric studies using the concrete compressive strength f'_c, and the quantities of horizontal and vertical reinforcement as the variable parameters and by comparing a series of experimental data with non-linear finite element analyses. From this Warwick and Foster concluded that concrete strength and the ratio of the shear span to member depth were the main contributors that affected the efficiency factor.

Based on panel testing performed by Vecchio and Collins (1986), Collins and Mitchell proposed Equation 2-47.

$$k_3 v = \frac{1}{0.8 + 170\varepsilon_1}$$

(2-47)

where

$$\varepsilon_1 = \varepsilon x + \frac{(\varepsilon_x - \varepsilon_2)}{\tan^2 \theta}$$

(2-48)

Variables were defined as:

ε_1 = major principal strain, normal to strut

ε_2 = minor principal strain, parallel to strut

ε_x = strain in the horizontal direction

θ = angle of strut to horizontal

Foster and Gilbert demonstrated in 1996 that the relationship defined by Collins and Mitchell could be modified as a function of f'_c and the ratio a'/d. In doing so the strut angle was approximated as $tan\theta \approx d/a'$; more precisely $tan\theta \approx z/a$. This produced the result shown in Equation 2-49.

$$k_3 v = \frac{1}{1.14 + \left(0.64 + \frac{f'_c}{470}\right)\left(\frac{a}{z}\right)^2} \quad (SI)$$

(2-49)

Foster and Gilbert further simplified this equation, termed the modified Collins and Mitchell relationship, based on the insensitivity of v to f'_c to produce Equation 2-50.

$$k_3 \nu = \frac{1}{1.14 + 0.75\left(\dfrac{a}{z}\right)^2} \quad (SI)$$

(2-50)

For special situations where $a/z = 0$, i.e. $\varepsilon_l = 0$ the MCFT infers that $\nu = 1$ and thus the relationship is further modified to yield Equation 2-51.

$$\nu = \frac{1}{1. + 0.66\left(\dfrac{a}{z}\right)^2}$$

(2-51)

It must be noted that when Equation 2-51 is used $k_3 = 0.88$.

MacGregor proposed that the efficiency factor be defined by Equation 2-52

$$k_3 \nu = \nu_1 \nu_2$$

(2-52)

where

$$\nu_2 = 0.55 + \frac{1.25}{\sqrt{f'_c}} \quad (MPa)$$

(2-53)

The variable ν_l in Equation 2-52 was defined as a factor dependant on the potential of damage to the strut(s) under consideration.

Vecchio and Collins later revised their efficiency factor based on newly available data of the time to produce Equation 2-54.

$$\nu = \frac{1}{1 + k_c k_f}$$

(2-54)

where

$$k_c = 0.35\left(\frac{-\varepsilon_1}{\varepsilon_2} - 0.28\right)^{0.80}$$ (2-55)

and

$$k_f = 0.1825\sqrt{f'_c} \geq 1.0 \ \ (MPa)$$ (2-56)

Using an assumed value for ε_2 of -0.0025 and the relationship shown in Equation 2-57

$$\varepsilon_1 = \varepsilon x + \frac{(\varepsilon_x - \varepsilon_2)}{\tan^2 \theta}$$ (2-57)

The following is obtained for k_c

$$k_c = 0.35\left(0.52 + 1.8\left(\frac{a}{z}\right)^2\right)^{0.80}$$ (2-58)

For cases where $a/z = 0$ the MCFT implied an efficiency factor value of $v = 1$ and $k_f = 1.0$ and substituting Equation 2-58 into Equation 2-54 with these special case values produced Equation 2-59.

$$v = \frac{1}{0.83 + k_c k_f}$$ (2-59)

Based on the development of a reinforced concrete cracked membrane model for plane stress elements the efficiency factor define by Equation 2-60 was adopted

$$v = \frac{1}{(0.4 + 30\varepsilon_1)f'^{1/3}_c}$$ (2-60)

When the major principal strain ε_l, is treated as a function of both ε_x and $1/\tan^2 \theta$ then Equation 2-60 takes the form of Equation 2-61.

$$\nu = \frac{1}{\left[c_1 + c_2 (a/z)^2\right] f'_c{}^{1/3}} \leq 1 \qquad (2\text{-}61)$$

where c_1 and c_2 are empirically derived constants

From their review of sixteen previous studies, 135 specimens that had been determined to have failed in compression were analyzed and efficiency factors assigned based on concrete strength f'_c, multi-parameter model predictions and MCFT. Equations 2-51, 2-59 and 2-61 were compared against the experimental data and models proposed by the AS3600 model with cutoff and models proposed by Batchelor and Campbell, Chen, MacGregor and Warwick and Foster.

Two parameters were used to define the efficiency factors, f'_c and a/z and the following observations were made:

- Poor correlation with high degrees of variability existed between experimental data and efficiency factor models based solely on concrete strength f'_c

- Multi-parameter efficiency factor models also exhibited poor correlation with high degrees of variability between experimental data and predicted behavior

- MCFT models provided coefficients of variation from 0.22-0.24 when compared to the experimental data

- Boundary conditions play are a significant factor in obtaining data that is reliable and has a low degree of scatter

- Strut angle was the most significant factor and models based on the shear span to depth ratio a/z, provided the best predictions for efficiency factors

Most of the reviewed articles addressed topics other than the same two specific areas of pure flexure and deep beams covered by this thesis; this was attributable to the paucity of relevant available literature. However their inclusion was justified by the wide array of examples contained within these articles. The examples illustrated that there has always been division between the codes on approach to analysis and design as well as the actual formulae to be utilized when designing or analyzing a reinforced concrete section, member or structure.

3.0 <u>THEORY OF FLEXURE</u>

3.1 Background

In the classical approach to solving for the flexural strength of a section generally there are two assumptions required in order to provide a simplified method to the solution of the required calculations. These two assumptions form the backbone of the elastic case for flexural theory that states that normal stresses within a beam due to bending vary linearly with the distance from the neutral axis.

The assumptions are:

1) Plane sections remain plane.

2) Hooke's Law can be applied to the individual fibers within the beam section.

There are two components to the first assumption as discussed in §6.4 of Mechanics of Materials: The first component is based on rigorous mathematical solutions from the theory of elasticity that demonstrate some warpage does actually occur along plane sections and that this warpage is greatest when shear is applied along with a moment. However adjoining planes are also similarly warped and therefore the distance between any two points on adjoining sections for all practical purposes remains constant whether or not warpage is considered. Flexural theory is based upon the relative distances between sections and because it has been proven that warpage does not violate

this relationship between plane sections and the assumption that plane sections remain plane remains valid.

The second part of this assumption is that when a beam is subjected to pure bending the positive strains on the outermost tensile surface are accompanied by negative transverse strains, this curvature is classified as anticlastic curvature. Likewise the negative strains along the outermost compressive surface are accompanied by positive transverse strains; this type of curvature is classified as anti-synclastic curvature. See Figure 3-1. The classical approach to solutions of reinforced concrete sections ignore this behavior.
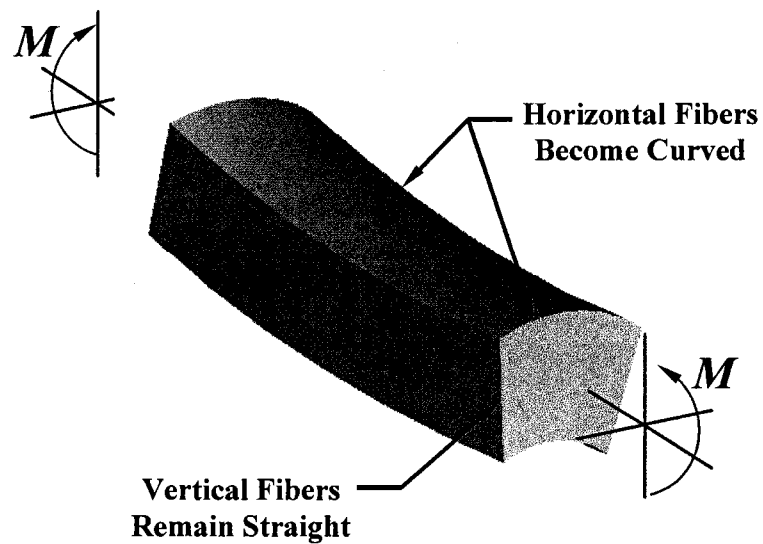

Figure 3-1 Beam in flexure with saddling effect

The second assumption, based on Hooke's law, Equation 3-1, states that individual fiber strains can be used to calculate individual fiber stresses and visa-versa.

$$\varepsilon = \frac{\sigma}{E}$$
<div align="right">(3-1)</div>

Where the variables are defined as follows:

ε = strain

E = modulus of elasticity of the material, commonly referred to as Young's Modulus

σ = stress

3.2 Theory of Flexure in Shallow Reinforced Concrete Sections

In the study of reinforced concrete additional assumptions are made in series with the first two presented; assumptions 4, 6 and 7 are generally attributed to Charles S. Whitney but they were obtained from "Design of Reinforced Concrete ACI 318-08 Code Edition" for this thesis.

3) The strain in the reinforcing steel is the same as the surrounding concrete prior to cracking of the concrete or yielding of the steel – this is a continuation of the second assumption

4) The tensile strength of concrete is negligible and assumed to be zero

5) The stress-strain curve of the steel is elastically perfectly plastic

6) The total force in the compression zone can be approximated by a uniform stress block with magnitude equivalent to $0.85 f'_c$ multiplied by a depth of a

7) The maximum allowable strain of concrete is 0.003

The general arguments that form the basis of Hooke's Law remain as valid for reinforced concrete sections as they do for isotropic homogenous material sections when subjected to small strains.

In general the tensile strength of concrete is around 10% of the compressive strength. When loaded the tension zone of a concrete section will begin to crack under very light loads destroying the continuity of the section and any tensile reinforcement will be forced to carry the tensile load in its entirety.

The assumption that the stress-strain curve of steel is elastically perfectly plastic implies that the ultimate strength of steel is equivalent to its yield strength. In effect, this results in an underestimation of the overall ultimate strength of a given section due to the reinforcing steel but it produces a more predictable mode of member failure.

The stress distribution in the compressive region does not maintain a linear relationship with respect to distance from the neutral axis due to the nature of the constituent materials used to manufacture concrete. Rather the stress distribution is in the form of a parabola as shown in Figure 3-2 c.

Whitney developed an equivalent rectangular stress block that provides results of equal accuracy for the compressive strength of a concrete section that avoids the rigorous mathematical calculations required to compute the area of a parabola. This block has

depth, a, and an average compressive strength equivalent to $0.85f'_c$. The value of 0.85

was derived from extensive laboratory testing of core test results of concrete in structures

where the concrete was a minimum of 28 days old.

To calculate the depth of the compression block the distance from the extreme

compressive fiber c, is multiplied by a modification coefficient β_l yielding the result

shown in Equation 3-2.

$$a = \beta_1 c \qquad (3\text{-}2)$$

The coefficient β_l varies as summarized in Equation 3-3.

$$\beta_1 = \begin{cases} 0.85 & for \quad f'c \le 4000\,psi \\ 0.85 - 0.05\left(\dfrac{f'c - 4000}{1000}\right) & for \quad 4000 < f'c \le 8000\,psi \\ 0.65 & for \quad f'c > 8000\,psi \end{cases} \qquad (3\text{-}3)$$

The ACI has adopted a strain of 0.003 in the extreme compressive fiber as the

assumed maximum allowable strain, or limit strain, for a concrete section. Compared

with results determined from extensive empirical data this value represents the lower

bound of the limit strain.

Using these seven basic assumptions a series of equations can be derived that

provide quantitative values for the equivalent, counteracting force required for a beam to

remain in equilibrium while under the application of an external force. This can be

explained by visualizing the two forces as vectors, equal in magnitude and opposite in

direction, acting at any two locations along the centerline of the cross section. Summing

the forces in the axial direction $T = C$, i.e. the tensile forces provided by the

reinforcement present in a section are opposite and equal to the sum of the compressive

force provided by the concrete; reference Equations 3-4 through 3-8.

$$T = A_s f_y \tag{3-4}$$

$$C = 0.85 f'_c \beta_1 cb \tag{3-5}$$

where

$$a = \beta_1 c \tag{3-6}$$

$$\therefore c = a / \beta_1 \tag{3-7}$$

$$T = C \Rightarrow A_s f_y = 0.85 f'_c ab \tag{3-8}$$

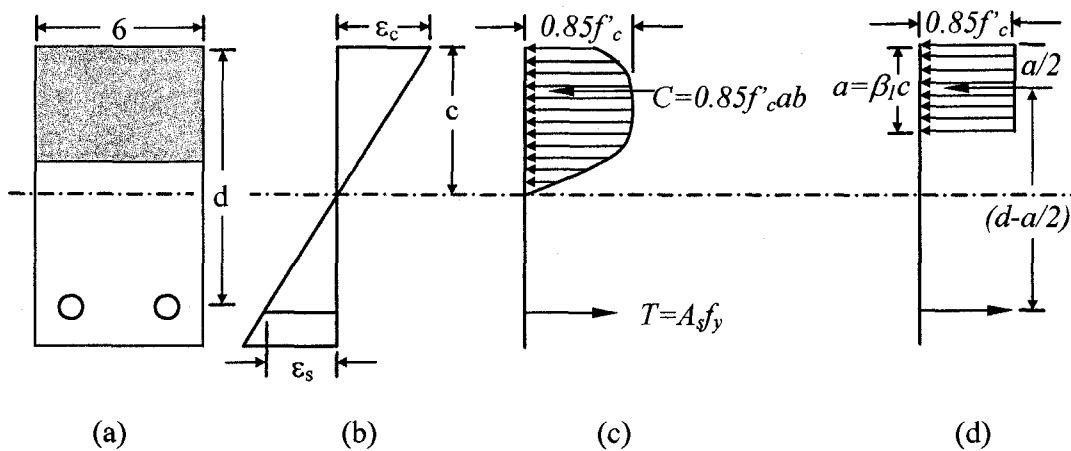(a)   (b)   (c)   (d)

Figure 3-2 Graphic representation of forces within a reinforced concrete section

Variables are defined as:

a = effective depth of the compressive block

A_s = area of non-prestressed steel

f_y = yield strength of non-prestressed steel

f'_c = compressive strength of the concrete

b = the width of the section

c = distance from extreme compressive fiber to neutral axis

Using the relationships show in Equations 3-4 through 3-8 and solving for a yields the result shown in Equation 3-9.

$$a = \frac{A_s f_y}{0.85 f'_c b} \qquad (3\text{-}9)$$

Solving for the internal resisting couple between the tensile and compressive forces yields the nominal strength or moment resistance of the section M_n, shown in Equation 3-10.

$$M_n - A_s f_y \left(d - \frac{a}{2} \right) = 0.85 f'_c \, ab \left(d - \frac{a}{2} \right) \qquad (3\text{-}10)$$

3.3   Theory of Flexure in Deep Beams

Deep beams are a common structural member for which an accurate solution cannot be reached using the aforementioned techniques. Deep beams are structural members defined by the relationship between beam width b_w, beam depth h and clear

span l_n. Per ACI 318-08 §10.7.1, deep beams are members loaded on one face and supported on the opposite face so that compression struts can develop between the loads and the supports and have either:

  a) clear spans l_n, equal to or less than four time the overall member depth; or,

  b) regions with concentrated loads within twice the member depth from the face of the support

Deep beams or deep beam regions begin to show crack propagation at loads in the range of $^1/_3P_u$ to $^1/_2P_u$, where P_u represents the concentrated load, and plane sections are no longer assumed to remain plane. This invalidates the first and most fundamental assumption discussed in this paper for the solution of reinforced sections. Therefore other more advanced methods must be employed. One of these is the method of Strut-and-Tie Model (STM) an inherently conservative method for solving the forces within these member's sections. The overarching motivation of STM is weighted toward conservatism in the solutions it provides and to transfer as much of the applied loading as possible into compression using the fewest number of members.

The foundations of STM are attributed to the truss method work done by Ritter in 1899 developed as a means to explain the dowel action of stirrup reinforcement. However it was not until the 1980s that the truss method transformed into STM and was used to find solutions for the discontinuous regions within deep beams.

The method of strut and tie models is not exclusively limited to deep beams, it also has valid applications in corbels, dapped-end beams and the discontinuous regions, or D-regions, within shear spans. Mathematically a D-region is defined as a region located within a distance equal to the member depth h, from the beam/support interface or a region located a distance h from each side of a concentrated load; reference Figure 3-3 for examples.

(a) Geometric discontinuities

(b) Loading and geometric discontinuities
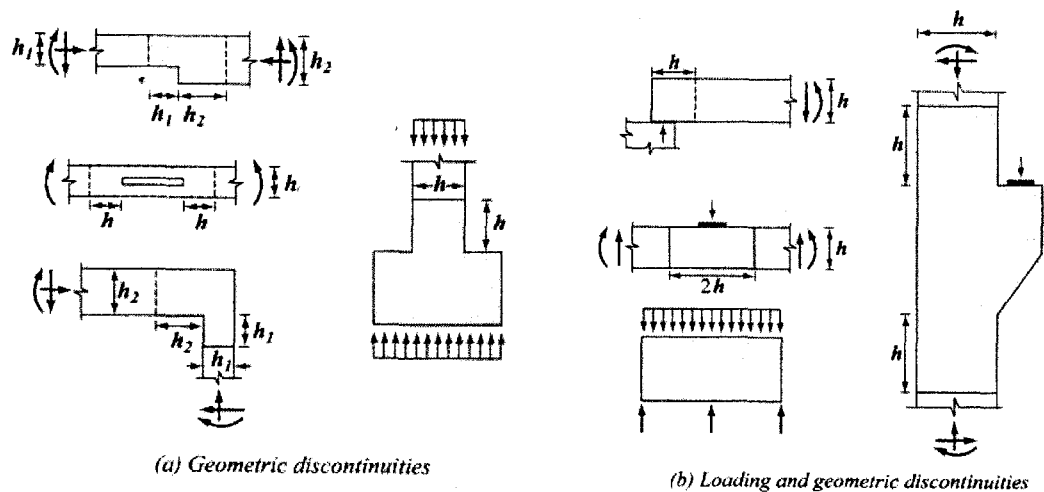
Figure 3-3 ACI 318-08 Fig. RA.1.1 (a and b) – D-regions and discontinuities (Reprinted with permission from the American Concrete Institute)

A D-region within a beam is defined as an inter-beam span where traditional moment and shear strength theory no longer applies as based on the assumption that plane sections remain plane, and loads are not reacted by beam action but rather they are reacted primarily by arch action, as such these D-regions can be isolated and viewed as a

deep beam. In these regions the ratio of shear deformations to flexural deformations can no longer be considered negligible.

At its core STM disregards kinematic restraints, only gives an estimation of member strength, and it conforms to the lower boundary of theory of plasticity, i.e. only equilibrium and yield conditions need be satisfied. The solutions for the capacity of members found using the application of this lower bound theory are estimates that will provide member capacities which will be less than or equal to the load required to fail the member; thus the inherently conservative nature of STM solutions.

The two greatest similarities between the ACI 318-08 and AASHTO LRFD code provisions are the basic set up of the solution, and how the truss members are chosen. After the global forces have been determined for a particular member, a truss model is chosen to represent the flow of forces within that member. The goal for development of any truss model is to use the lowest number of members required to satisfy equilibrium and safely transmit the forces into the supports. After a truss model has been developed the forces within that truss are analyzed by using the method of joints, the method of sections, a combination of both or using a CAD program.

Members in compression are designated struts and members in tension are designated ties. The intersection of any two or more members is designated a node, as shown in Figure 3-4.

(a) CCC Node (b) CCT Node
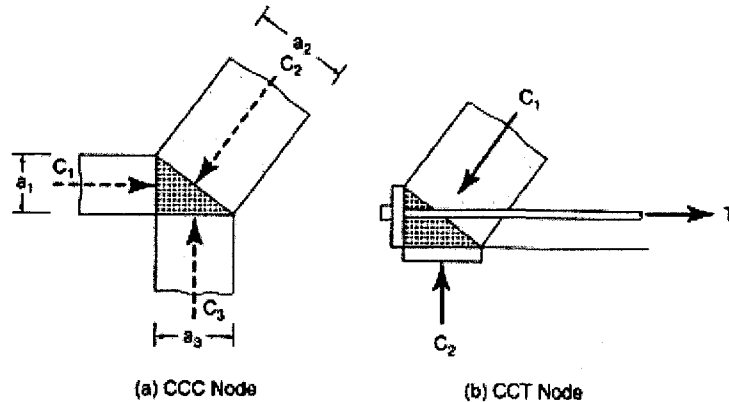
**Figure 3-4 ACI 318-08 Fig. RA.1.5 (a and b) - Hydrostatic nodes
(Reprinted with permission from the American Concrete Institute)**

There are few similarities that exist between the ACI 318-08 and AASHTO

LRFD codes with respect to STM efficiency factors. The basic premise for the

implementation of the method using either code is the same but the way that these forces

are resolved within the individual strut and nodal members is the area of greatest

divergence between the two codes. § 4.2 provides a comprehensive explanation of the

differences in the STM between the ACI 318-08 and the AASHTO LRFD 2nd Ed. and §

5.2 discusses the differences in the results obtained from each code.

4.0 <u>ANALYTICAL PROCEDURE</u>

4.1   Shallow Beams

In order to simplify the programming phase of the project, an analytical approach was used rather than a design approach. Doing so reduced the required number of IF logic statements, shortened the overall length of the EXCEL program, simplified the program used and focused the project on the analysis of results rather than programming. All spreadsheets used in the shallow beam analysis were vetted via direct comparison against example problems 7.4 and 7.5 from the Notes on ACI 318-08 Building code Requirements for Structural Concrete. Results from the spreadsheets matched those in the example problems exactly.

Each series of analytical calculations were performed using sections having similar geometric and identical material properties. The yield strength of the reinforcing steel f_y, was set at 60ksi and the crushing strength of the concrete f'_c, was set at 4ksi. Ten different geometries were analyzed in a series of four different calculations with each calculation using three different values for the following variables; flange width b, web width b_w, flange depth t_f, and the depth of reinforcement d. Ten arbitrary sections with the following geometries, graphically described in Figure 4-1, were chosen for analysis.
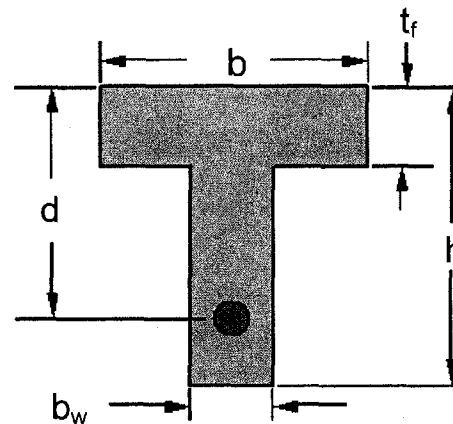
Figure 4-1 Section geometry

The values used for each variable's analytical case are listed below in Table 4-1.

Table 4-1 Values for variable and fixed geometry for each case

VARIABLE VALUES		FIXED GEOMETRY	
b	36in.	t_f	4in.
	42in.	b_w	14in.
	54in.	d	24in.
b_w	14in.	b	36in.
	18in.	t_f	4in.
	21in.	d	24in.
d	24in.	b	36in.
	30in.	b_w	14in.
	36in.	t_f	4in.
t_f	2in.	b	36in.
	6in.	b_w	14in.
	10in.	d	24in.

For each case the assumed area of provided reinforcing steel was varied from zero to an arbitrary value of 20 square inches. This was accomplished in incremental steps of 0.50 square inches. However only data within and inclusive of the boundaries determined by A_{smin} and A_{smax} would be considered for final analysis.

Because each code specifies a unique analytical procedure, the focal crux of this paper, separate programming approaches were required for both the ACI 318-08 and the AASHTO LRFD in order to reach solutions. Each procedure is described in detail in the following sections.

4.1.1 Stress Block Depth Factor β_1

The sole quantity that was independent of the code provision used and could be calculated simultaneously was the stress block depth factor, β_1. Used in computation of the location of the neutral axis the method for computing the value of β_1, is identical for both ACI 318-08 and AASHTO LRFD codes and was computed using a simple nested IF statement as described in Figure 4-2 below.
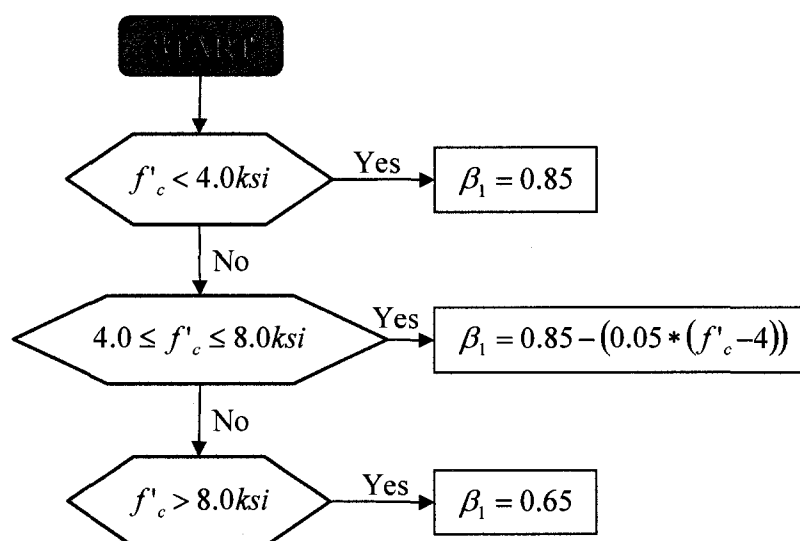

Figure 4-2 IF logic statement for computation of stress block depth factor β_1

4.1.2   ACI 318-08

4.1.2.1   Limits of Reinforcement

As defined by ACI 318-08 the minimum area of reinforcement A_{smin}, is the maximum value of the following two equations; both of which are functions of section geometry, the yield strength of reinforcement and the crushing strength of concrete.

$$A_{s\,min} = Maximum\left[\left(\left(\frac{3\sqrt{f'_c}1000}{f_y 1000}\right)b_w d\right), \left(\left(\frac{200}{f_y 1000}\right)b_w d\right)\right]$$ (4-2)

ACI 318-08 defines the maximum area of reinforcement A_{smax}, as a fraction of the balanced area of steel for a section.

$$A_{s\,max} = 0.63375 A_{sbal}$$ (4-3)

Where the balanced area of reinforcement A_{sbal}, is computed as shown in Equation 4-4. A_{sbal} is also a function of section geometry, yield strength of reinforcement f_y, stress block depth factor β_1, and the crushing strength of concrete f'_c.

$$A_{sbal} = 0.85\left(\frac{f'_c}{f_y}\right)\left((b - b_w)t_f + 0.375\beta_1 b_w d\right)$$ (4-4)

4.1.2.2 Location of Neutral Axis c and Depth of Compressive Block a

The ACI 318-08 utilizes a variable called the reinforcement index ϖ, based on the ratio of reinforcement and computed as shown in Equation 4-5.

$$\varpi = \frac{A_s f_y}{b d f'_c} = \rho \frac{f_y}{f'_c} \tag{4-5}$$

ϖ was used to evaluate the preliminary value for the depth of the compressive section, denoted in this paper as a' for clarity, as shown in Equation 4-6.

$$a' = 1.18\varpi d \tag{4-6}$$

This preliminary value a' was used in the calculation of the preliminary depth of the neutral axis which has been denoted in this paper for clarity as c' shown in Equation 4-7.

$$c' = \frac{a'}{\beta_1} \tag{4-7}$$

Both of these preliminary values were used only for the evaluation of section behavior via comparison to the flange depth t_f, i.e. the determination as to whether the section was in rectangular action or flanged action and therefore if the web carried any compressive load.

These preliminary results for a' and c' determined the method used to calculate the working value for the depth of the compressive section a, and the working value for

the depth of the neutral axis c, by means of IF logic statements. The grayed out cells on the left hand side of the flow chart in Figure 4-6 offers a comprehensive view of this procedure.

After a value for the depth of the compressive section a, had been obtained and the depth of the neutral axis c, had been established, an IF statement was used to determine whether the section behaved under T-section or rectangular action, i.e. if the depth of the compressive section was greater than or equal to the flange depth $a \leq t_f$. This in turn provided the appropriate formula to solve for the factored moment capacity for the section. See Figure 4-6.

4.1.2.3 Strength Reduction Factor ϕ

The depth of the neutral axis was also used in the determination of the strength

reduction factor ϕ based on ACI 318-08 reproduced below in Figure 4-3.
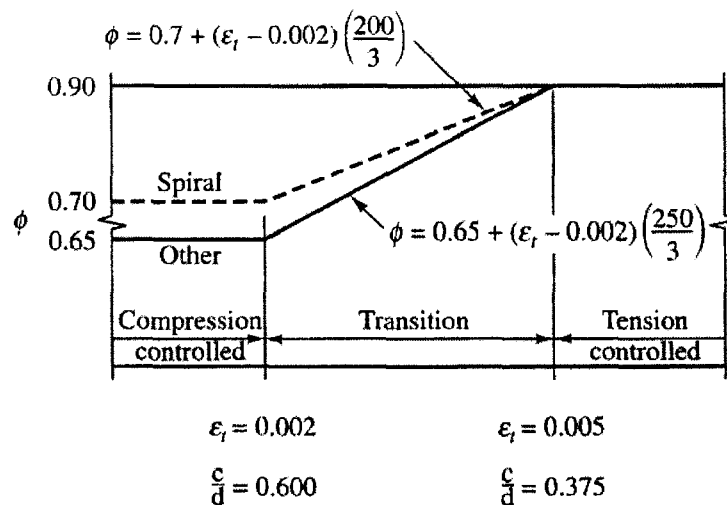
**Figure 4-3 ACI 318-08 Fig. R9.3.2 - Strength reduction factor
(Reprinted with permission from the American Concrete Institute)**

Another nested IF statement was used within the Excel program to determine this

value as shown in Figure 4-4.

The moment capacity could then be computed using the given values for A_s,

section geometry, f_y, f'_c, and the calculated values for c, β_1, and if required the web and

flange moment capacities, M_{n1} and M_{n2} respectively. A sample Excel worksheet is shown

in Figure 4-5.

Figure 4-6 shows the preliminary calculations which were contained in hidden cells, these cells are represented by lightly shaded columns. This procedure is illustrated by the flowchart in Figure 4-7.
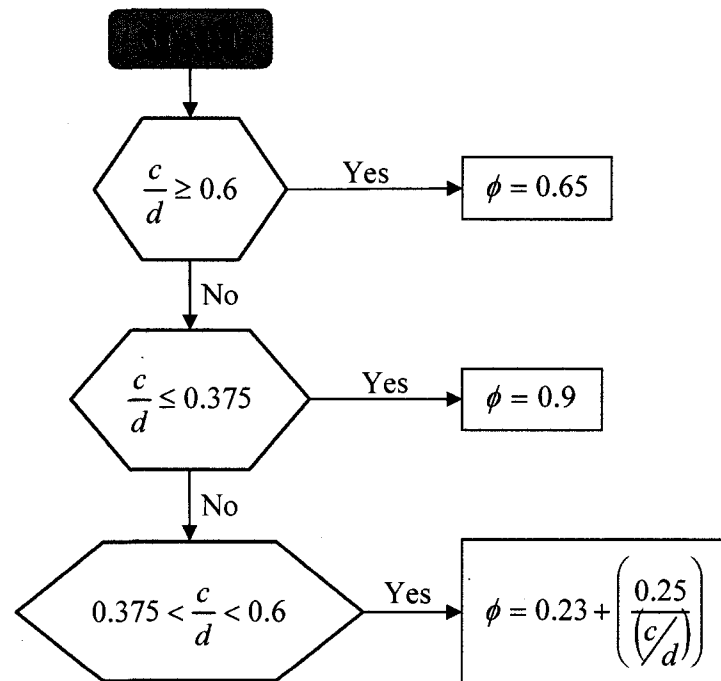

Figure 4-4 ACI 318-08 calculation of strength reduction factor ϕ

ACI 318-05					
	Moment k*in.	As	c	a	c/d	φ, Bending
	0.0	0.000	0.000	0.000	0.000	0.900
	644.7	0.500	0.288	0.245	0.012	0.900
	1282.8	1.000	0.577	0.490	0.024	0.900
As_{min}	1362.1	1.063	0.613	0.521	0.026	0.900
	1914.2	1.500	0.865	0.735	0.036	0.900
	2539.1	2.000	1.153	0.980	0.048	0.900
	3157.3	2.500	1.442	1.225	0.060	0.900
	3768.9	3.000	1.730	1.471	0.072	0.900
	4373.9	3.500	2.018	1.716	0.084	0.900
	4972.2	4.000	2.307	1.961	0.096	0.900
	5564.0	4.500	2.595	2.206	0.108	0.900
	6149.1	5.000	2.884	2.451	0.120	0.900
	6727.6	5.500	3.172	2.696	0.132	0.900
	7299.5	6.000	3.460	2.941	0.144	0.900
	7864.8	6.500	3.749	3.186	0.156	0.900
$c>=t_f$	8352.3	6.936	4.000	3.400	0.167	0.900
	8423.5	7.000	4.037	3.431	0.168	0.900
	8975.5	7.500	4.325	3.676	0.180	0.900
	9520.9	8.000	4.614	3.922	0.192	0.900
$a>=t_f$	9894.1	8.160	4.706	4.000	0.196	0.900
	10057.3	8.500	5.210	4.429	0.217	0.900
	10577.3	9.000	5.952	5.059	0.248	0.900
	11080.2	9.500	6.693	5.689	0.279	0.900
	11566.1	10.000	7.435	6.319	0.310	0.900
	12034.9	10.500	8.176	6.950	0.341	0.900
	12486.8	11.000	8.917	7.580	0.372	0.900
As_{max}	12536.0	11.056	9.000	7.650	0.375	0.900

Figure 4-5 Sample excel spreadsheet analysis

	Asf	Mn1	Mn2	ω	a	c
			ACI 318-05			
	4.987	-7180.80	6582.40	0.000	0.000	0.000
	4.987	-6427.81	6582.40	0.009	0.246	0.289
	4.987	-5682.17	6582.40	0.017	0.492	0.578
As$_{min}$	4.987	-5989.45	6582.40	0.018	0.622	0.616
	4.987	-4943.89	6582.40	0.026	0.738	0.868
	4.987	-4212.96	6582.40	0.035	0.983	1.157
	4.987	-3489.38	6582.40	0.043	1.229	1.446
	4.987	-2773.15	6582.40	0.052	1.475	1.735
	4.987	-2064.28	6582.40	0.061	1.721	2.025
	4.987	-1362.76	6582.40	0.069	1.967	2.314
	4.987	-668.59	6582.40	0.078	2.213	2.603
	4.987	18.22	6582.40	0.087	2.458	2.892
	4.987	697.68	6582.40	0.095	2.704	3.181
	4.987	1369.79	6582.40	0.104	2.950	3.471
	4.987	2034.54	6582.40	0.113	3.196	3.760
c>=t$_f$	4.987	2608.21	6582.40	0.120	3.410	4.012
	4.987	2691.95	6582.40	0.122	3.442	4.049
	4.987	3341.99	6582.40	0.130	3.688	4.338
	4.987	3984.69	6582.40	0.139	3.933	4.627
a>=t$_f$	4.987	4185.80	6582.40	0.142	4.012	4.720
	4.987	4592.43	6582.40	0.148	4.179	4.917
	4.987	5170.12	6582.40	0.156	4.425	5.206
	4.987	5728.90	6582.40	0.165	4.671	5.495
	4.987	6268.77	6582.40	0.174	4.917	5.784
	4.987	6789.74	6582.40	0.182	5.163	6.074
	4.987	7291.80	6582.40	0.191	5.408	6.363
As$_{max}$	4.987	7346.52	6582.40	0.192	5.435	6.395

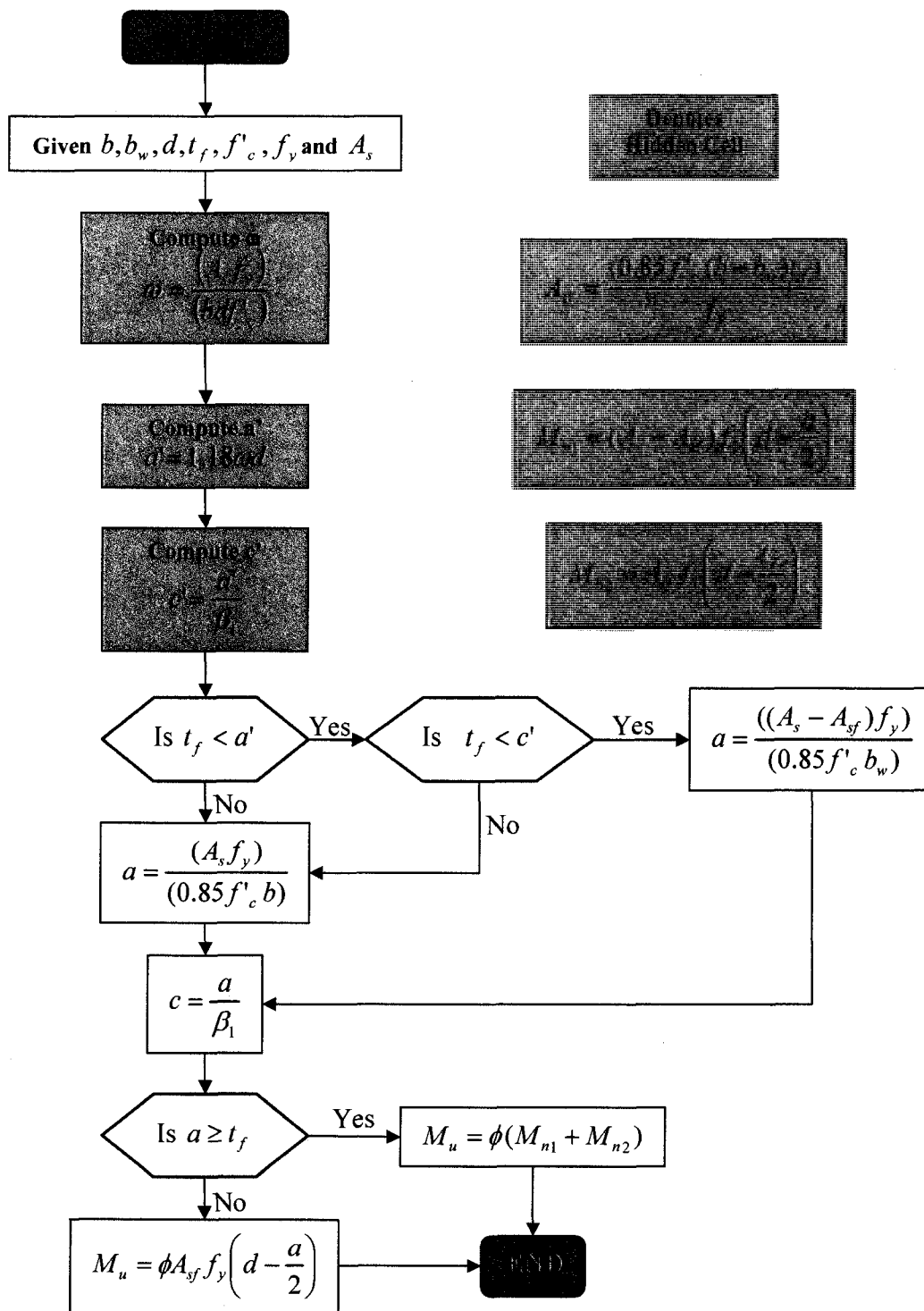Figure 4-6 Sample excel spreadsheet showing preliminary ACI 318-08 calculations

Given $b, b_w, d, t_f, f'_c, f_y$ and A_s

Compute a
$a = \dfrac{(A_s f_y)}{(bd f'_c)}$

Compute a'
$a' = 1.18 \omega d$

Compute c'
$c' = \dfrac{a'}{\beta_1}$

$A_{sf} = \dfrac{(0.85 f'_c (b - b_w) t_f)}{f_y}$

$M_{n1} = (A_s - A_{sf}) f_y \left(d - \dfrac{a}{2}\right)$

$M_{n2} = A_{sf} f_y \left(d - \dfrac{t_f}{2}\right)$

Is $t_f < a'$ — Yes → Is $t_f < c'$ — Yes → $a = \dfrac{((A_s - A_{sf}) f_y)}{(0.85 f'_c b_w)}$

No (from $t_f < a'$): $a = \dfrac{(A_s f_y)}{(0.85 f'_c b)}$

No (from $t_f < c'$) → $a = \dfrac{(A_s f_y)}{(0.85 f'_c b)}$

$c = \dfrac{a}{\beta_1}$

Is $a \geq t_f$ — Yes → $M_u = \phi(M_{n1} + M_{n2})$ → END

No → $M_u = \phi A_{sf} f_y \left(d - \dfrac{a}{2}\right)$ → END

Figure 4-7 ACI 318-08 excel program logic flowchart

4.1.3   AASHTO LRFD

4.1.3.1   Limits of Reinforcement

The procedure for determining A_{smin} as specified by AASHTO LRFD Equation

5.7.3.3.2-1 did not require the use of any IF logic statements and was determined as

shown in Equation 4-8.

$$A_{s\min} = 0.7 b_w d \left(\frac{f'_c}{f_y} \right)$$
(4-8)

However, determination of the AASHTO LRFD value for A_{smax} did require an IF

statement that was dependent on the value calculated for the maximum depth of neutral

axis c. AASHTO LRFD § 5.7.3.3.1 defines the limitation for maximum reinforcement as

follows:

> 5.7.3.3.1 Maximum Reinforcement
> The maximum amount of prestressed and nonprestressed reinforcement
> shall be such that:
>
> $$\frac{c}{d_e} \leq 0.42 \qquad (5.7.3.3.1\text{-}1)$$
>
> in which:
>
> $$d_e = \frac{A_s f_y d_s + A_{ps} f_{ps} d_p}{A_s f_y + A_{ps} f_{ps}} \qquad (5.7.3.3.1\text{-}2)$$
>
> where:
> c = the distance from the extreme compressive fiber to the neutral
> axis (in.)
>
> d_e = the corresponding effective depth from the extreme
> compressive fiber to the centroid of the tensile force in the tensile
> reinforcement (in.)
>
> If Equation 1 is not satisfied the section shall be considered to be
> overreinforced.

The final statement leads to the conclusion that is summed up mathematically in Equation 4-9, also reference Figure 4-9.

$$\frac{c}{d} > 0.42 \rightarrow \text{Overreinforced} \qquad (4\text{-}9)$$

Setting AASHTO LRFD Equation 5.7.3.3.1-1 equivalent to Equation 4-9 and using the known depth for the centroid of reinforcement the maximum value for the depth of the neutral axis for a section while remaining underreinforced can be found simply, as shown in Equation 4-10. For clarity within this paper this preliminary value for c will be denoted max$c$.

$$\max c = 0.42d \qquad (4\text{-}10)$$

Using one of the two approaches described in detail in §4.1.3.2 and solving for c one can readily determine the limiting area of reinforcement allowed.

4.1.3.2 Location of Neutral Axis c, and Depth of Compressive Block a

The AASHTO LRFD code provides two methods of determining the depth of the neutral axis; the conservative approach and the refined approach.

When using the refined approach the method used to determine the depth of the neutral axis is based on the action experienced by the section, i.e. whether or not the beam is under rectangular action or T-section action.

If the beam is under T-section action then c is computed as shown in Equation 4-11.

$$c = \frac{A_s f_y - A_{s'}|f_{y'}| - 0.85 f'_c \beta_1 (b - b_w) h_f}{0.85 f'_c \beta_1 b_w}$$

(4-11)

Otherwise c is computed by the method described as the conservative approach which is identical to the method used by ACI 318-08, reference Equation 4-12. The gray box in Figure 4-11 highlights this process within the overall AASHTO LRFD analytical procedure.

$$c = \frac{A_s f_y - A_{s'}|f_{y'}|}{0.85 f'_c \beta_1 b}$$

(4-12)

All AASHTO LRFD analysis performed and discussed in this paper utilized the refined approach during the calculation of the depth of the neutral axis and an EXCEL IF statement was programmed using the value for *maxc* from Equation 4-10 as shown in Figure 4-8.
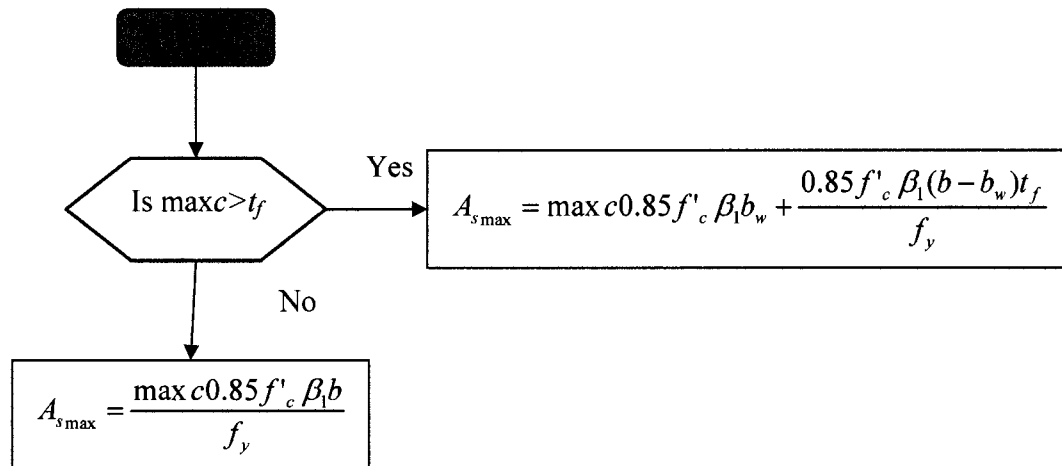
Figure 4-8 Determination of AASHTO LRFD A_{smax}

4.1.3.3 Strength Reduction Factor ϕ

The strength reduction factor ϕ, as defined by AASHTO LRFD also uses the limit of A_{smax} to determine its value. If the area of reinforcement is less than A_{smax} then $\phi = 0.9$, otherwise $\phi = 0.7$. See Figure 4-9.
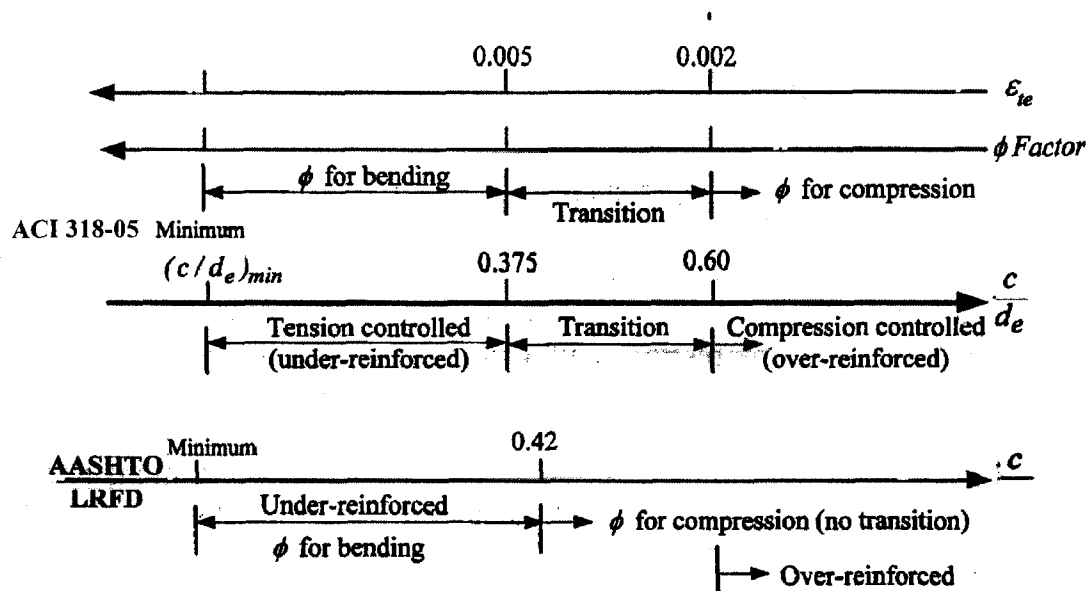
Figure 4-9 AASHTO LRFD and ACI 318-08 limits of reinforcement

The AASHTO LRFD moment capacity was computed using the identical values for A_s,

section geometry, reinforcement yield strength f_y, and concrete crushing strength f'_c, as

for the ACI 318-08 test cases along with the AASHTO LRFD specific calculated values

for depth of neutral axis c, and strength reduction factor ϕ. A sample EXCEL worksheet

is shown in Figure 4-10 and Figure 4-11 illustrates this procedure by means of a

flowchart.

	AASHTO - LRFD						
	Moment		C				
	k*in.	As	kip	c	a	c/d$_e$	ϕ, Bending
	0.0	0.000	0.0	0.000	0.000	0.000	0.9
	644.7	0.500	30.0	0.288	0.245	0.012	0.9
As$_{min}$	864.9	0.672	40.3	0.388	0.329	0.016	0.9
	1282.8	1.000	60.0	0.577	0.490	0.024	0.9
	1914.2	1.500	90.0	0.865	0.735	0.036	0.9
	2539.1	2.000	120.0	1.153	0.980	0.048	0.9
	3157.3	2.500	150.0	1.442	1.225	0.060	0.9
	3768.9	3.000	180.0	1.730	1.471	0.072	0.9
	4373.9	3.500	210.0	2.018	1.716	0.084	0.9
	4972.2	4.000	240.0	2.307	1.961	0.096	0.9
	5564.0	4.500	270.0	2.595	2.206	0.108	0.9
	6149.1	5.000	300.0	2.884	2.451	0.120	0.9
	6727.6	5.500	330.0	3.172	2.696	0.132	0.9
	7299.5	6.000	360.0	3.460	2.941	0.144	0.9
	7864.8	6.500	390.0	3.749	3.186	0.156	0.9
c>=t$_f$	8283.7	6.936	416.2	4.000	3.400	0.167	0.9
	8354.7	7.000	420.0	4.095	3.481	0.171	0.9
a>=t$_f$	8805.5	7.412	444.7	4.706	4.000	0.196	0.9
	8900.2	7.500	450.0	4.836	4.111	0.202	0.9
	9428.7	8.000	480.0	5.578	4.741	0.232	0.9
	9940.2	8.500	510.0	6.319	5.371	0.263	0.9
	10434.7	9.000	540.0	7.061	6.002	0.294	0.9
	10912.1	9.500	570.0	7.802	6.632	0.325	0.9
	11372.5	10.000	600.0	8.544	7.262	0.356	0.9
	11816.0	10.500	630.0	9.285	7.892	0.387	0.9
	12242.4	11.000	660.0	10.027	8.523	0.418	0.9
As$_{max}$	12272.4	11.036	662.2	10.080	8.568	0.420	0.9

Figure 4-10 Sample excel spreadsheet for AASHTO LRFD analysis
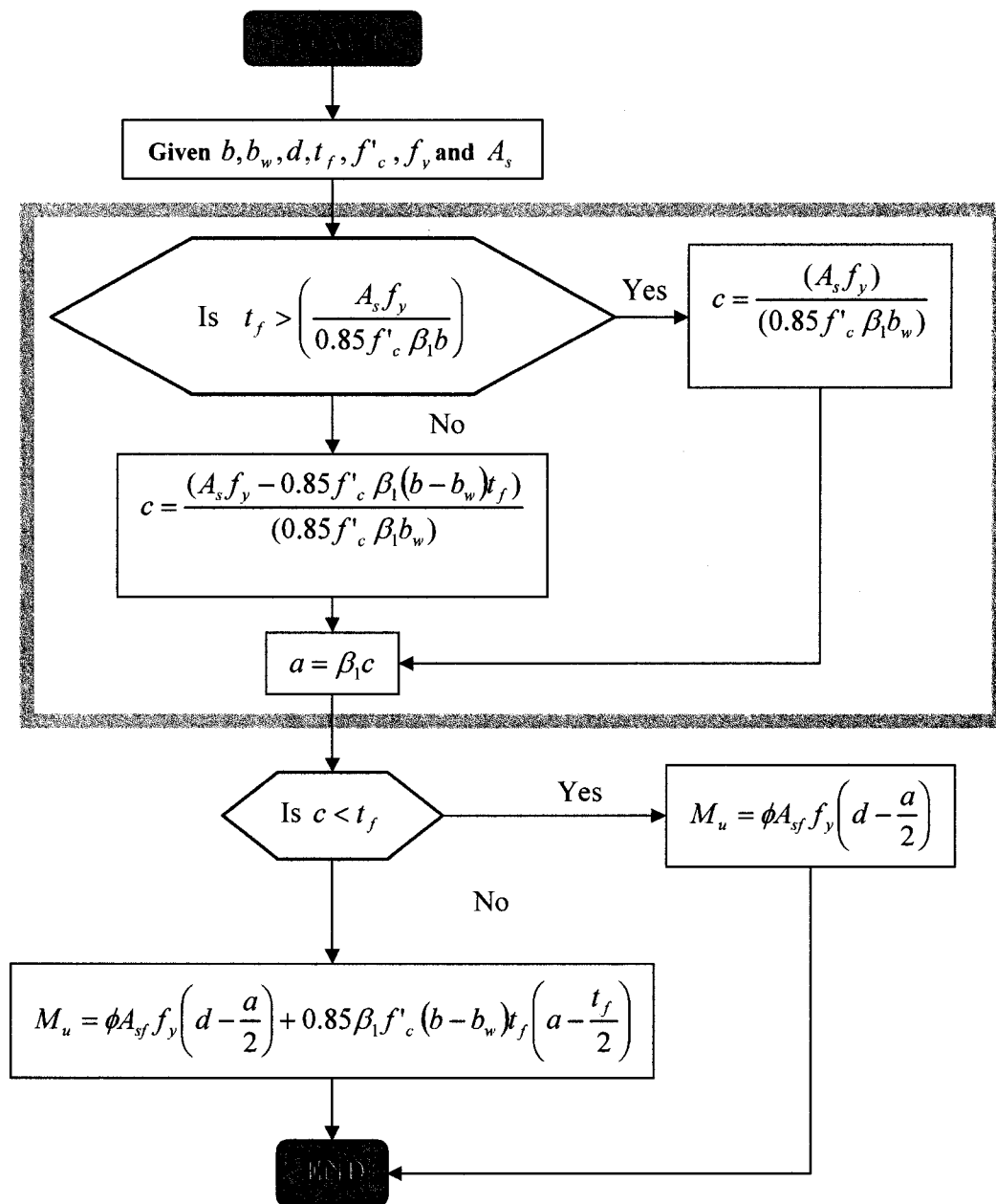
Figure 4-11 AASHTO LRFD flowchart

4.2 STM

4.2.1 Introduction

Each series of deep beams was analyzed using the STM method as described by both the ACI 318-08 and AASHTO LRFD 2nd Ed. code provisions. Results were then compared to the work performed by Ha on identical sections and compared as a percentage of the maximum allowable load to the test load.

The solutions for this series of beams were worked in three phases; first a graphical STM solution was solved to determine the maximum allowable strut and tie member sizes, then the truss geometries from the first step were solved for using a unit load and classical hand calculations; finally an EXCEL spreadsheet created specifically to solve for the STM model element capacities (struts and ties) based on the previously defined geometry from step 1 was utilized. This spreadsheet then converted the unit load into an equivalently proportioned maximum allowable service load which led to the final solution to the problem.

Concrete strength was assumed to be 7ksi, the lowest value used by Ha, and reinforcing steel strength was assumed to be 60ksi. Geometric section properties were matched to those used by Ha with identical beam sections measuring 44in. x 36in. x 4in. The location of the openings was specific to each series and constituted the only variable

within this problem the locations of which matched those used by Ha. Reference Figure

4-12 and Table 4-2.
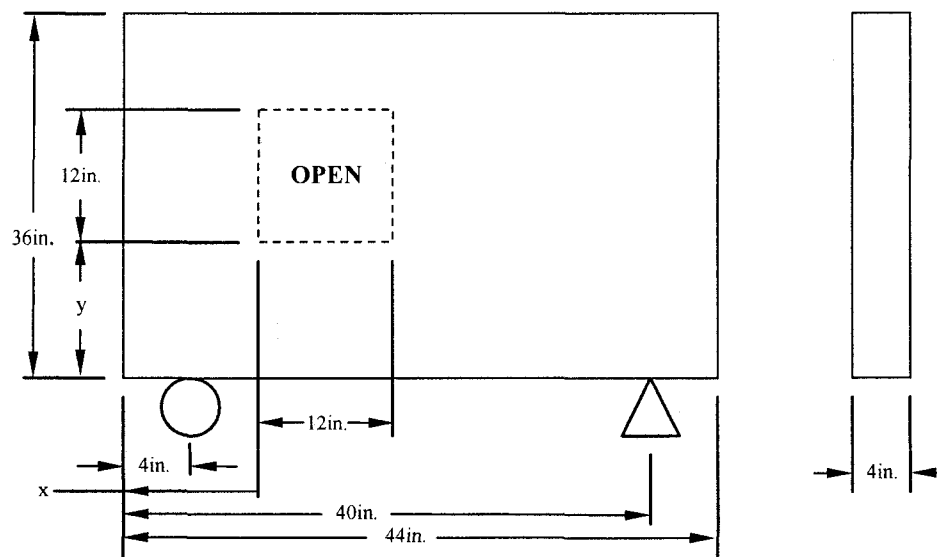
Figure 4-12 Generic beam with and without opening

Table 4.2.1-1 lists the values used for the x and y coordinates of the lower left

corner of the 12in. x 12in. cutout.

Table 4-2 Cutout locations from lower left corner in inches

Opening Location		
	x	y
SERIES 1	N/A	N/A
SERIES 2	16	12
SERIES 3	16	8
SERIES 4	16	16
SERIES 5	20	12

The method of STM analysis as employed for purposes of this thesis were for all intents and purposes identical.

Use was made of Naaman's proposal regarding the compressive strength of concrete that "...the value of f_{cu} recommended by ACI in Equation (15.7) and Table 15.1 is appropriate enough, given the uncertainty on the evaluation of the state of strain in the struts."

For completeness Equation 15.7 from the Naaman text reads:

$$f_{cu} = \text{smaller of } 0.85\beta_s f'_c \text{ or } 0.85\beta_n f'_c \tag{4-13}$$

This upper limit of the effective strength as defined by the AAHTO LRFD of $0.85\beta_n f'_c$ was used for all AASHTO LRFD based STM calculations performed in this paper.

This assumptions greatly reduced the complexity of many of the iterative steps required during the analytical process; when these assumptions were used the method of STM as described by both ACI 318-08 and AASHTO LRFD 2nd Ed. outside of the values for strength reduction factors was identical; the strength reduction factors remained unique to each code.

4.2.1.1   Graphical Solution

Pro/E 3-D design software was utilized to provide true scale models and drawings of each deep beam section to ensure that the largest possible strut and tie members had been placed in the section. Geometric model constraints were used to ensure that no strut possessed cross sectional area greater than that of any adjacent node and that all STM members remained prismatic. See Appendix A – Deep Beam STM Models, Figures A-1 through A-5.

It should be noted that Figures A-2 through A-5 are unstable trusses; that is they do not satisfy all of the necessary requirements for a stable and determinate structure. The convention for calculating the determinacy and stability of a structure is shown below.

$$r + b = 2n \quad \text{Stable and Determinate} \tag{4-14}$$

$$r + b > 2n \quad \text{Stable and Indeterminate} \tag{4-15}$$

$$D = r + b - 2n \quad \text{Degree of Indeterminacy} \tag{4-16}$$

$$r + b < 2n \quad \text{Unstable} \tag{4-17}$$

With variables defined as:

r = number of reactions

b = number of beams/truss members

n = number of nodes

Using Figure A-2 as an example one can see that the number of members is 9, the number of reactions is 3 and the number of nodes is 7. Therefore r + b = 3 + 9 < 2*7 demonstrating that the structure is unstable. Due to the symmetry of the truss models unique solutions for each member were possible. A thorough examination of "Examples for the Design of Structural Concrete with Strut and Tie Models" reveals that many effective STM models are not considered stable truss structures when evaluated using Equation 4-17; but they are symmetric trusses and provide satisfactory support because the members are confined by the surrounding concrete. However, for the asymmetric truss model shown in Figure B-6 this is not the case and unique solutions for each member were not found.

4.2.1.2 Hand Calculations

After the truss geometry had been determined as shown in Appendix B – Deep Beam STM Truss Models Figures B-1 through B-5, the individual truss member forces were solved for using a unit load, basic equations of equilibrium and the method of joints. Results from these calculations were used as the input into the EXCEL Spreadsheets. See Appendix C – STM Truss Free Body Diagrams & Solutions Series 1 through Series 5.

4.2.1.3 Excel Spreadsheets

A series of Excel spreadsheets was developed that used concrete strength $f'c$, strength reduction factor(s) ϕ, reinforcement yield strength f_y, and beam member

geometry as inputs to calculate the maximum concentrated load that could be applied. An iterative process that determined STM applicability was used, i.e. after all maximum equivalent forces had been determined and converted into a single point load placed at the midsection of the beam the validity of $V_u \leq \phi V_n$ was checked. If the criteria of $V_u \leq \phi V_n$ was met then the magnitude of the maximum point load was considered acceptable.

Spreadsheet logic flow followed the procedure shown in Figure 4-12 and verification of the strut capacity at midlength and nodal interface was computed using the code specific relationship details described in Table 4-3.

For all cases documented for this thesis all struts were treated as bottle shaped with the cross sectional area at strut midlength assumed to be greater than the maximum area available at the strut-node interface.

Unit load values found during the hand analysis portion were input into the spreadsheet and the minimum required member width was determined using $P_r = \phi P_n$ and $P_n = f_{cu} A_{cs}$, where P_r is the calculated force within the strut member, A_{cs} represents the cross sectional area of the strut and $f_{cu} = 0.85 f'c \min(\beta_n, \beta_s)$. Since member depth was held constant at 4.0 inches to remain consistent with Ha's experimental beams the specific version of the equation used was,

$$w_{\min} = \frac{P_n}{4.0in.0.85 f'c \min(\beta s, \beta n)} \tag{4-18}$$

The minimum required "unit width" calculated from Equation 4-18 was then divided into the maximum attainable widths as determined using Pro/E to obtain the percentage increase available. The limiting case was selected and used to calculate the individual member forces. This value was then used with the previously worked hand solutions and converted into the maximum applied concentrated load, to be compared against the test loads used by Ha in his work. These comparisons formed the basis of this portion of this thesis.

4.2.2 ACI 318-08 vs. AASHTO LRFD

As shown in Table 4-3 the effective concrete compressive strength f_{cu}, is calculated the same regardless of which code is used; however the member effectiveness factors and strength reduction factors used by the two codes were very different.

4.2.3 Strength Reduction Factor ϕ

ACI 318-08 provision used 0.75 for all STM cases whereas the AASHTO LRFD provided two distinct strength reduction factors based on the member type; $\phi = 0.7$ for struts and $\phi = 0.9$ for ties. Reference Table 4-3 for application.

4.2.4 Strut Effectiveness Factors β_s

ACI 318-08 contained five distinct strut effectiveness factors β_s, based on strut geometry, provided strut reinforcement and weight of concrete used. In cases where the provided strut reinforcement does not meet the requirements of ACI 318-08 section A.3.3 the weight of concrete is used to determine the strut effectiveness factor via the modification factor λ which was related to the unit weight of concrete; $\lambda = 1.0$ for normal-weight concrete, $\lambda = 0.85$ for sand-lightweight concrete and $\lambda = 0.75$ for all-lightweight concrete. However for purposes of simplicity the requirements of ACI 318-08 A.3.3 were always assumed satisfied and therefore $\beta_s = 0.75$. The AASHTO LRFD 2nd Ed. code only provided two strut effectiveness factors based solely on strut geometry, i.e. if they were prismatic or bottle shaped struts.

4.2.5 Node Effectiveness Factors β_n

The number of node effectiveness factors β_n, defined by each code was equal at three; however the two values provided by the AASHTO LRFD 2nd Ed. for C-C-C and C-C-T nodes were conservative when compared against their counterparts in the ACI 318-08. See Table 4-3 for exact values.

Table 4-3 ACI 318-08/AASHTO LRFD effective strength coefficients

	ACI 318-08	AASHTO - LRFD
Strength Reduction Factor ϕ	0.75	0.7 Compression
		0.9 Tension
Strength of Struts	$f_s = f_{cu}A_s$	$f_s = f_{cu}A_s$
	$f_{cu} = 0.85\beta_s f'_c$	$f_{cu} = 0.85\beta_s f'_c$
Uniform Cross Section β_s	1.0	1.0
w/Reinforcement Satisfying A.3.3 β_s (ACI 318-08 Only)	0.75	0.75
w/o Reinforcement Satisfying A.3.3 β_s (ACI 318-08 Only)	0.60λ	
Struts in Tension β_s (ACI 318-08 Only)	0.40	
All other Cases β_s (ACI 318-08 Only)	0.60	
Strength of Nodes	$f_n = f_{cu}A_n$	$f_n = f_{cu}A_n$
	$f_{cu} = 0.85\beta_s f'_c$	$f_{cu} = 0.85\beta_s f'_c$
C-C-C Nodes β_n	1.0	0.85
C-C-T Nodes β_n	0.8	0.75
C-T-T, T-T-T Nodes β_n	0.6	0.65
Strength of Ties	$f_T = f_y A_s$	$f_T = f_y A_s$
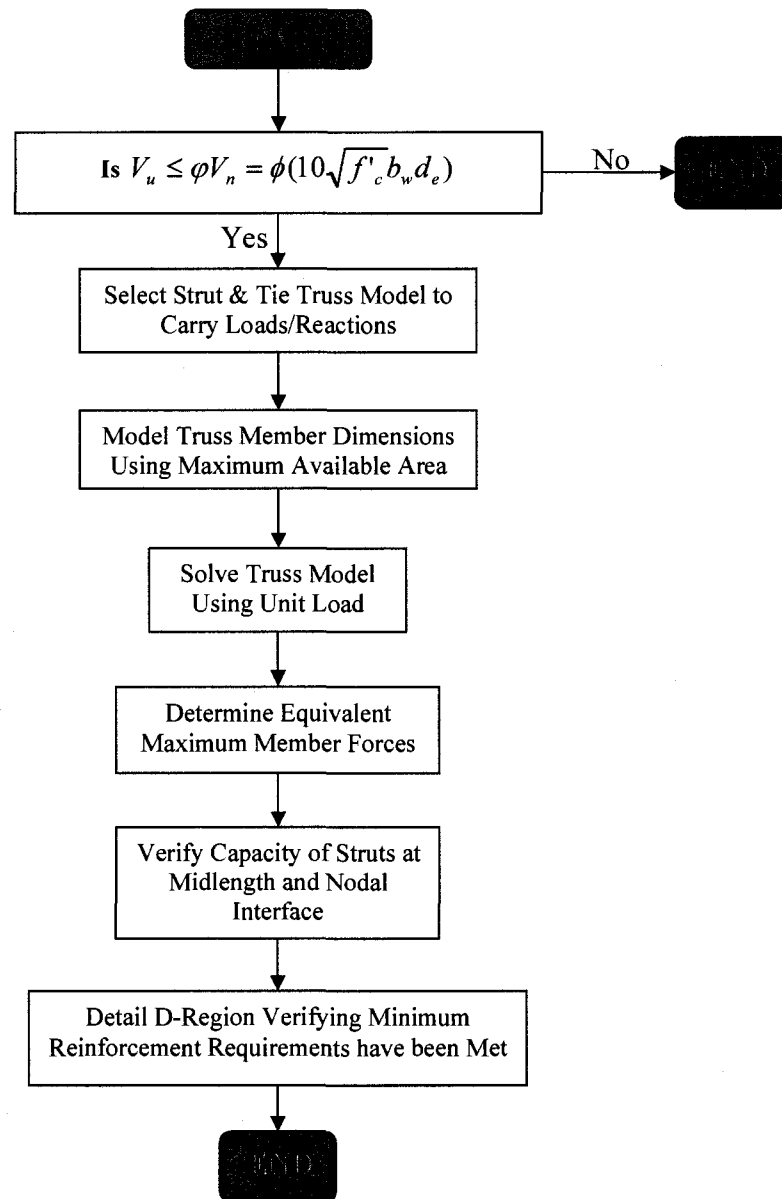
Figure 4-13 Strut and tie modeling procedure

5.0 <u>RESULTS and DISCUSSION</u>

5.1 Flexure

Twelve beam sections were analyzed using both the ACI 318-08 and AASHTO

LRFD code provisions. The reinforcement provided was varied over the range and

inclusive of the limits A_{smin} to A_{smax}; reinforcement limits were held respective to the

provisions of each code.

The section geometry and variables used were:
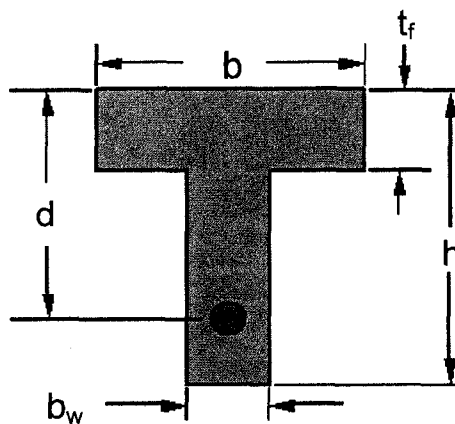
Figure 5-1 Graphic representation of section geometry

Where the fixed values used for these dimensions were as follows:

Flange width $b = 36\text{in.}$

Flange depth $t_f = 4\text{in.}$

Web depth $b_w = 14\text{in.}$

Depth to centroid of reinforcement $d = 24\text{in.}$

5.1.1 A_{smin} and A_{smax}, ACI 318-08 versus ASHTO LRFD

There were no cases where the ACI 318-08 calculated value for A_{smax} would allow the ratio of c/d to be greater than 0.375.

The difference between results for A_{smin} and A_{smax} as calculated using the ACI 318-08 and AASHTO LRFD varied greatly depending on the variable in question. Table 5-1 highlights these differences via comparison of the slope of the lines generated when the limits A_{smin} and A_{smax} were calculated using different section variables.

Table 5-1 Rates of change for ACI 318-08 and AASHTO LRFD A_{smin} and A_{smax}

Variable	Slope ACI-381-05		Slope AASHTO LRFD		% ACI - AASHTO	
	A_{smin}	A_{smax}	A_{smin}	A_{smax}	A_{smin}	A_{smax}
b	0.000	0.227	0.000	0.193	0.00	117.65
b_w	0.076	0.207	0.048	0.293	63.25	70.63
d	0.044	0.253	0.028	0.283	63.25	89.29
t_f	0.000	0.880	0.000	1.060	0.00	83.09

From Table 5-1 several things become obvious: section flange depth, b and t_f have no impact on the minimum amount of reinforcement allowed; regardless of the code used, a change in web width will have the greatest impact upon the difference between the slope of the lines generated when determining the minimum allowable area of reinforcement between the ACI 318-08 and the AASHTO LRFD; whereas flange depth will have the greatest impact upon the difference between the slope of the lines generated when determining the maximum allowable area of reinforcement as provided by the ACI 318-08 and the AASHTO LRFD. The percentage difference between these results is

tabulated in the far right columns of Table 5-1. These percentages were calculated by dividing the values for the slopes of the results found using the ACI 318-08 by the slopes of the results found using the AASHTO LRFD.

It is of interest to note that the difference between the codes for minimum reinforcement when based on section flange width and section flange depth, b and t_f respectively, was consistent between the codes while the difference between the codes for maximum reinforcement was always less when using the ACI 318-08 than the AASHTO LRFD except when comparing results found using the flange width b as the variable. In this case the slope of the results found using ACI 318-08 increased by a rate of 17.65% faster than for those produced when using the AASHTO LRFD provisions.

The slopes of the results found using ACI 318-08 for all other variables were an average 81% less than the corresponding values calculated using the AASHTO LRFD. Reference Figures 5-2 through 5-5.
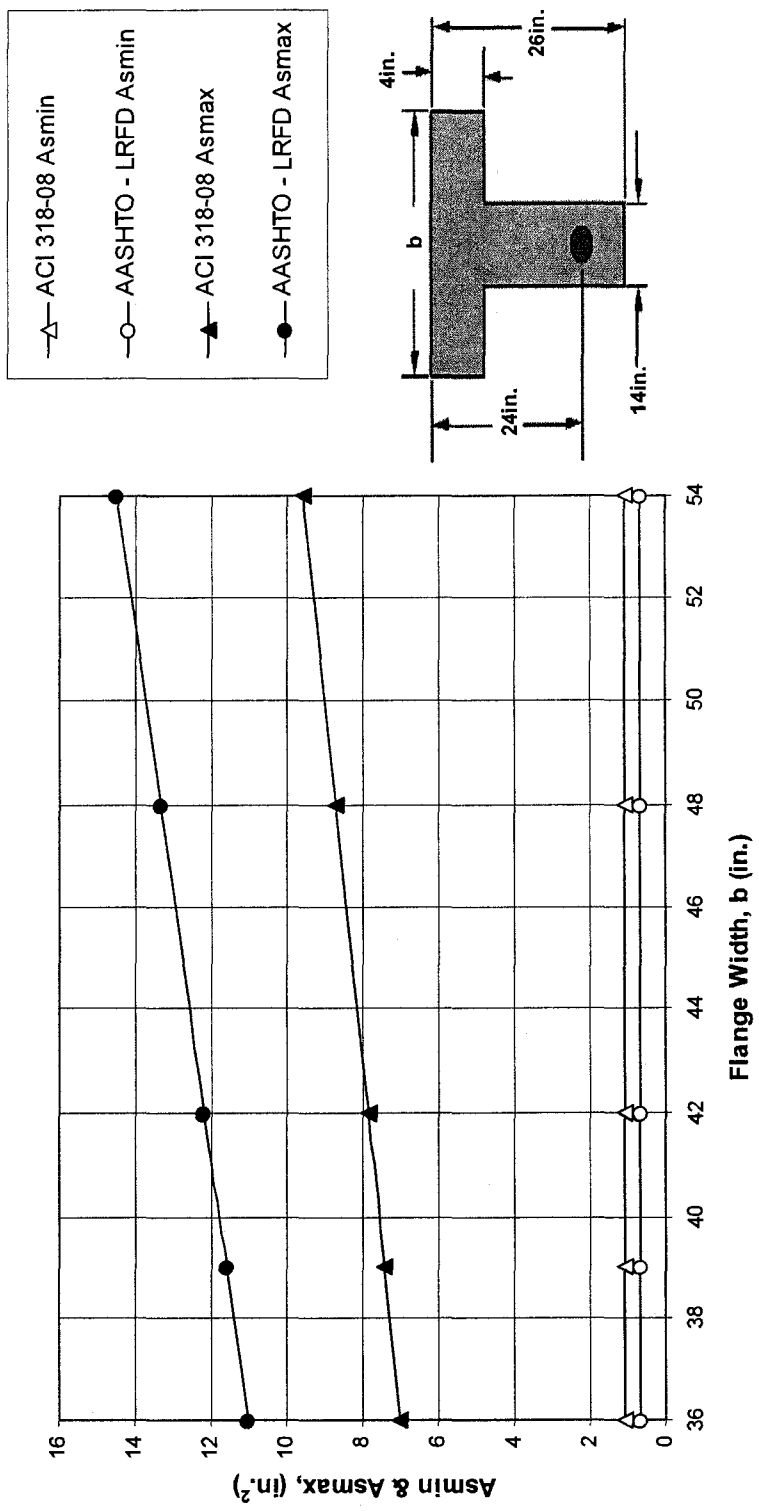
Figure 5-2 A_{smax} and A_{smin} as a function of b
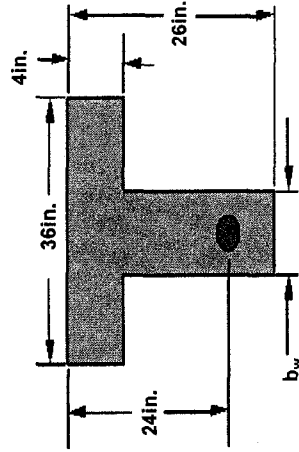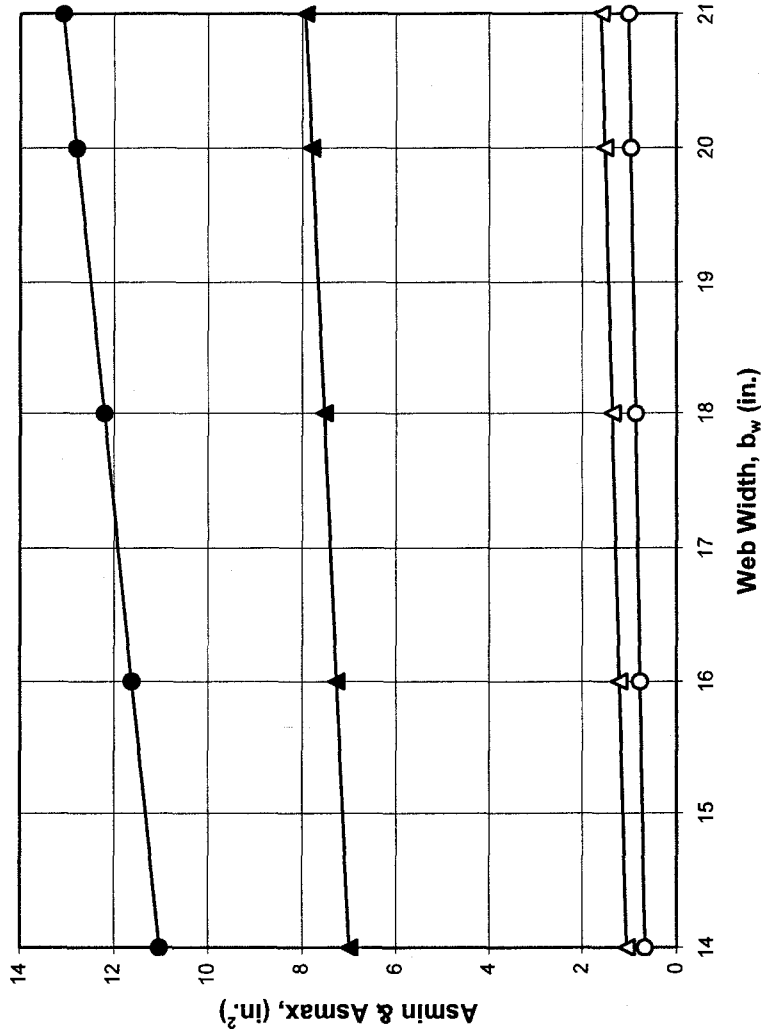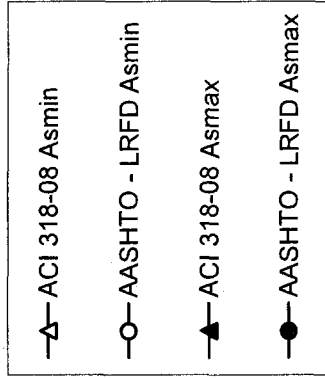
Figure 5-3 A_{smax} and A_{smin} as a function of b_w
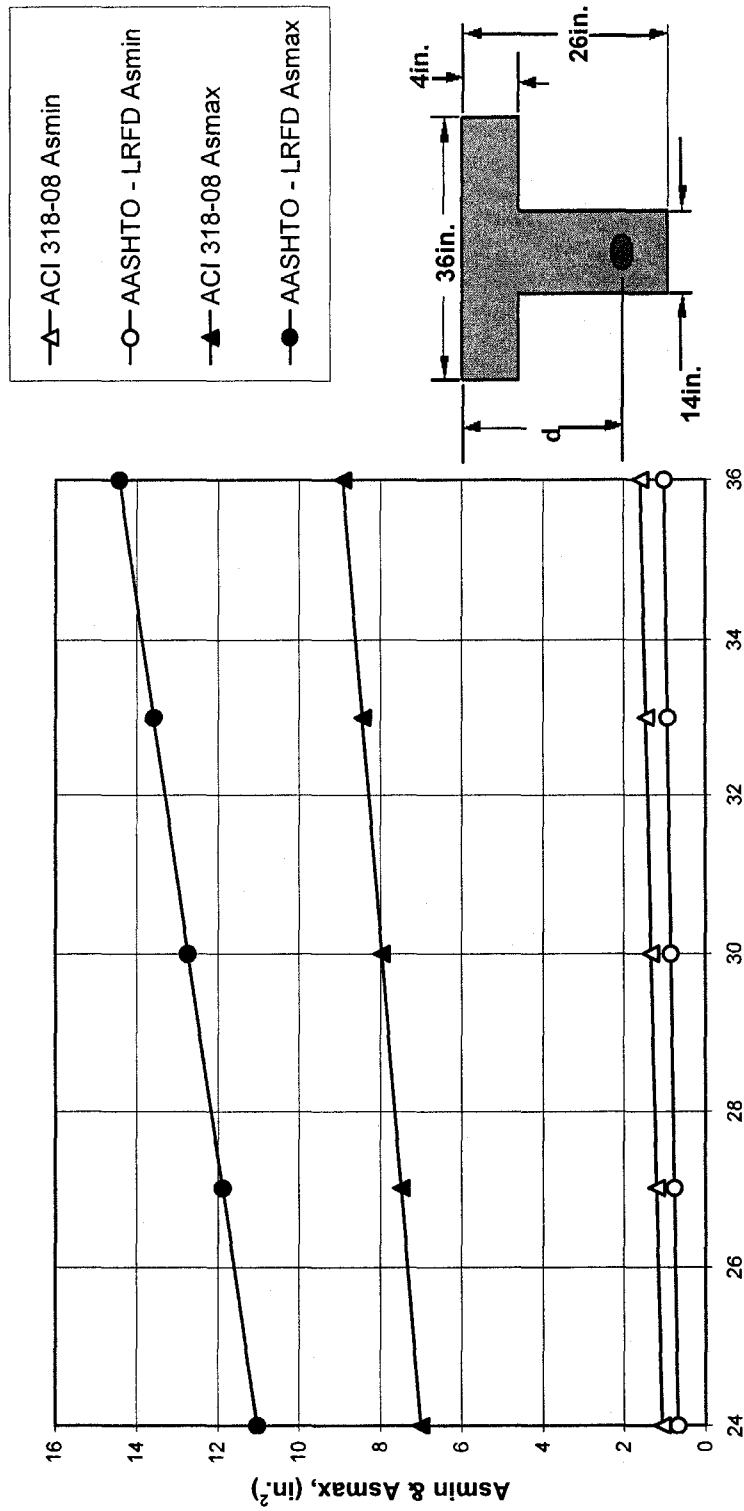
Figure 5-4 A_{smax} and A_{smin} as a function of d
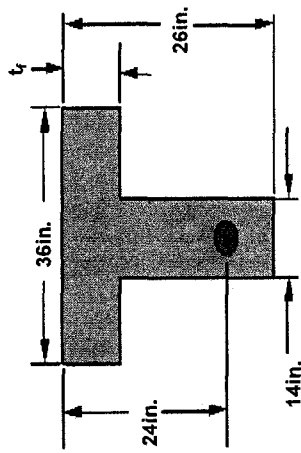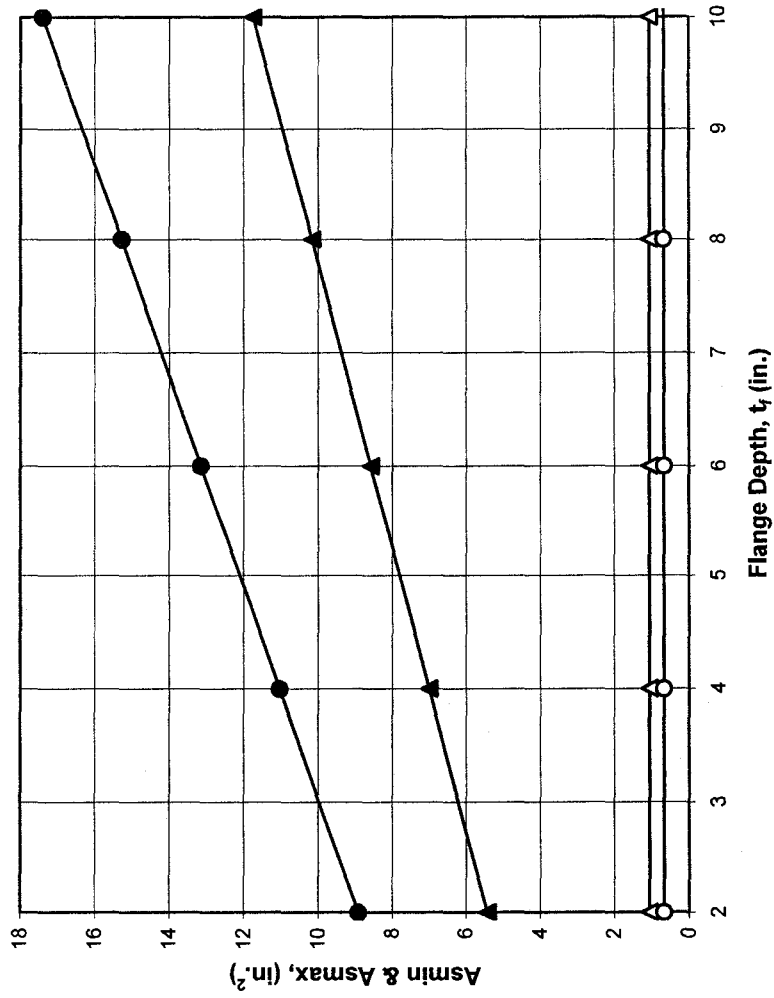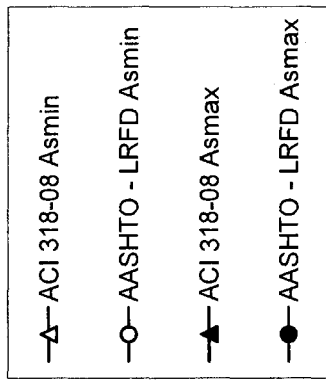
Figure 5-5 A_{smax} and A_{smin} as a function of t_f

5.1.2 A_s versus M_u

During the determination of the flexural strength of a section based on the area of

reinforcing steel by either ACI 318-08 or AASHTO LRFD code, the difference in

corresponding moment capacity was never greater than 1.4%; the average difference was

0.93%. It was observed that sections analyzed using AASHTO LRFD code consistently

required a larger area of steel to support the same moment than that required for an

otherwise equivalent ACI 318-08 section. All results presented in this section in the form

of tables or percentages represent a ratio between the results found for the ACI 318-08

and AASHTO LRFD code requirements for determining flexural capacity, reference

Equations 5-1 through 5-3.

For all cases analyzed, certain geometric dimensions were found to have greater

influence than others on the amount of reinforcement required to resist a given moment;

results are summarized in Table 5-2 and Figures 5-6 through 5-9.

Table 5-2 Ratio of AASHTO LRFD to ACI 318-08 for M_u per unit A_s

VARIABLE	VALUE	ACI 318-05	AASHTO LRFD	%	Δ AVG	% AVG	Δ MAX	% MAX
b	36	1189.10	1178.79	99.13	9.31	99.22	10.31	99.34
	42	1196.27	1186.56	99.19				
	54	1201.20	1193.30	99.34				
b_w	14	1189.11	1178.79	99.13	12.22	98.97	13.66	99.13
	18	1185.04	1171.39	98.85				
	21	1176.01	1163.34	98.92				
d	24	1189.11	1178.79	99.13	13.53	99.10	16.35	99.13
	30	1495.58	1481.67	99.07				
	36	1798.78	1782.43	99.09				
t_f	2	1197.49	1186.04	99.04	11.54	99.01	19.63	99.69
	6	1167.61	1164.05	99.69				
	10	1152.80	1133.17	98.30				

The percentage difference ratio as shown in Table 5-2 is the sum of the applied

factored moments divided by the sum of the areas of reinforcement required for a section

analyzed using the AAASHTO LRFD to carry that moment over the entire viable range

of reinforcement, divided by the area of reinforcement required for the ACI section, i.e.

the range A_{smin} to A_{smax} as defined by each code. Equations 5-1 through 5-3 describe the

formulae used in the calculation of this percentage more concisely. This was considered

a convenient method of quantifying the difference in results produced by each code for

the area of reinforcement required to resist an applied moment on a per unit basis, i.e.

applied moment per unit area of reinforcement. The applied moment is a representation

of the applied loads only however it is used in the determination of required

reinforcement during design or analysis of a section via the calculated resistive moment

of the section, $M_n = \phi M_u$. Therefore in essence this percentage represents a comparison

between the ACI 318-08 and the AASHTO LRFD of the allowable applied load as

defined by each code for based on each cross section's geometry.

$$\Delta\% = \left(1 - \frac{(AASHTO)M_u : A_s}{(ACI)M_u : A_s}\right)100 \qquad (5\text{-}1)$$

where

$$AASHTO\text{--}M_u : A_s = \frac{\sum\limits_{As\,min}^{As\,max} M_u}{\sum\limits_{As\,min}^{As\,max} A_s} \qquad (5\text{-}2)$$

and

$$ACI-M_u : A_s = \frac{\sum\limits_{As\,min}^{As\,max} M_u}{\sum\limits_{As\,min}^{As\,max} A_s} \qquad (5\text{-}3)$$

Examination of the data in Table 1 highlights two consistent traits between the codes: a) a section designed using the AASHTO LRFD code will always require a larger area of reinforcing steel than an equivalent section designed using the ACI 318-08 code, i.e. the AASHTO LRFD will provide a more conservative solution for the resistive moment per unit of reinforcing steel; b) web width b_w, has the greatest effect on the ratio of steel to flexural strength for any arbitrary T or L flanged section, although this amount averaged only 1.40% for the section geometries studied.
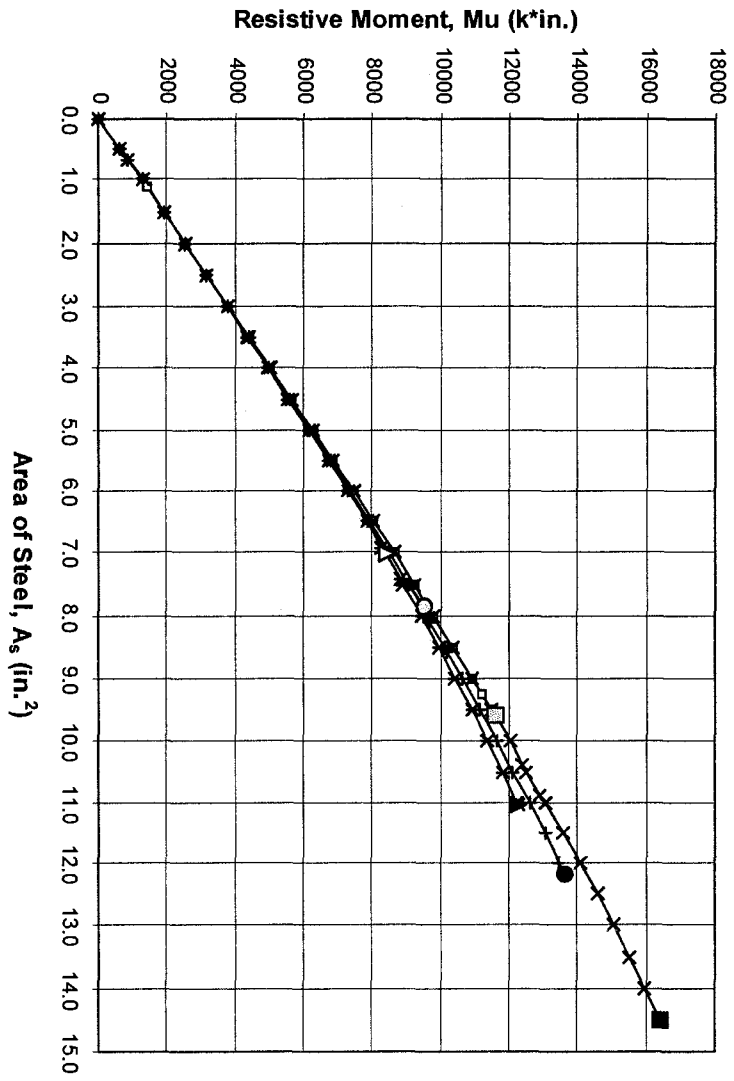
Figure 5-6 A_s versus M_u for variable b

Figure 5-7 A_s versus M_u for variable b_w

88
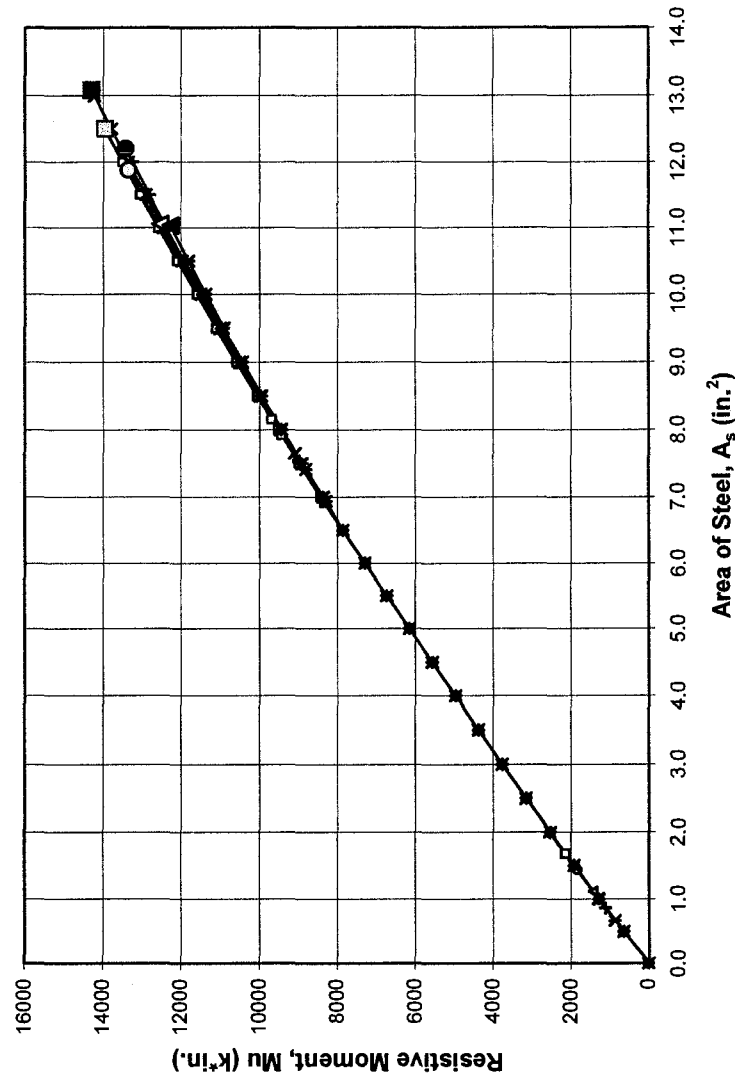
Figure 5-8 A_s versus M_u for variable d
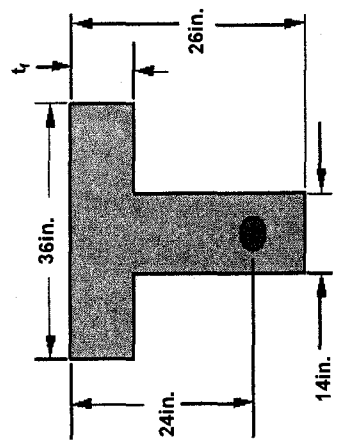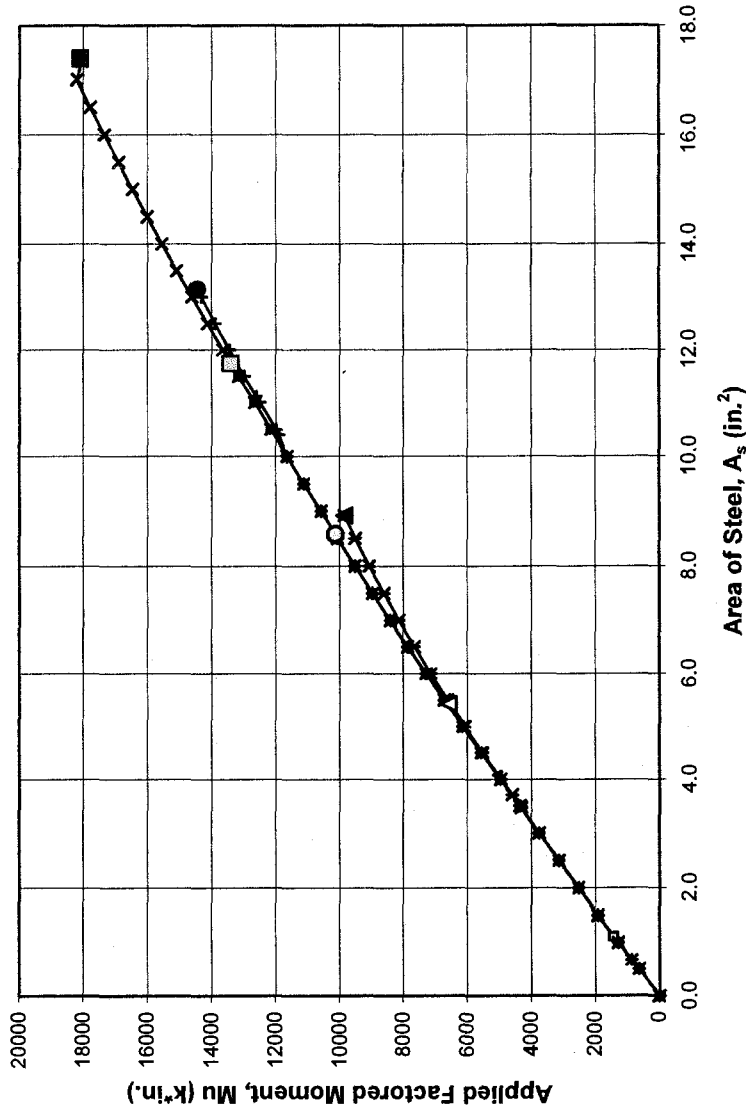
Figure 5-9 A_s versus M_u for variable t_f

5.1.3 Location of Neutral Axis *c*, and Depth of Compressive Block *a*

The depth of the neutral axis has been conventionally defined as described by Equation 5-4 which is used by both the ACI 318-08 and AASHTO LRFD. This equation applies regardless of section geometry, that is rectangular or flanged, or whether the section is in rectangular or T-section behavior when using ACI or AASHTO LRFD Simplified Conservative Approach.

$$c = \frac{A_s f_y - A'_s f'_y}{0.85 f'_c \beta_1 b}$$ (5-4)

The AASHTO LRFD refined approach, which was the method used for all AASHTO LRFD based calculations in this paper, differs when sections exhibit flanged behavior as described earlier in §4.1.3.2. The formulae are repeated below for convenience.

$$c = \frac{A_s f_y - A'_s f'_y}{0.85 f'_c \beta_1 b}$$ (5-5)

$$c = \frac{A_s f_y - A'_s f'_y - 0.85 f'_c \beta_1 (b - b_w) h_f}{0.85 f'_c \beta_1 b_w}$$ (5-6)

The results for the depth of the neutral axis using Equation 5-6 were computed for every 0.250 square inches increase in the area of reinforcement provided; this range was inclusive of the lower limit of A_{smin} and the upper limit of A_{smax} as found by the ACI 318-08. Because the value for A_{smax} that was produced by the ACI 318-08 was always less

than that found by using the AASHTO LRFD it was used as the limiting value for this comparison. From these values the arithmetic mean was calculated. The results are listed in Table 5-3.

This option to choose the level of fidelity in the calculation of the depth of the neutral axis was a significant difference between the two codes; both in the approach used in and the results obtained. The AASHTO LRFD provided the option to neglect any additional compressive strength contributions that the flanged area, minus the web width, would provide. When the option to use the AASHTO LRFD refined approach was not taken both codes would produce identical values for the depth of the neutral axis.

Table 5-3 Results for location of neutral axis

Depth of Neutral Axis ACI vs. AASHTO							
		AVERAGE c					
VARIABLE	VALUE	ACI	AASHTO	Δ AVG	Δ %AVG	Δmax	Δ %max
b	36	2.540	2.409	0.140	93.95	0.167	94.83
	42	2.224	2.102				
	54	2.181	2.014				
b_w	14	2.539	2.409	0.073	97.27	0.130	100.43
	18	2.681	2.580				
	21	2.827	2.839				
d	24	2.539	2.409	0.056	98.02	0.130	102.04
	30	2.695	2.750				
	36	3.234	3.141				
t_f	2	2.130	2.158	0.086	97.06	0.143	101.31
	6	2.874	2.732				
	10	3.745	3.602				

As shown in Table 5-3 the results using the refined approach of Equations 5-5 and 5-6 produced a greater depth for the location of the neutral axis; this provided a larger compressive area and hence required a larger area of tensile reinforcement to obtain force equilibrium, i.e. a balanced section, $T = C$. Web width b_w, had the greatest impact on the difference between results obtained from ACI 318-08 and AASHTO LRFD codes. This effect was maximized when b_w was equal to one-half the value of flange width b, or 18 inches for the sections analyzed. Reference Figures 5-10 through 5-13. Notice should be made of the abrupt change in slope that is attributable to the effect of provided reinforcement in the calculation of the location of the neutral axis. This abrupt change in slope is due to the direct proportionality of the tensile force T to the compressive force C, i.e. $T = C$, and the role the location of the neutral axis has in the calculation of the compressive force as shown in Equation 3-5, $C = 0.85 f'_c \beta_1 cb$. The point at which the slope change occurs is when the depth of the neutral axis exceeds the flange depth t_f, of the section; that is when the section is no longer in rectangular action and the refined approach described by Equation 5-6 was utilized.

5.1.4   Strength Reduction Factor ϕ

Due to limits placed on the sections analyzed in this paper on the allowable amount of reinforcement, artificial or otherwise, the strength reduction factor ϕ, was equal to 0.9 for every test point. Indirectly this states that the ratio c/d was always less than or equal to 0.375 for all ACI 318-08 analyses and c/d was always less than or equal

to 0.42 for all AASHTO LRFD analyses. Because the value of ϕ never differed between the ACI 318-08 and the AASHTO LRFD for the shallow beam flexural analyses performed in this paper no additional comparisons on this particular code provision were made.

94
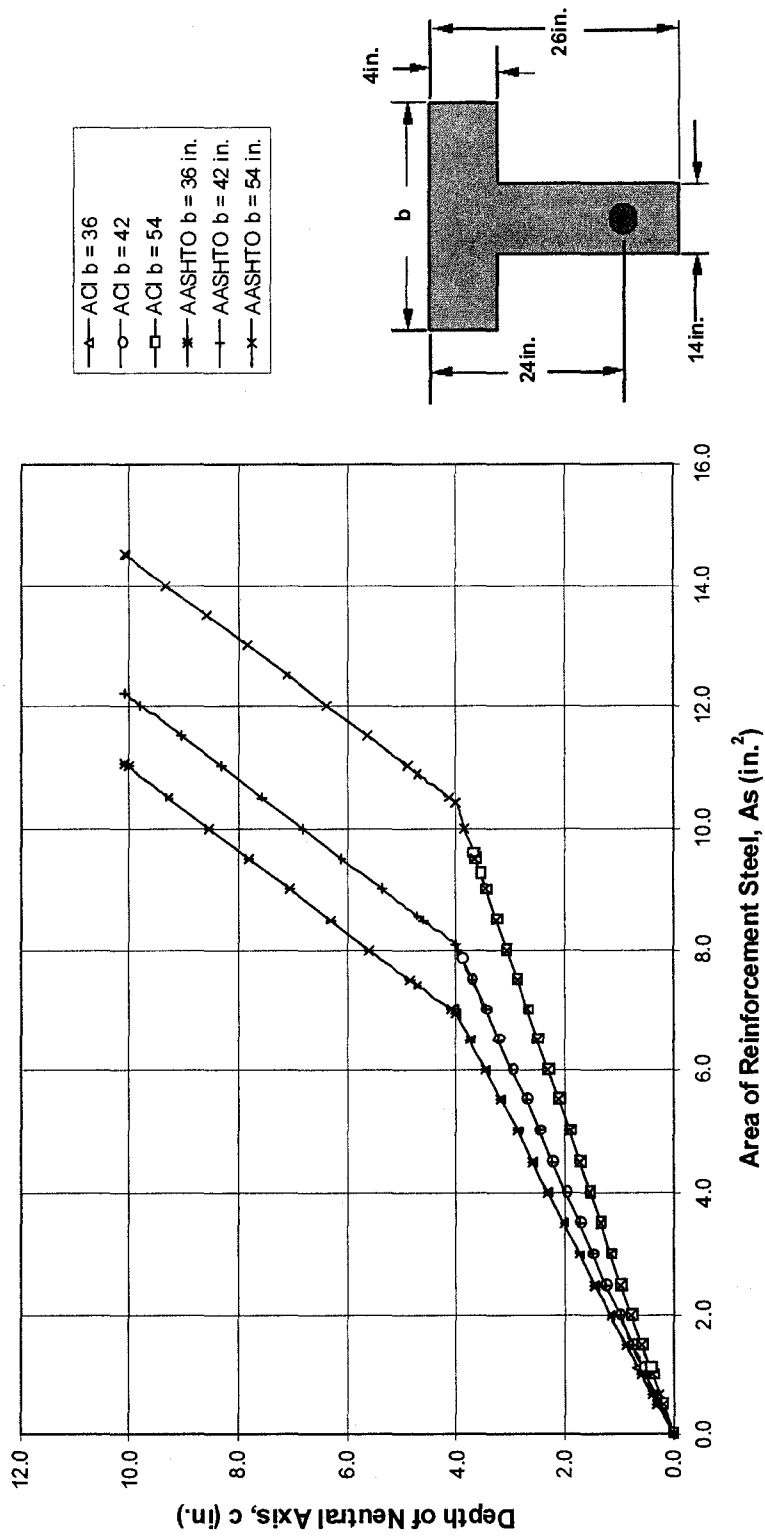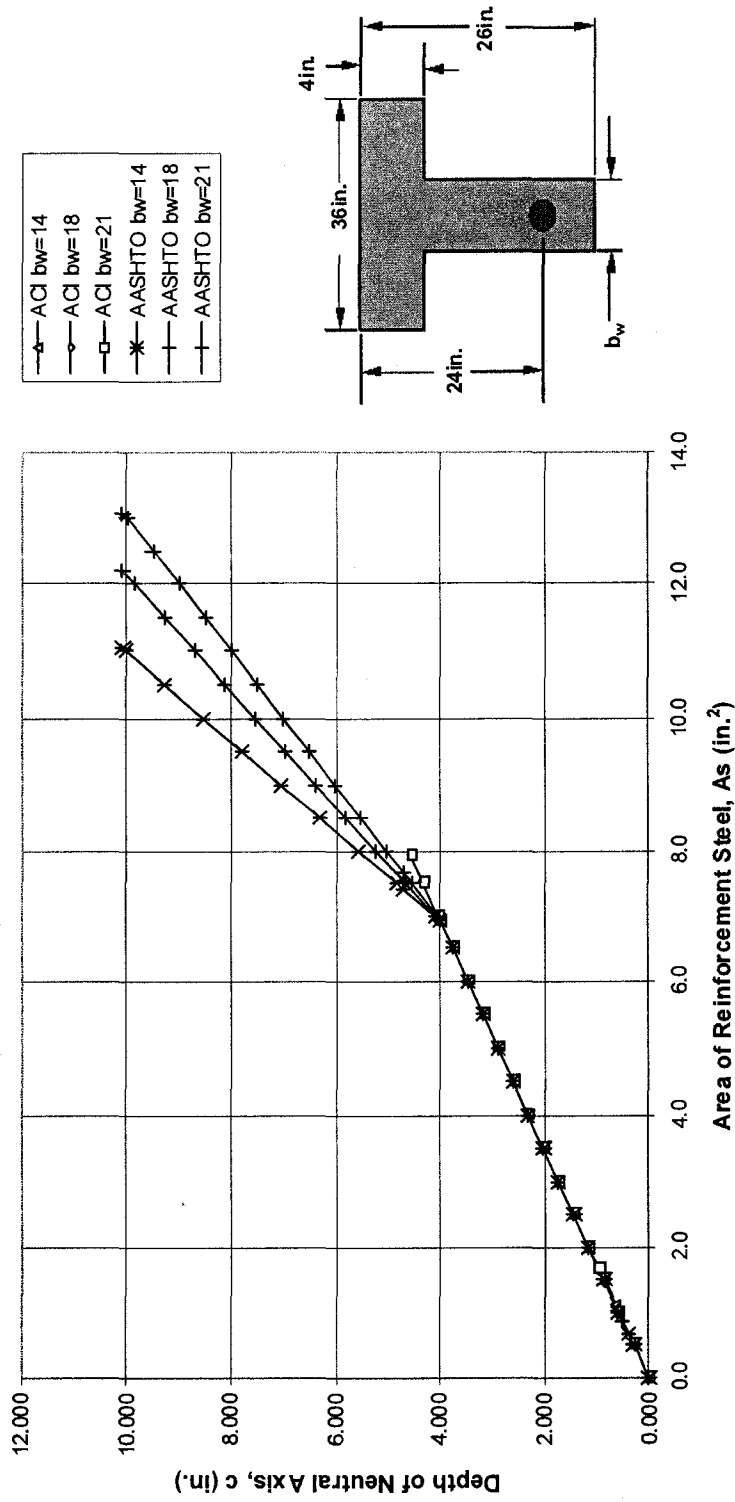

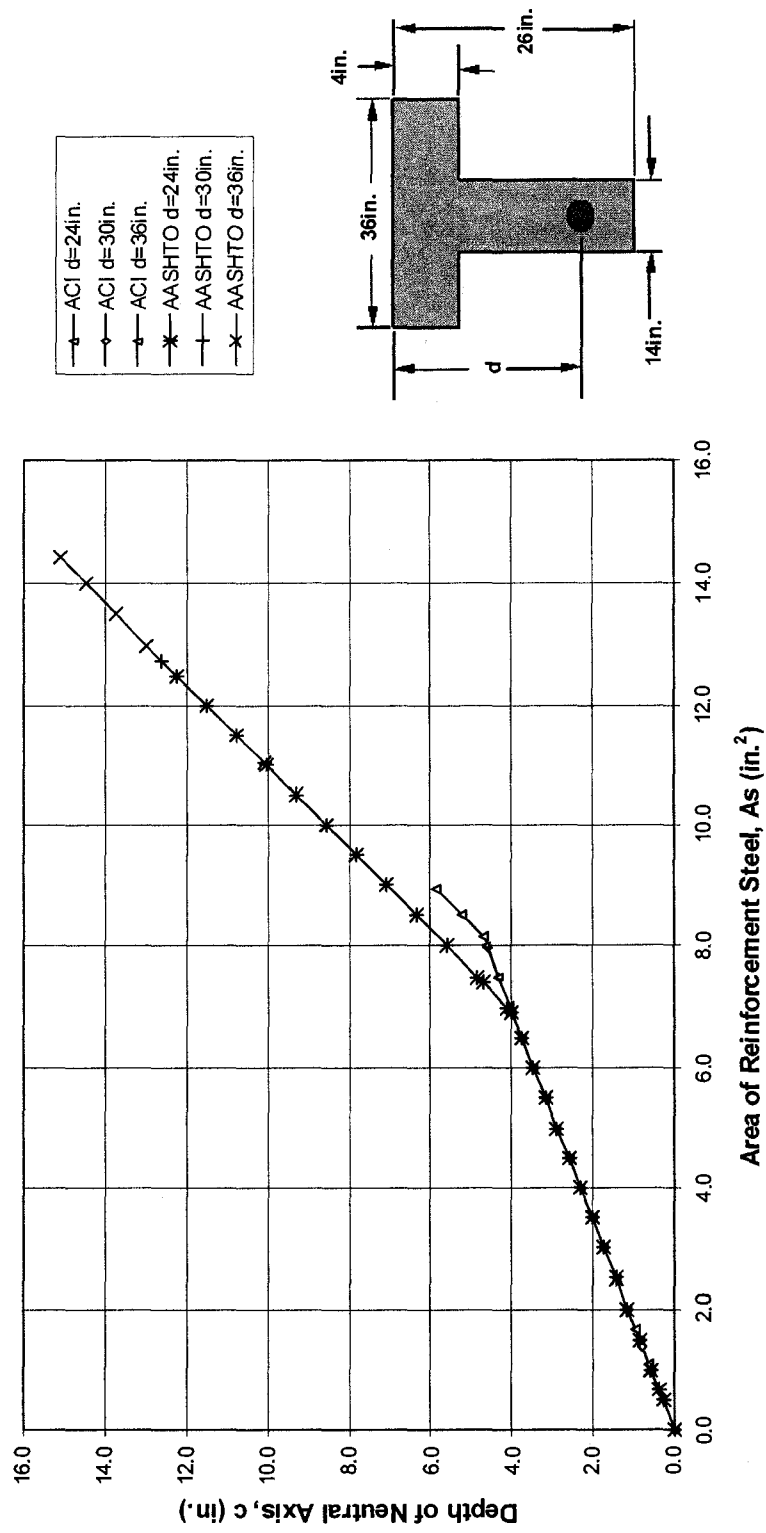Figure 5-10 A_s versus c for variable b

Figure 5-11 A_s versus c for variable b_w

Figure 5-12 A_s versus c for variable d
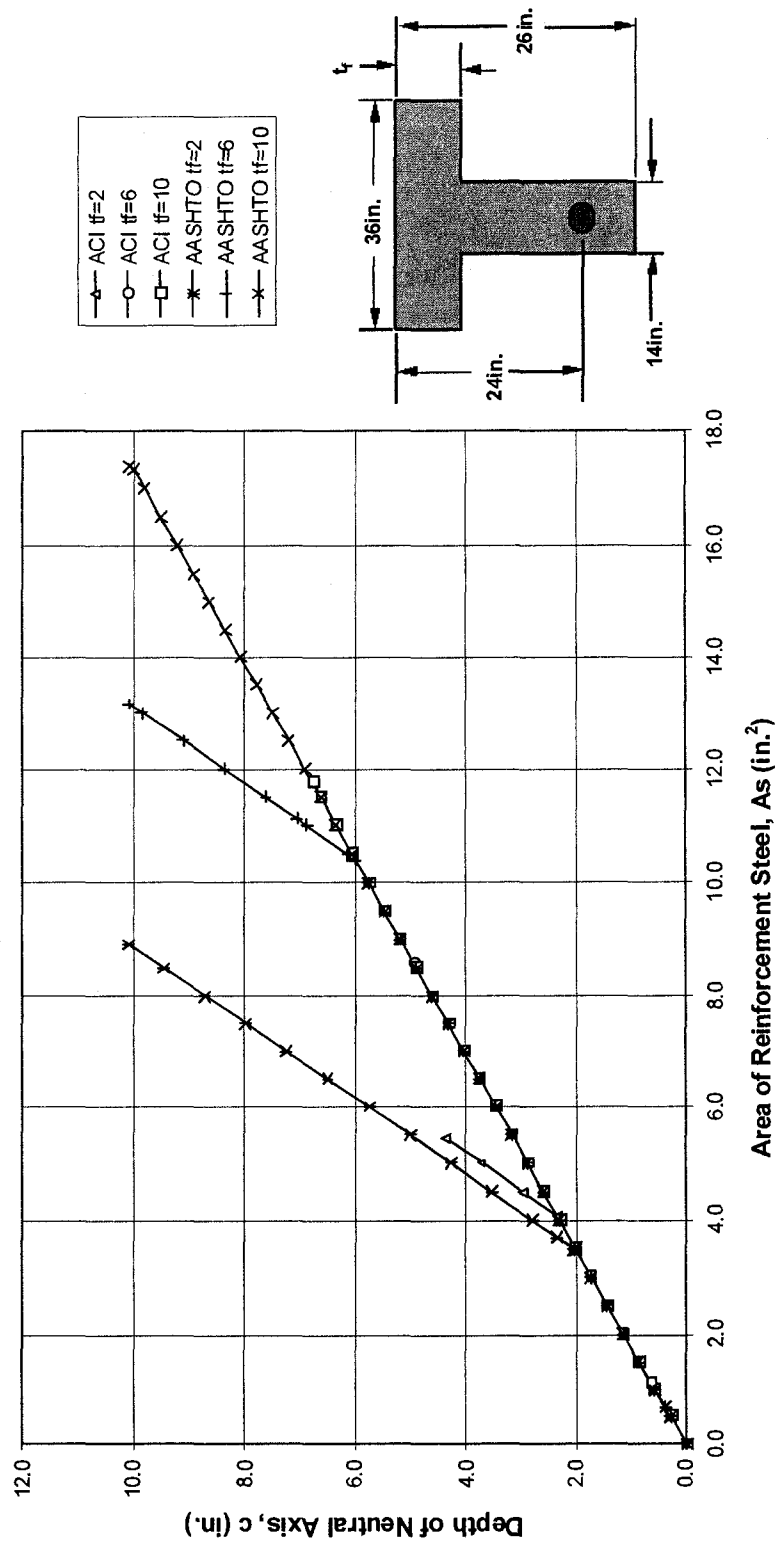
Figure 5-13 A_s versus c for variable t_f

5.2 STM

Five deep beams previously tested by Ha were reevaluated using the Strut and Tie

Method (STM) as described by both the ACI 318-08 and AASHTO LRFD code

provisions.

Section geometry and variables are shown in Figure 5-14 and Table 5.4.
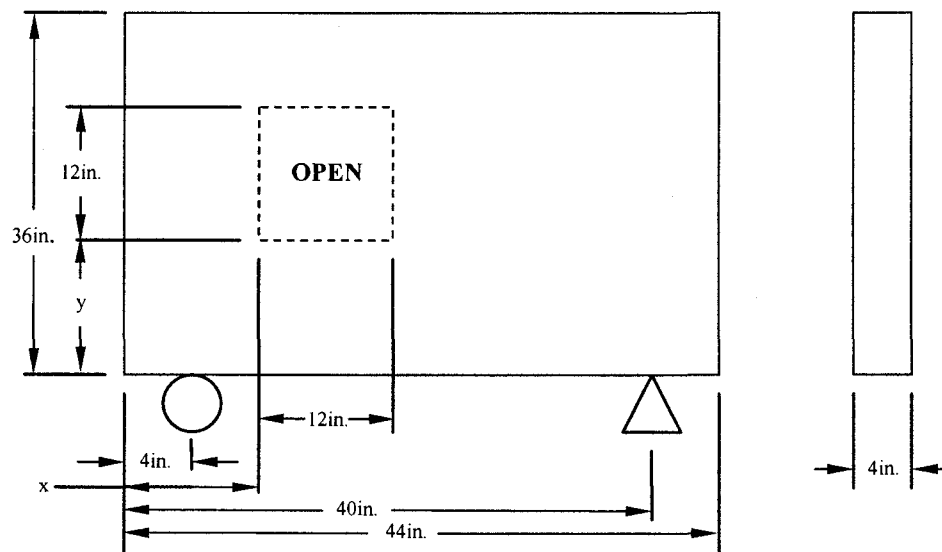
Figure 5-14 Generic beam with and without opening

Table 5-4 Cutout locations from lower left corner in inches

12in. x 12in. Cutout Location		
	x	y
SERIES 1	N/A	N/A
SERIES 2	16	12
SERIES 3	16	8
SERIES 4	16	16
SERIES 5	20	12

5.2.1 Maximum Allowable Concentrated Load – STM versus FEA

In the work performed by Ha the maximum test loads applied to the sections

varied from 70kips to 175kip depending on the beam geometry. All design loads and

their corresponding ACI 318-08 and AASHTO LRFD counterparts are summarized in

Table 5-5 and are shown graphically in Figure 5-15. The gray columns in Table 5-5

represent the STM method predicted loads as a percentage of Ha's test loads.

Table 5-5 Predicted load versus maximum test load comparisons

SERIES	Ha	ACI 318-08	%	AASHTO - LRFD	%	Δ%
1	175.00	127.96	73.12	119.43	68.25	4.87
2	125.00	85.68	68.54	79.97	63.98	4.57
3	150.00	106.35	70.90	99.26	66.17	4.73
4	70.00	73.53	105.04	68.63	98.04	7.00
5	100.00	86.67	86.67	80.89	80.89	5.78

Of the five comparisons made only series 4 produced predicted load values that

exceeded the test load used by Ha; this was only true when the ACI 318-08 code

provisions were utilized and this exceedance was 5.04%. The magnitude of the predicted

loads calculated using the AASHTO LRFD in series 4 were 98.04% of the actual test

load value used by Ha of 70 ksi. The predicted values for all other cases analyzed were

well below the experimental test loads used by Ha; this was consistent with expectations

given the conservative nature of the STM model process.

In the instance of series 4 several factors can explain the fact that the predicted

safe design load inclusive of safety factors was greater than the load actually reached

during Ha's laboratory testing. Analytical and predictive calculations make several

assumptions any of which can be the source of this discrepancy:

- compressive strength of concrete is consistent throughout the section

- placement of the concrete is without voids or inconsistencies

- area and depth of reinforcement are exact

- cross section geometry and member length are exact

In every series the maximum load the beam was predicted to be capable of

carrying was greater when the ACI 318-08 code was used. The load predicted as

analyzed using AASHTO LRFD was always 93.3% of that analyzed using ACI 318-08.

When a comparison was made between the area of reinforcing steel required by each

code the AAHSTO–LRFD code requirement was 77.8% of that of the ACI 318-08

sections. Reference Equations 5-7 and 5-8. These percentages were directly attributable

to the different values specified for the strength reduction factors by each code.

$$\%Load\frac{\phi ACI318-08}{\phi AASHTO-LRFD} \Rightarrow 93.3 \tag{5-7}$$

$$\%Load\frac{\phi ACI318-08}{\phi AASHTO-LRFD} \Rightarrow 93.3\frac{0.75}{0.9} = 77.8 \tag{5-8}$$

5.2.2 Maximum Allowable Concentrated Load without ϕ – STM versus FEA

A second comparison was made between the experimental design loads used by

Ha and the analytical results derived in this paper without application of the strength

reduction factor ϕ. All design loads and their corresponding ACI 318-08 and AASHTO

LRFD counterparts without the application of ϕ are summarized in Table 5-6 and are shown graphically in Figure 5-16. Again the gray columns in Table 5-5 represent the STM method predicted loads as a percentage of Ha's test loads.

Table 5-6 Predicted load without ϕ versus maximum test load comparisons

SERIES	T.H.	ACI 318-08	%	AASHTO - LRFD	%	Δ%
1	175.00	170.62	97.50	170.62	97.50	0.00
2	125.00	114.24	91.39	114.24	91.39	0.00
3	150.00	141.79	94.53	141.79	94.53	0.00
4	70.00	98.04	140.06	98.04	140.06	0.00
5	100.00	115.56	115.56	115.56	115.56	0.00

In the cases of both series 4 and 5 it can be observed that the predicted strengths have exceeded the actual test loads as determined by Ha. This finding clearly demonstrates the importance of using the strength reduction factor to account for any imperfections during the mixing and placement of concrete as well as the location of reinforcing steel.

The removal of the strength reduction factors also illustrated the significance of largest difference between the ACI 318-08 and AASHTO LRFD when using the method of strut and tie models as shown in Table 5-6. The strength reduction factors assigned by the ACI 318-08 and AASHTO LRFD codes are very different from each other and therefore would never produce identical results for the same section same regardless of truss or member geometry; only by ignoring the contribution of the strength reduction factors altogether could identical results be achieved for each code.

Load Comparison
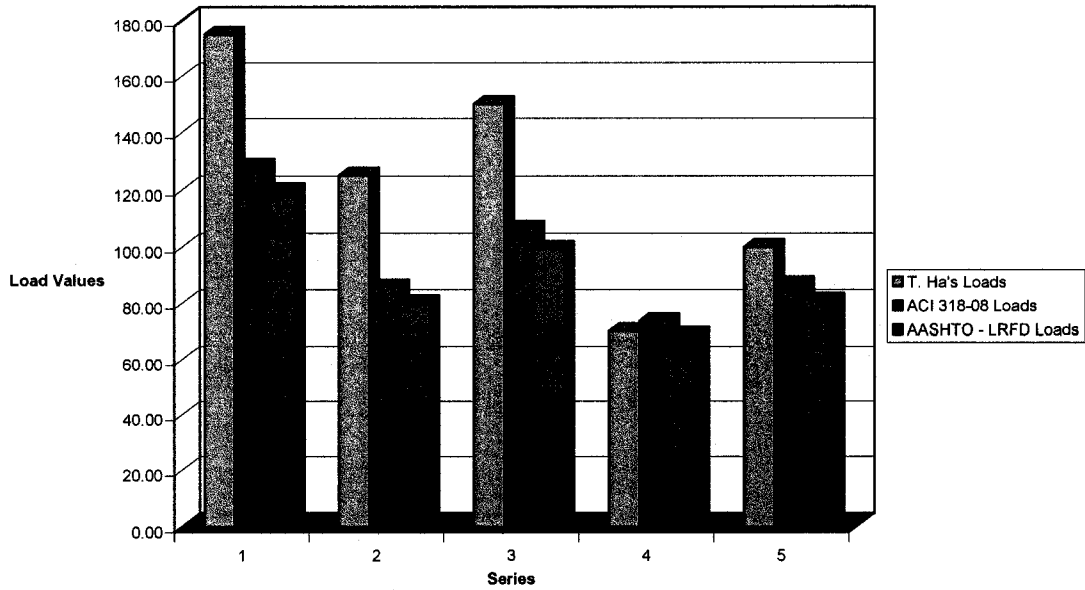
Figure 5-15 Predicted load vs. maximum test load comparisons

Load Comparison Without ϕ
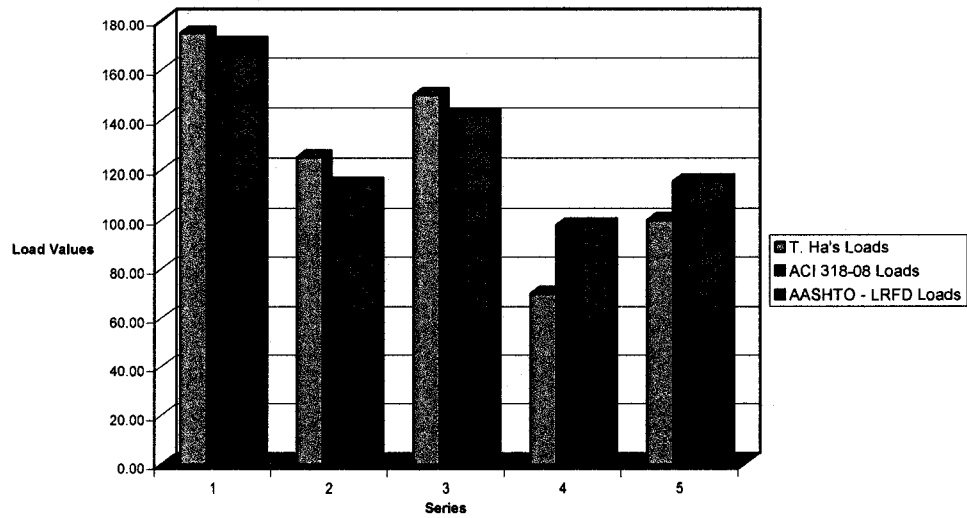
Figure 5-16 Predicted load without ϕ vs. maximum test load comparisons

6.0 <u>SUMMARY and CONCLUSIONS</u>

6.1 Summary

Twelve different flanged shallow beam sections were designed and analyzed for flexural resistance by applying both the ACI 318-08 and the AASHTO LRFD code provisions using hand calculations and analytical software developed by the author. An additional five rectangular deep beam sections were analyzed using the method of strut and tie models by applying both the ACI 318-08 and AASHTO LRFD code guidelines, utilizing Pro/E CAD software, hand calculations and analytical software developed by the author. Flexural shallow beam sections were divided into four categories; each category represented a geometric feature to be varied; flange width b, flange depth t_f, web width b_w, and the depth of the centroid of reinforcement d_t. Factored moment capacity M_u, for each section was calculated for reinforcing steel amounts that were increased by increments of 0.50 square inches. The deep beam sections investigated were identical, apart from the inclusion and location of a 12in. x 12in. opening. Maximum load capacity was predicted for a concentrated load located at the center on the top face of the beam.

Differences found between the code provisions included but were not limited to the method prescribed for finding the allowable limits of reinforcement or the method used for determining the location of the neutral axis. Many other differences existed but would only be noticed if prestressed reinforcement was incorporated into the design; this fell beyond the scope of this study. The methods employed to reach solutions for both

sets of problems could vary greatly between the two codes however there were no significant differences in the end results derived from using either set of provisions.

6.2   Conclusion

6.2.1 A_{smin} and A_{smax} for Flexure

Web width b_w, had the greatest impact upon the minimum allowable reinforcement for a given section; whereas the minimum allowable reinforcement A_{smin}, and the flange depth t_f, had the greatest influence upon the maximum allowable reinforcement A_{smax} for a section.

6.2.2 A_s versus M_u for Flexure

Web width b_w, had the greatest effect on a given section's moment capacity regardless of what code was utilized. Significant differences were encountered between the ACI 318-08 and AASHTO LRFD provisions when analyzing or designing sections for moment capacity in regards to the method prescribed for finding the allowable limits of reinforcement. In spite of these differences the results obtained from both codes for all cases analyzed within this paper were always within 1.4% of each other.

6.2.3   Depth of Neutral Axis c for Flexure

The method for calculating the depth of the neutral axis c, was the most noticeable difference between the ACI 318-08 and AASHTO LRFD code provisions. However the results calculated for sections from either code discussed in this paper were

never more than 9% apart. This was attributed to the fact that only non-prestressed, plain reinforced sections were analyzed. Results using non-reinforced sections were never considered for this thesis.

6.2.4 Strength Reduction Factor ϕ for Flexure

Due to the limits of reinforcement placed each section by both codes, the strength reduction factor, ϕ, was always equal to 0.9 and therefore ϕ did not have a differing affect on the results obtained from either code.

6.2.5 Maximum Load Capacity for STM

Maximum predicted load capacity for any of the beam series studied was always greater when analyzed using the ACI 318-08 Appendix A STM method provisions than when using the AASHTO LRFD provisions. These differences in maximum predicted load capacity ranged from 4.57% to 7.00%. Inherent differences in member effectiveness factors and the strength reduction factors were the source of this variance.

Works Cited

ACI Committee 318. <u>Building Code Requirements for Structural Concrete 318-02, and Commentary (318R-02)</u>. Farmington Hills. American Concrete Institute. 2002.

ACI Committee 318. <u>Building Code Requirements for Structural Concrete 318-08, and Commentary (318R-08)</u>. Farmington Hills. American Concrete Institute. 2005.

American Association of State Highways and Transportation Officials, AASHTO LRFD. <u>AASHTO LRFD Bridge Design Specifications</u>, 3rd ed. Washington DC. 2004.

Beres, Attila. <u>Notes on ACI 318-02 Building Code Requirements for Structural Concrete with Design Applications.</u> 8th ed. Portland Cement Association. Skokie, IL. 2002.

Brown, Michael D., Sankovich et al. "Behavior and Efficiency of Bottle Shaped Struts." <u>ACI Structural Journal</u> 103.3 (2006): 348-55.

Foster, Stephen J., and Adrian R. Malik. "Evaluation of Efficiency Factor Models used in Strut-and-Tie Modeling of Nonflexural Members." <u>Journal of Structural Engineering</u> 128.5 (2002): 569-77.

Gupta, Pawan R., and Michael P. Collins. "Evaluation of Shear Design Procedures for Reinforced Concrete Members under Axial Compression." <u>ACI Structural Journal</u> 100.4 (2001): 537-47.

Ha, Sun Thuc. <u>Design of Concrete Deep Beams with Openings and Repair Using Carbon Fiber Laminates</u>. San Jose State University. San Jose, CA. 2002.

Hibbeler, R.C. <u>Mechanics of Materials</u>. 6th ed. Upper Saddle River, NJ. Pearson; Prentice Hall. 2005.

Hsu, Thomas T. C., "Toward a Unified Nomenclature for Reinforced-Concrete Theory." <u>Journal of Structural Engineering</u> 122.3 (1996): 275-83.

Kamara, Mahmoud E., and Basile G. Rabbat. <u>Notes on ACI 318-05 Building Code Requirements for Structural Concrete with Design Applications</u> 9th ed. Portland Cement Association. Skokie, IL. 2005.

Leet, Kenneth M., and Chia-Ming Uang. <u>Fundamentals of Structural Analysis</u>. 1st ed. New York. McGraw-Hill. 2002.

Leu, Liang-Jeng, Huang, et al. "Strut-and-Tie Design Methodology for Three-Dimensional Reinforced Concrete Structures." Journal of Structural Engineering 132.6 (2006): 929-38.

MacGregor, James G. Reinforced Concrete – Mechanics and Design. 3rd ed. Englewood Cliffs, NJ. Pretence Hall. 1997.

McCormac, Jack C, and James K. Nelson. Design of Reinforced Concrete ACI 318-05 Code Edition. 7th ed. Hoboken, NJ. Wiley. 2006.

Naaman, Antoine E. Prestressed Concrete Analysis and Design Fundamentals. 2nd ed. Ann Arbor, MI. Techno Press 3000. 2004.

Naaman, Antoine E. Limits of Reinforcement in 2002 ACI Code: Transition, Flaws, and Solution. ACI Structural Journal 101.2 (2004): 209-18.

Rahal, Khaldoun N., and Khaled S. Al-Shaleh. "Minimum Transverse Reinforcement in MPa Concrete Beams." ACI Structural Journal 101.6 (2004): 872-78.

Rahal, Khaldoun N., and Michael P. Collins. "Experimental Evaluation of ACI and AASHTO LRFD Design Provisions for Combined Shear and Torsion." ACI Structural Journal 98.4 (2003): 277-82.

Reineck, Karl-Heinz. Examples for the Design of Structural Concrete with Strut and Tie Models. American Concrete Institute. Farmington Hills, MI. 2002.

Tan K. H., and G.H. Cheng. "Size Effect on Shear Strength of Deep Beams: Investigating with Strut-and-Tie Model." Journal of Structural Engineering 132.5 (2006): 673-85.

Wright, James T., and Gustavo J. Parra-Montesinos. Strut and Tie Model for Deep Beam Design – A Practical Exercise using Appendix A of the 2002 ACI Building Code. Concrete International. 2003.

Zwicky, Daia, and Thomas Vogel. "Critical Inclination of Compression Struts in Concrete Beams." Journal of Structural Engineering 132.5 (2006): 686-93.

Appendix A – Deep Beam STM Models

Load P
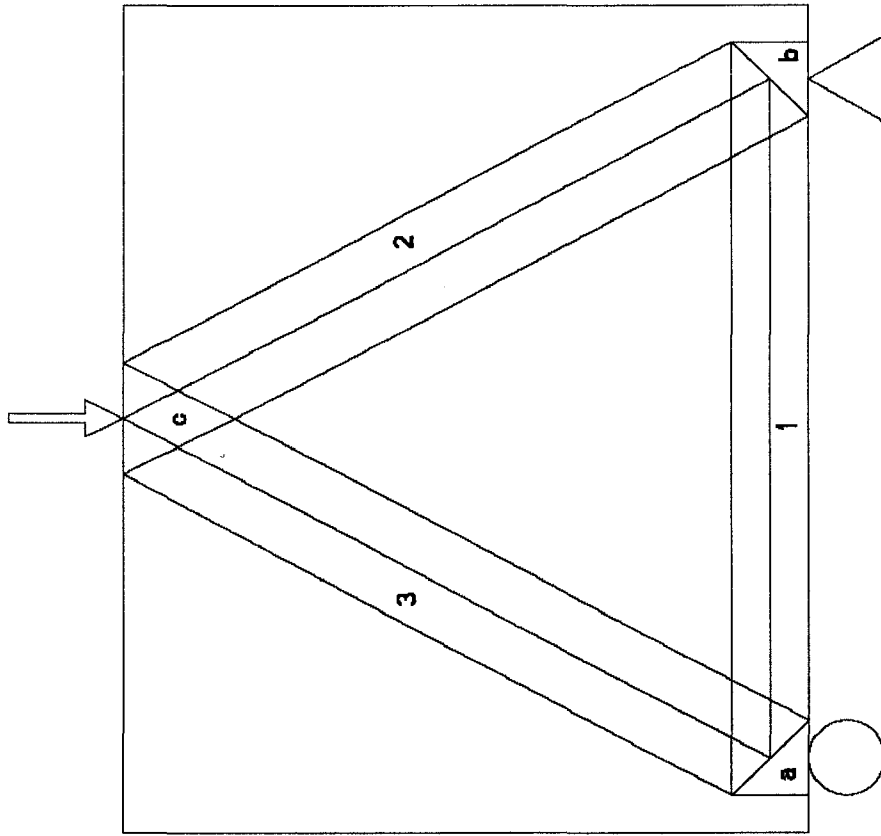
SERIES 1	
MEMBER	MINIMUM WIDTH
1	4.00
2	5.41
3	5.41

Figure A - 1 Deep beam series 1 STM model

SERIES 2	
MEMBER	MINIMUM WIDTH
1	5.62
2	4.00
3	5.62
4	4.00
5	5.64
6	5.64
7	4.00
8	4.00
9	4.00
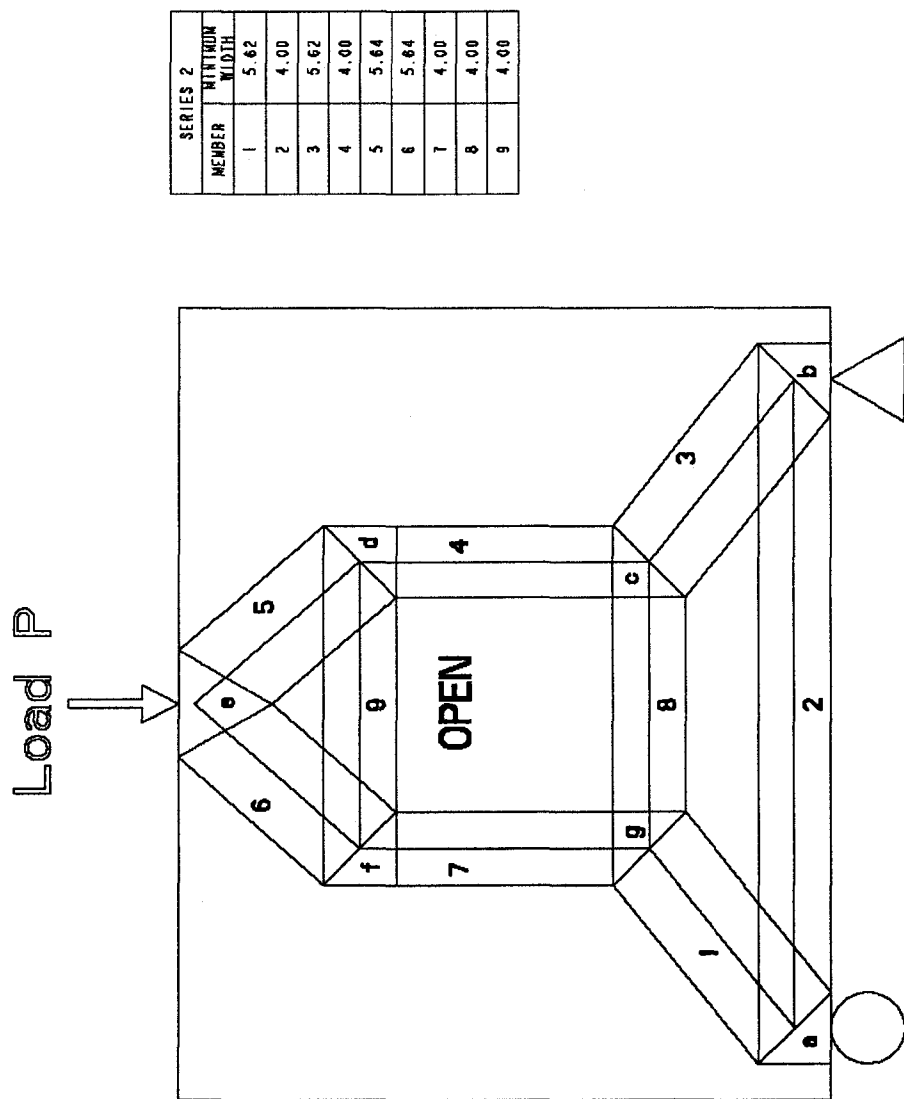
Figure A - 2 Deep beam series 2 STM model

SERIES 3	
MEMBER	MINIMUM WIDTH
1	5.60
2	4.00
3	5.60
4	4.00
5	5.64
6	5.64
7	4.00
8	4.00
9	4.00
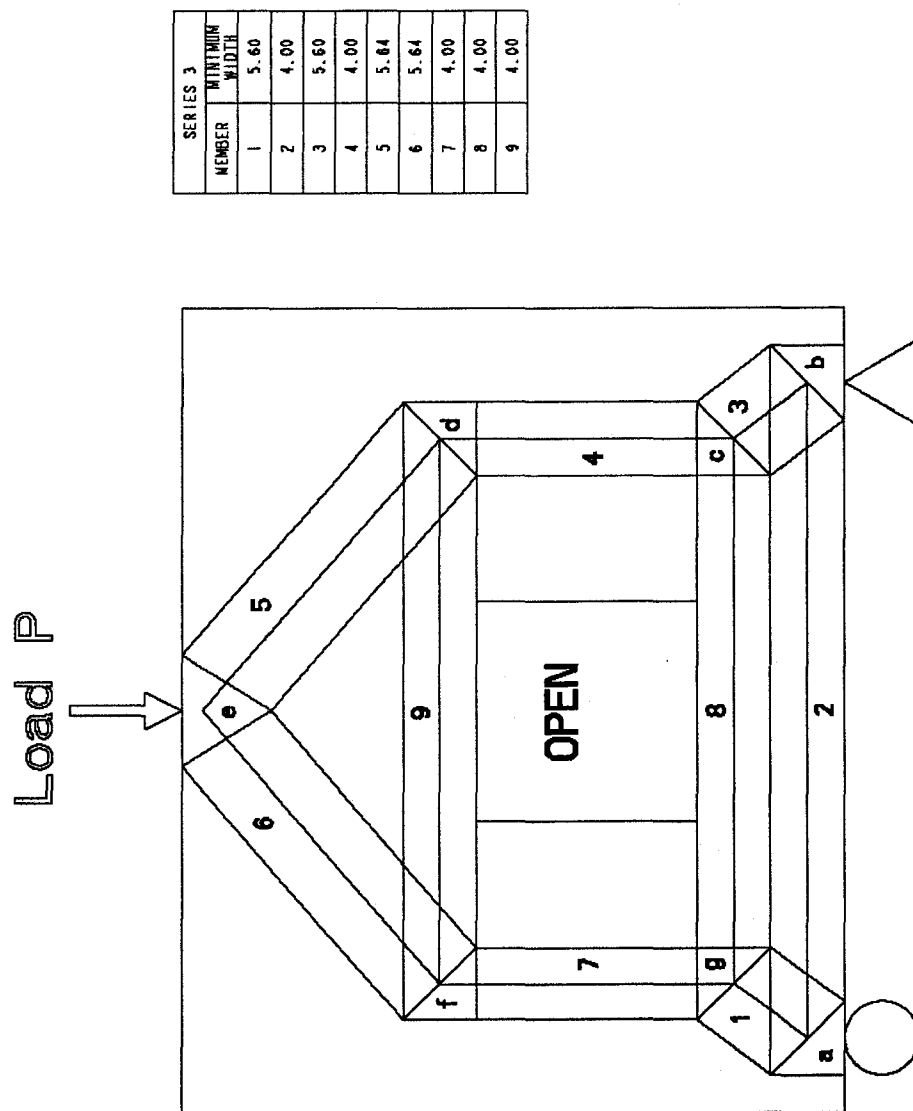
Figure A - 3 Deep beam series 3 STM model

111
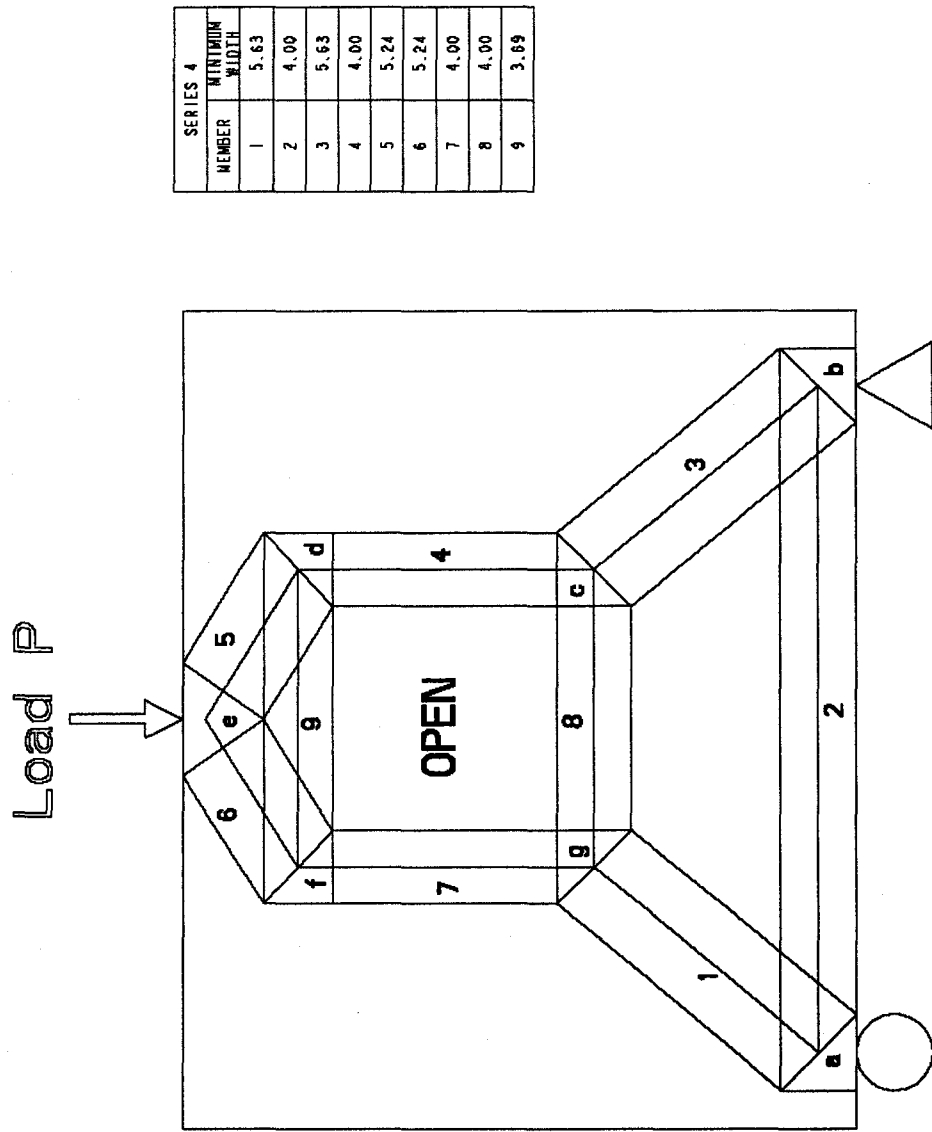
SERIES 4	
MEMBER	MINIMUM WIDTH
1	5.63
2	4.00
3	5.63
4	4.00
5	5.24
6	5.24
7	4.00
8	4.00
9	3.69

Figure A - 4 Deep beam series 4 STM model

SERIES 5	
MEMBER	MINIMUM WIDTH
1	5.62
2	4.00
3	5.62
4	3.63
5	5.38
6	5.38
7	3.63
8	4.47
9	4.00
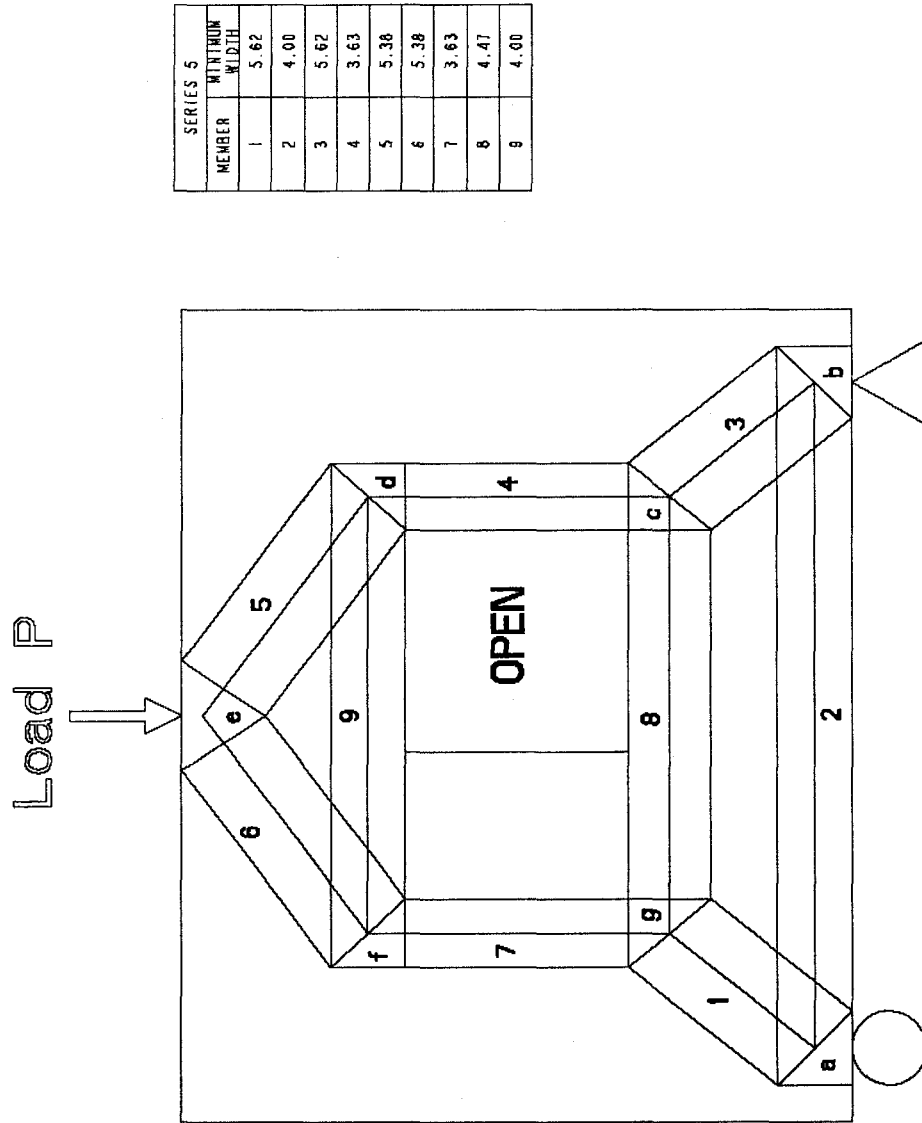
Figure A - 5 Deep beam series 5 STM model

Appendix B – Deep Beam STM Truss Models
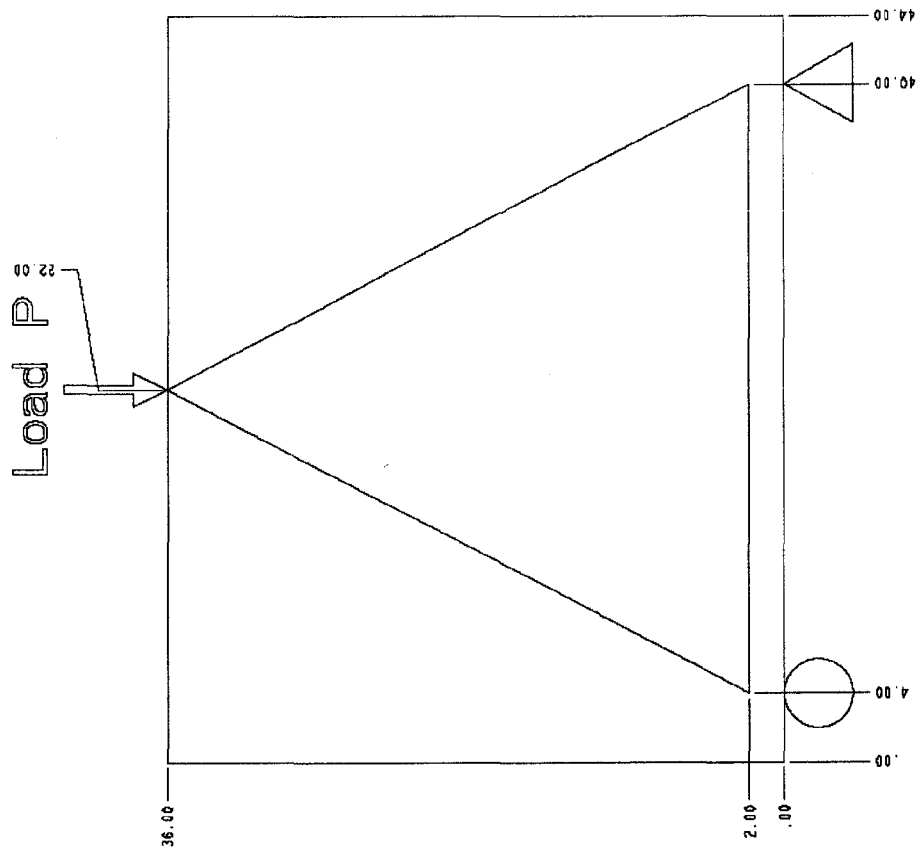
Figure B - 1 Deep beam series 1 STM truss model
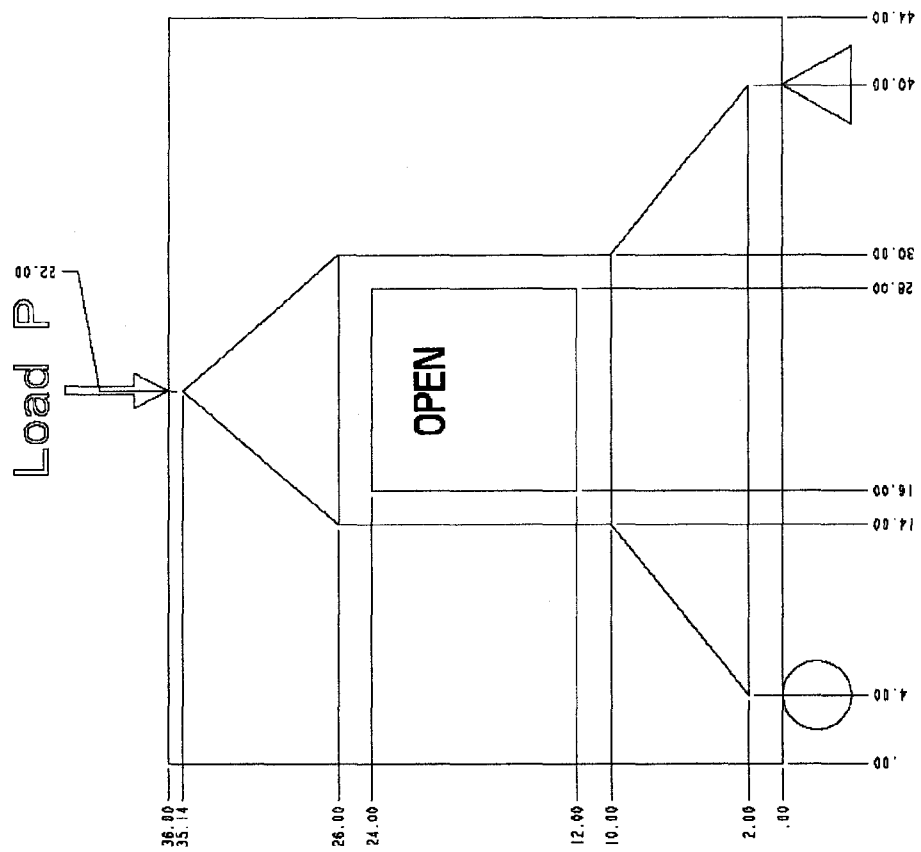
Figure B - 2 Deep beam series 2 STM truss model
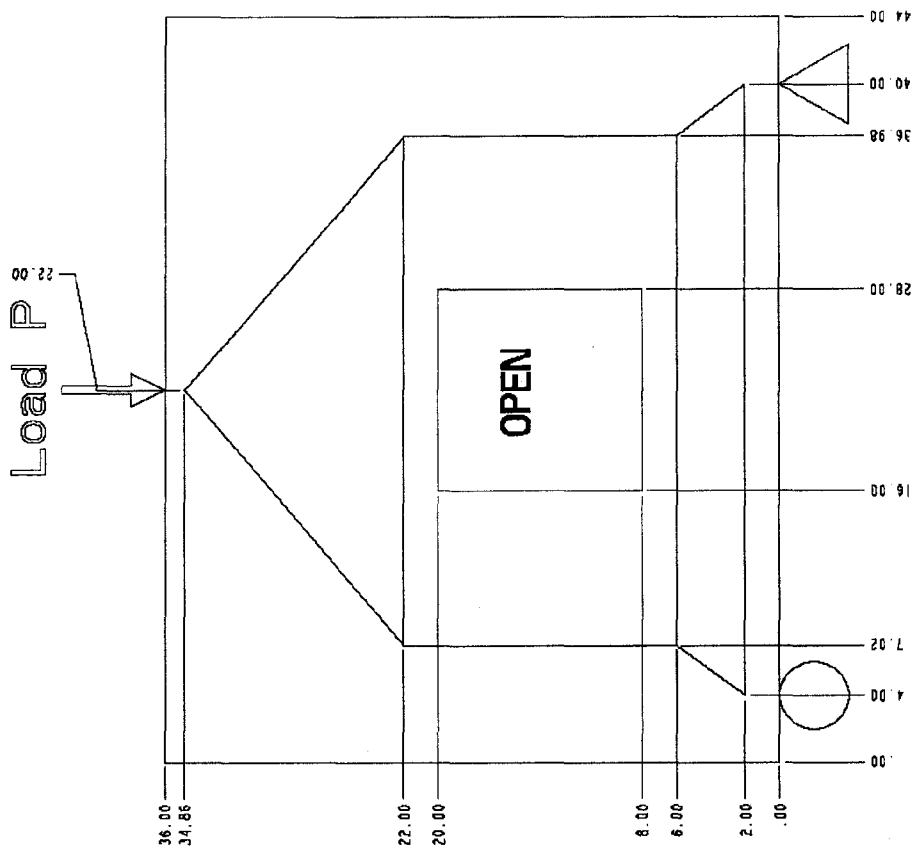
Figure B - 3 Deep beam series 3 STM truss model
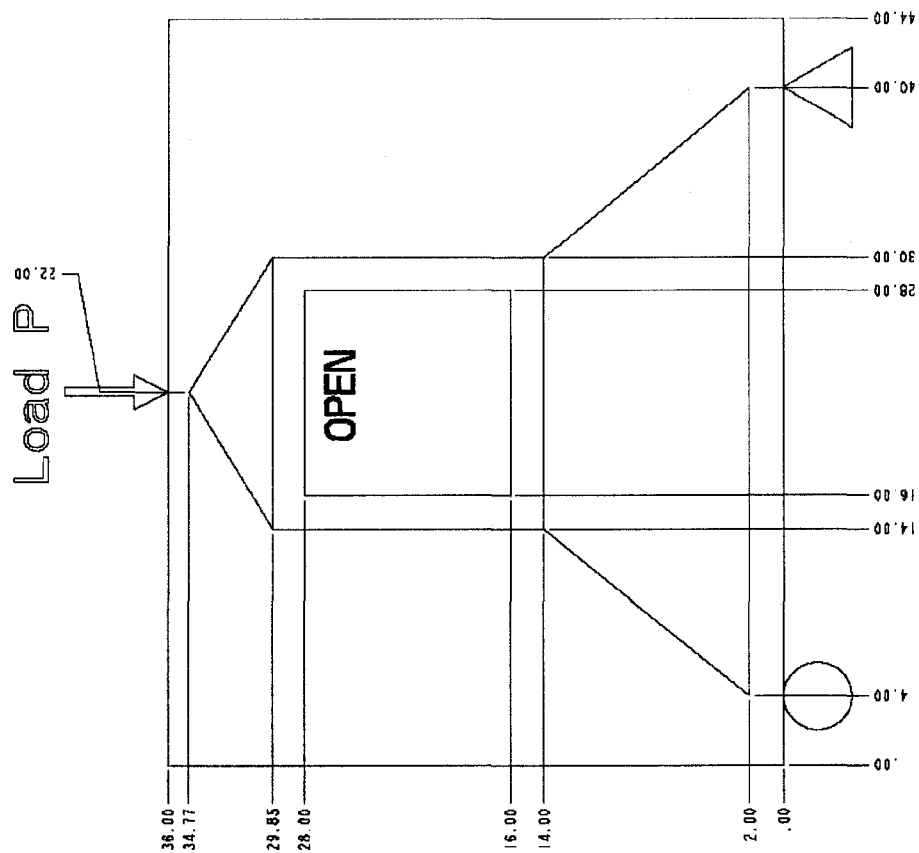
Figure B - 4 Deep beam series 4 STM truss model
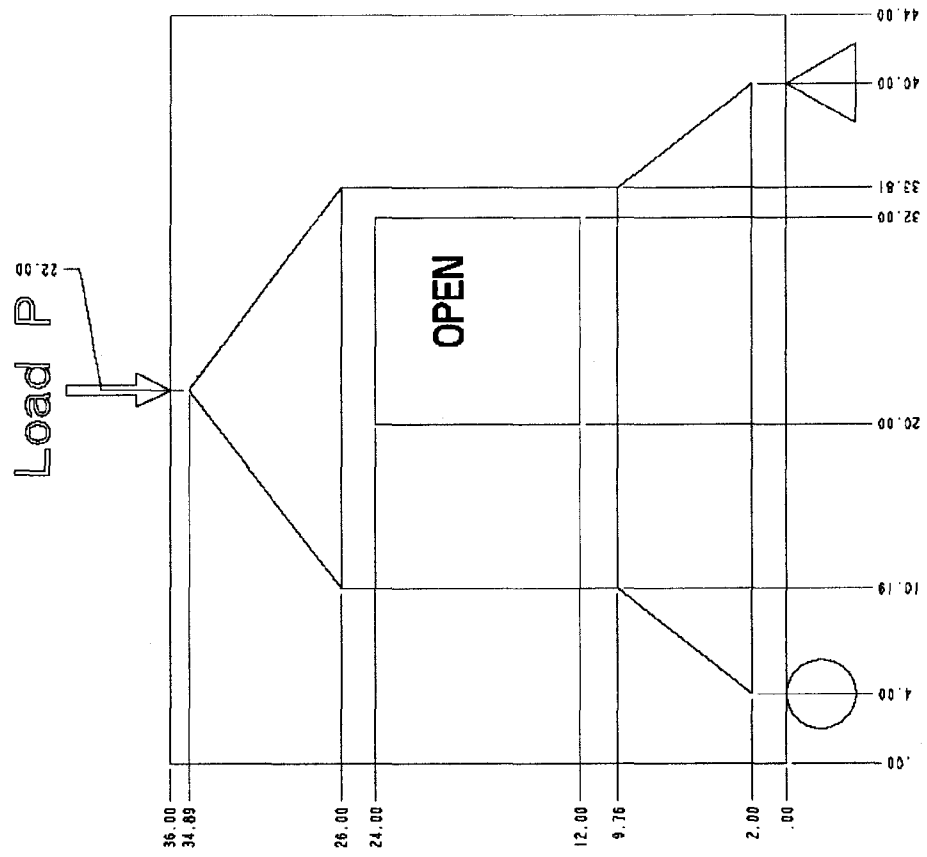
Figure B - 5 Deep beam series 5 STM truss model
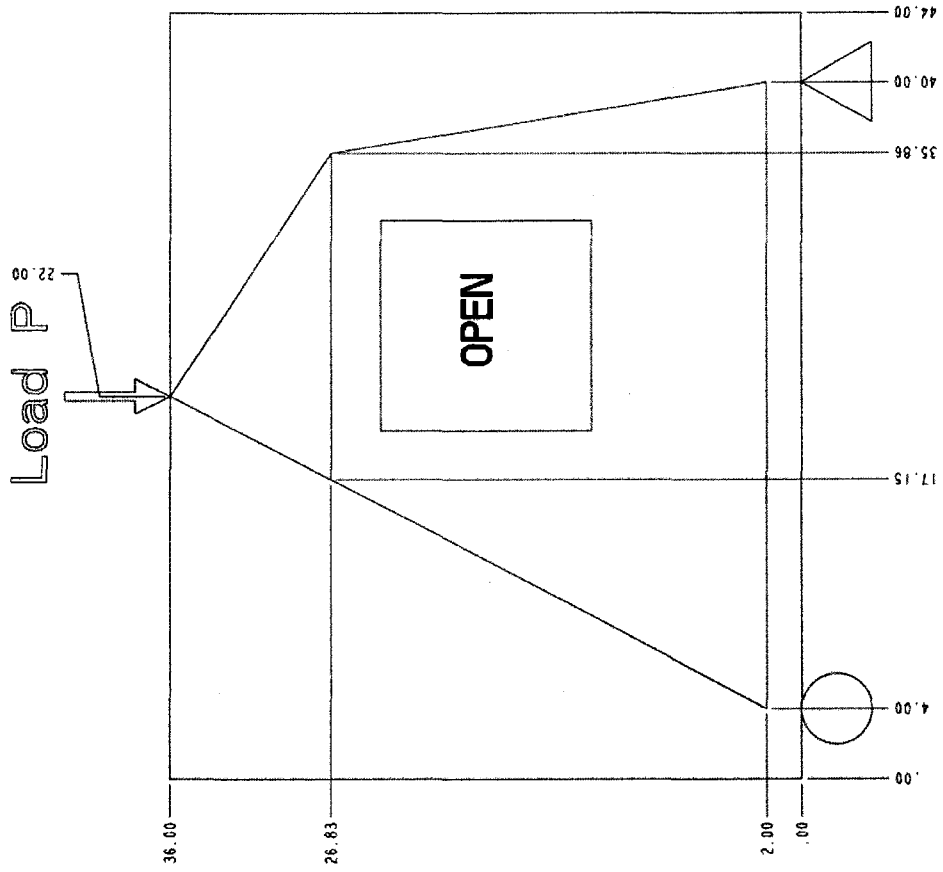
Figure B - 6 Deep beam series 5a Alternate STM truss model

Appendix C – STM Truss Free Body Diagrams & Solutions

Deep beam series 1 free body diagram and solution
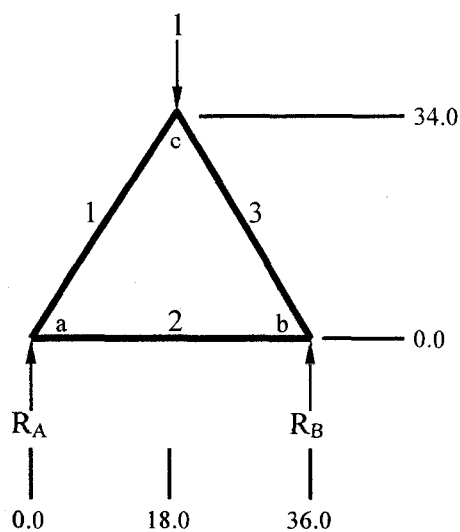
Truss Element	Element Force
1	0.566 C
2	0.464 T
3	0.566 C

$$\circlearrowleft + \Sigma M_A = 0 \Rightarrow R_B * 36in. - 1 = 0$$
$$R_B = 0.500$$

$$\uparrow + \Sigma F_Y = 0 \Rightarrow R_A + 0.500 - 1 = 0$$
$$R_A = 0.500$$
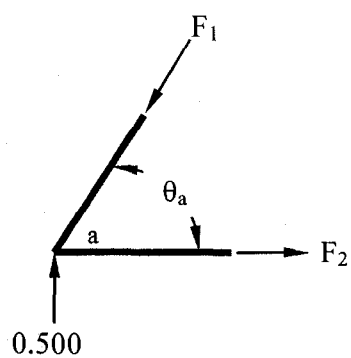
$$\theta_a = \tan^{-1} \frac{34}{18} \Rightarrow \theta_a = 62.10°$$
$$\uparrow + \Sigma F_Y = 0 \Rightarrow 0.500 - F_1 \sin 62.10° = 0$$
$$F_1 = 0.566$$
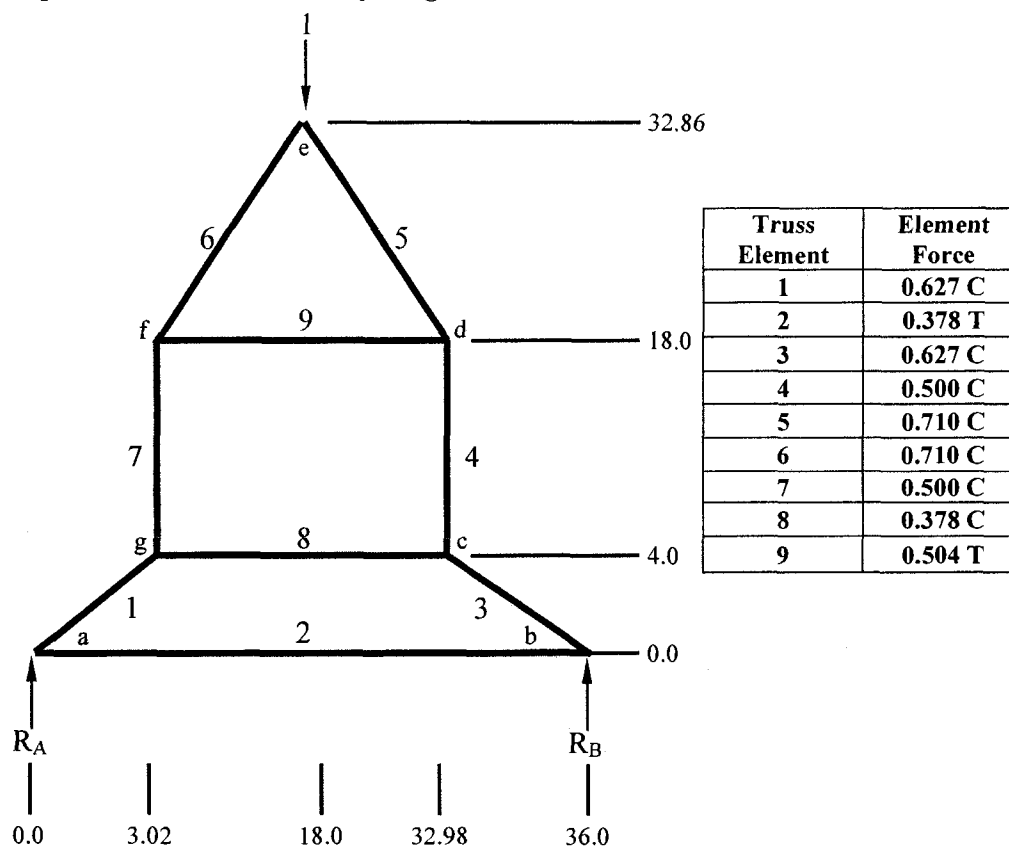$$\rightarrow + \Sigma F_X = 0 \Rightarrow F_2 - 0.566 \cos 62.10° = 0$$
$$F_2 = 0.468$$

From symmetry $F_1 = F_3 \therefore F_3 = 0.566$

Deep beam series 2 free body diagram and solution
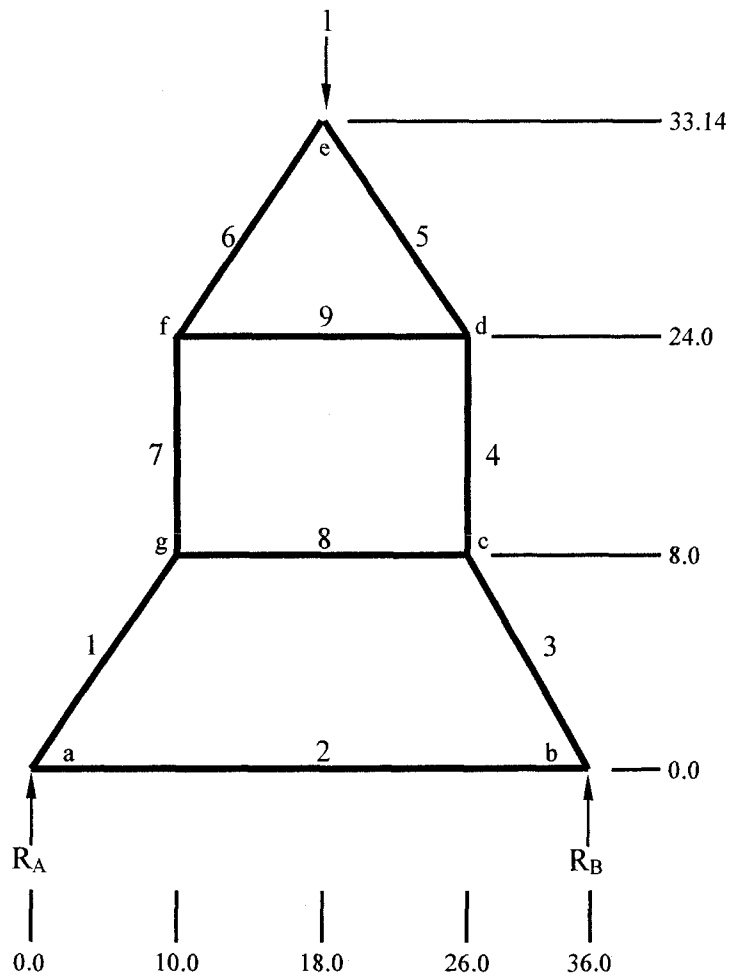
$$\text{↺}+ \Sigma M_A = 0 \Rightarrow R_B * 36in. - 1 = 0$$

$$R_B = 0.500$$

$$\text{↑} + \Sigma F_Y = 0 \Rightarrow R_A + 0.500 - 1 = 0$$
$$R_A = 0.500$$

Truss Element	Element Force
1	0.800 C
2	0.625 T
3	0.800 C
4	0.500 C
5	0.664 C
6	0.664 C
7	0.500 C
8	0.625 C
9	0.437 T
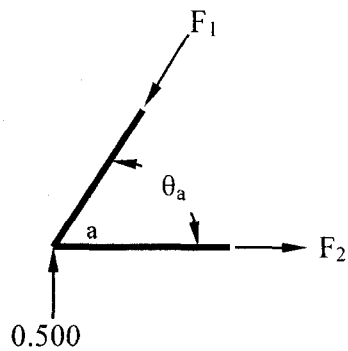
$$\theta_a = \tan^{-1}\frac{8}{10} \Rightarrow \theta_a = 38.66°$$

$$\uparrow +\Sigma F_Y = 0 \Rightarrow 0.500 - F_1 \sin 38.66° = 0$$

$$F_1 = 0.800$$

$$\rightarrow +\Sigma F_X = 0 \Rightarrow F_2 - 0.800\cos 38.66° = 0$$

$$F_2 = 0.625$$
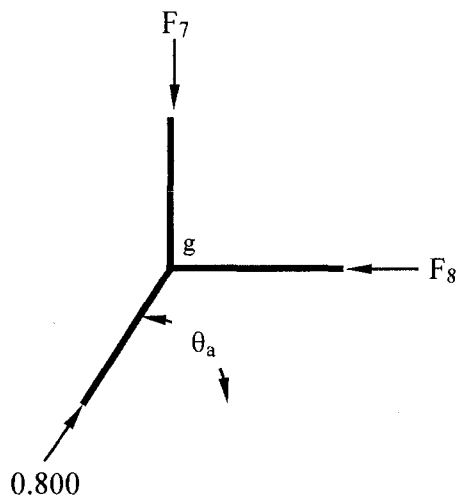
$$\uparrow +\Sigma F_Y = 0 \Rightarrow 0.800\sin 38.66° - F_7 = 0$$

$$F_7 = 0.500$$

$$\rightarrow +\Sigma F_X = 0 \Rightarrow 0.800\cos 38.66° - F_8 = 0$$

$$F_8 = 0.625$$
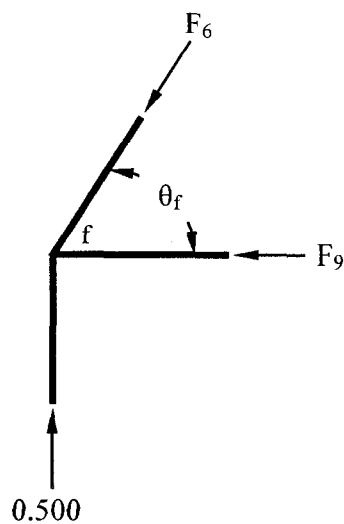
$$\theta_f = \tan^{-1}\frac{9.14}{8.0} \Rightarrow \theta_f = 48.81°$$

$$\uparrow +\Sigma F_Y = 0 \Rightarrow 0.500 - F_6 \sin 48.81° = 0$$

$$F_6 = 0.664$$

$$\rightarrow +\Sigma F_X = 0 \Rightarrow F_9 - 0.664\cos 48.81° = 0$$

$$F_9 = 0.437$$

From symmetry $F_1 = F_3, F_4 = F_7$ & $F_5 = F_6$

Deep beam series 3 free body diagram and solution

Truss Element	Element Force
1	0.627 C
2	0.378 T
3	0.627 C
4	0.500 C
5	0.710 C
6	0.710 C
7	0.500 C
8	0.378 C
9	0.504 T

$$\circlearrowleft + \Sigma M_A = 0 \Rightarrow R_B * 36in. - 1 * 18in. = 0$$
$$R_B = 0.500$$

$$\uparrow + \Sigma F_Y = 0 \Rightarrow R_A + 0.500 - 1 = 0$$
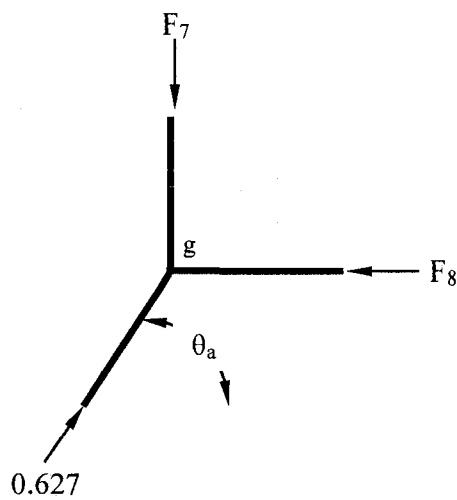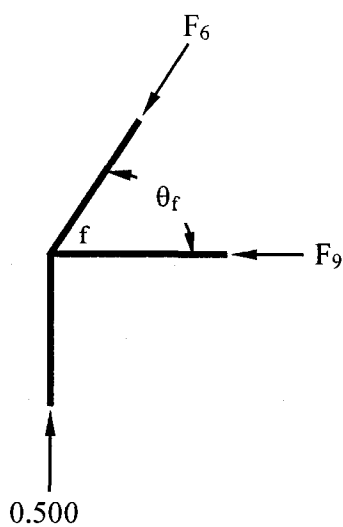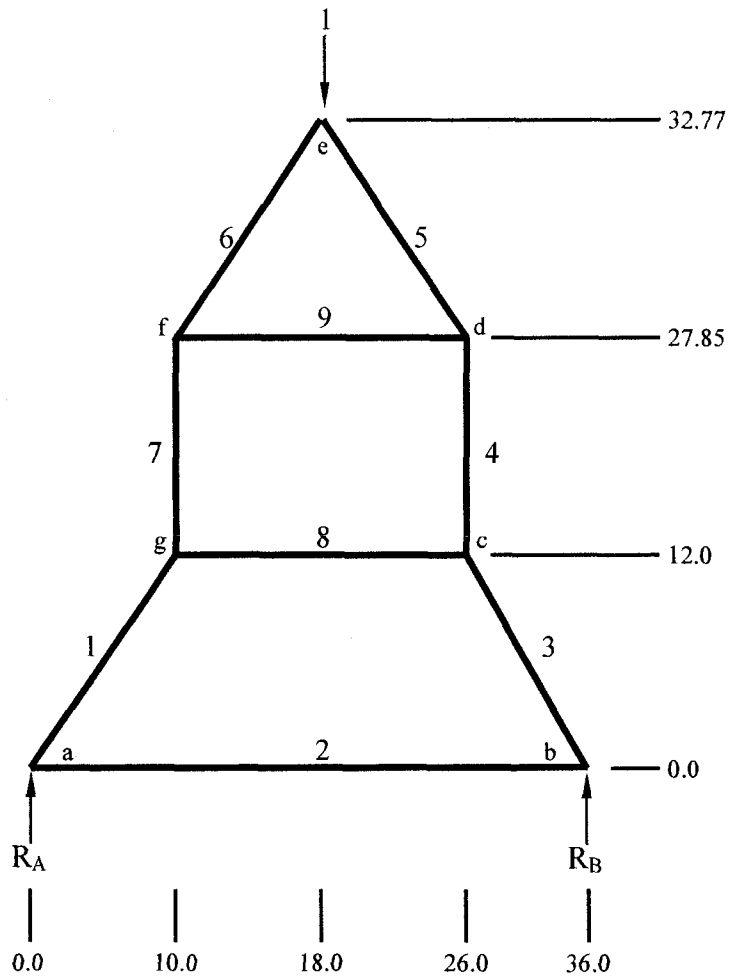$$R_A = 0.500$$
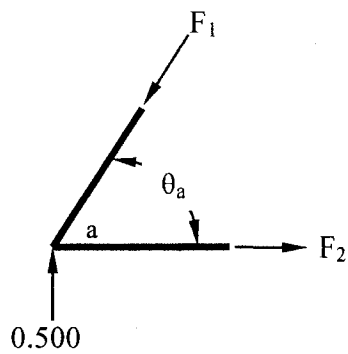
$$\theta_a = \tan^{-1}\frac{4}{3.02} \Rightarrow \theta_a = 52.95°$$

$$\uparrow +\Sigma F_Y = 0 \Rightarrow 0.500 - F_1 \sin 52.95° = 0$$

$$F_1 = 0.627$$

$$\rightarrow +\Sigma F_X = 0 \Rightarrow F_2 - 0.627\cos 52.95° = 0$$

$$F_2 = 0.378$$

$$\uparrow +\Sigma F_Y = 0 \Rightarrow 0.627\sin 52.95° - F_7 = 0$$

$$F_7 = 0.500$$

$$\rightarrow +\Sigma F_X = 0 \Rightarrow 0.627\cos 52.95° - F_8 = 0$$

$$F_8 = 0.378$$

$$\theta_f = \tan^{-1}\frac{14.86}{14.98} \Rightarrow \theta_f = 44.77°$$

$$\uparrow +\Sigma F_Y = 0 \Rightarrow 0.500 - F_6 \sin 44.77° = 0$$

$$F_6 = 0.710$$

$$\rightarrow +\Sigma F_X = 0 \Rightarrow F_9 - 0.710\cos 44.77° = 0$$

$$F_9 = 0.504$$

From symmetry $F_1 = F_3, F_4 = F_7$ & $F_5 = F_6$
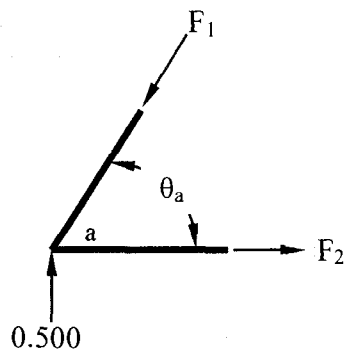
Deep beam series 4 free body diagram and solution

Truss Element	Element Force
1	0.651 C
2	0.417 T
3	0.651 C
4	0.500 C
5	0.954 C
6	0.954 C
7	0.500 C
8	0.417 C
9	0.813 T

$$\circlearrowleft + \Sigma M_A = 0 \Rightarrow R_B * 36in. - 1 = 0$$
$$R_B = 0.500$$

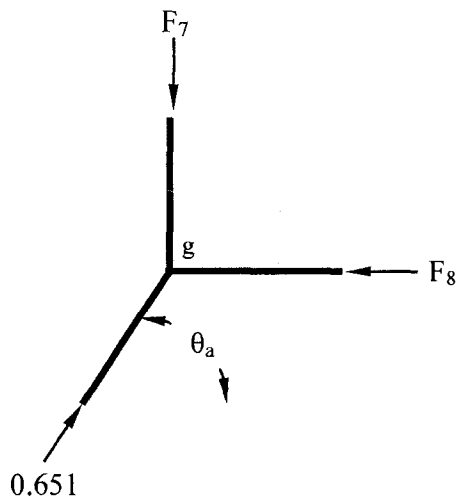$$\uparrow + \Sigma F_Y = 0 \Rightarrow R_A + 0.500 - 1 = 0$$
$$R_A = 0.500$$

$$\theta_a = \tan^{-1}\frac{12}{10} \Rightarrow \theta_a = 50.19°$$

$$\uparrow +\Sigma F_Y = 0 \Rightarrow 0.500 - F_1 \sin 50.19° = 0$$

$$F_1 = 0.651$$

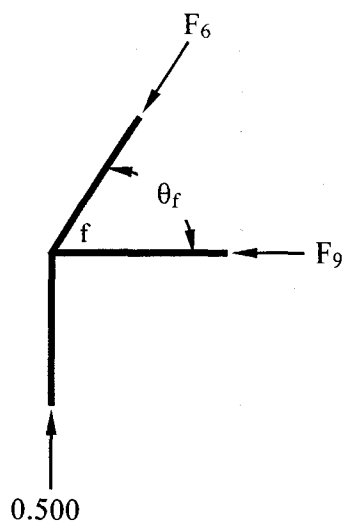$$\rightarrow +\Sigma F_X = 0 \Rightarrow F_2 - 0.651\cos 50.19° = 0$$

$$F_2 = 0.417$$

$$\uparrow +\Sigma F_Y = 0 \Rightarrow 0.651\sin 50.19° - F_7 = 0$$

$$F_7 = 0.500$$

$$\rightarrow +\Sigma F_X = 0 \Rightarrow 0.651\cos 50.19° - F_8 = 0$$

$$F_8 = 0.417$$

$$\theta_f = \tan^{-1}\frac{4.92}{8.0} \Rightarrow \theta_f = 31.59°$$

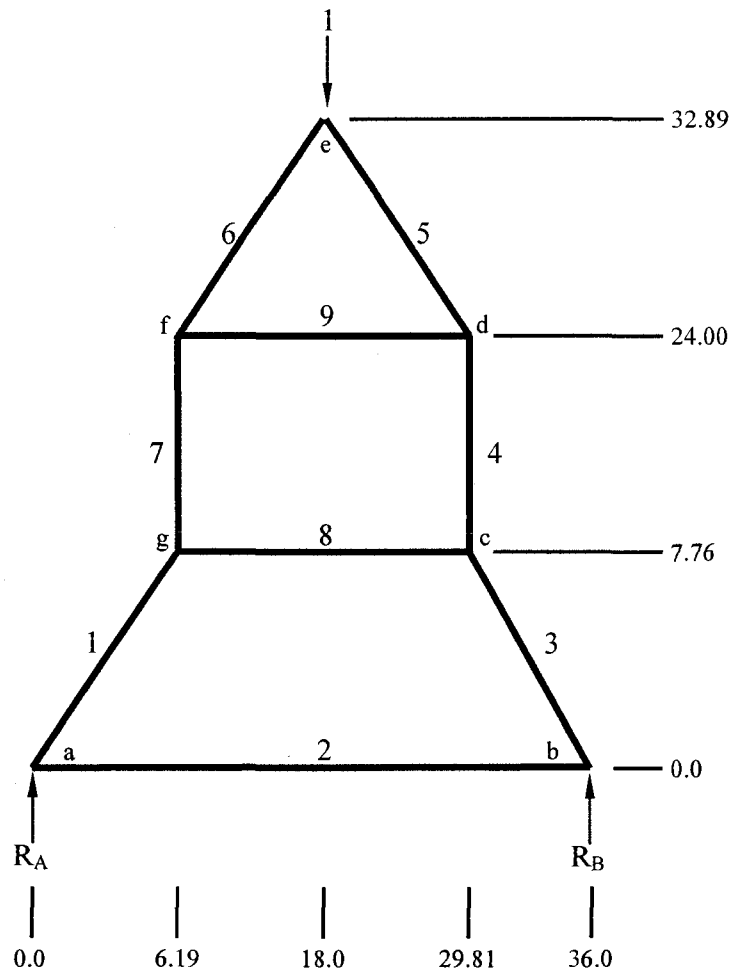$$\uparrow +\Sigma F_Y = 0 \Rightarrow 0.500 - F_6 \sin 31.59° = 0$$

$$F_6 = 0.954$$

$$\rightarrow +\Sigma F_X = 0 \Rightarrow F_9 - 0.954\cos 31.59° = 0$$

$$F_9 = 0.813$$

From symmetry $F_1 = F_3, F_4 = F_7$ & $F_5 = F_6$
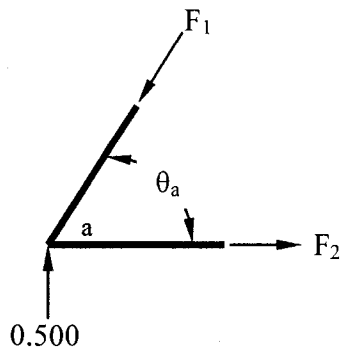
Deep beam series 5 free body diagram and solution

1

32.89

e

6 5

f   9   d 24.00

7   4

g   8   c 7.76

1   3

a   2   b   0.0

R_A R_B

0.0 6.19 18.0 29.81 36.0

Truss Element	Element Force
1	0.640 C
2	0.399 T
3	0.640 C
4	0.500 C
5	0.831 C
6	0.831 C
7	0.500 C
8	0.399 C
9	0.664 T

$$\circlearrowleft + \Sigma M_A = 0 \Rightarrow R_B * 36in. - 1 = 0$$
$$R_B = 0.500$$

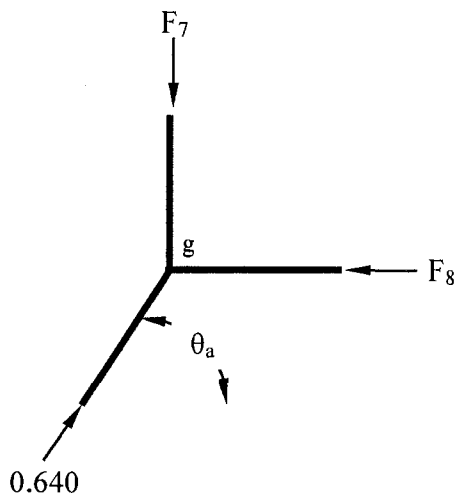$$\uparrow + \Sigma F_Y = 0 \Rightarrow R_A + 0.500 - 1 = 0$$
$$R_A = 0.500$$

$$\theta_a = \tan^{-1}\frac{7.76}{6.19} \Rightarrow \theta_a = 51.42°$$

$$\uparrow +\Sigma F_Y = 0 \Rightarrow .500 - F_1 \sin 51.42° = 0$$

$$F_1 = 0.640$$

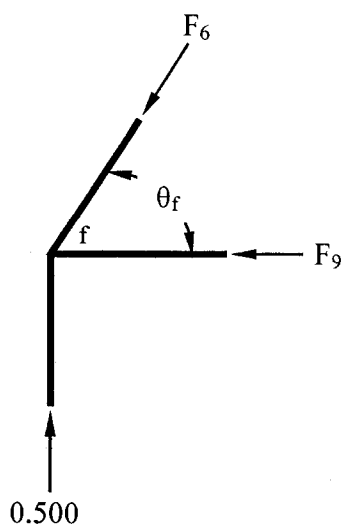$$\rightarrow +\Sigma F_X = 0 \Rightarrow F_2 - 0.640\cos 51.42° = 0$$

$$F_2 = 0.399$$

$$\uparrow +\Sigma F_Y = 0 \Rightarrow 0.640\sin 51.42° - F_7 = 0$$

$$F_7 = 0.500$$

$$\rightarrow +\Sigma F_X = 0 \Rightarrow 0.640\cos 51.42° - F_8 = 0$$

$$F_8 = 0.399$$

$$\theta_f = \tan^{-1}\frac{8.89}{11.81} \Rightarrow \theta_f = 36.97°$$

$$\uparrow +\Sigma F_Y = 0 \Rightarrow 0.500 - F_6 \sin 36.97° = 0$$

$$F_6 = 0.831$$

$$\rightarrow +\Sigma F_X = 0 \Rightarrow F_9 - 0.831\cos 36.97° = 0$$

$$F_9 = 0.664$$

From symmetry $F_1 = F_3, F_4 = F_7$ & $F_5 = F_6$